Late Cenozoic exhumation and drainage evolution of the Central and Western Alps revealed by detrital thermochronology

DISSERTATION

zur Erlangung des Doktorgrades der Naturwissenschaften
vorgelegt dem Fachbereich Geowissenschaften
der Universität Bremen
von

WOLFGANG STEFAN REITER

Bremen, 17. Mai 2013

Erstgutachter:	Prof. Dr. Cornelia Spiegel
Zweitgutachter:	PD Dr. Andreas Klügel
Datum des Kolloquiums:	20. Juni 2013

Erklärung

Hiermit versichere ich, daß ich

1. die Arbeit ohne unerlaubte fremde Hilfe angefertigt habe,
2. keine anderen als die von mir angegebenen Quellen und Hilfsmittel benutzt habe, und
3. die den benutzten Werken wörtlich oder inhaltlich entnommenen Stellen als solche kenntlich gemacht habe.

Bremen, den 17. Mai 2013 Wolfgang Stefan Reiter

Zusammenfassung

Die Zusammenhänge zwischen Klima, Tektonik und Änderungen in der Topographie eines Gebirges sind nur unzureichend verstanden. Der im späten Känozoikum beobachtete starke Anstieg globaler Sedimentationsraten, und vor allem der vermutete Zusammenhang mit einer zeitgleich auftretenden verstärkten Variabilität der klimatischen Verhältnisse bleibt trotz langjähriger Forschung umstritten. Es verdichten sich aber die Hinweise, daß die stark erhöhten Sedimentationsraten mit einer erhöhten Reliefbildung innerhalb der Gebirgsareale zusammenhängen könnten. Solchartige Beobachtungen, d.h. steigende Sedimentationsraten als auch stark erhöhte Reliefbildung, werden aus unterschiedlichen Zeiträumen innerhalb der Entwicklung von den Zentral- und Westalpen und deren Vorlandbecken berichtet. Die seit dem Unterpliozän ansteigenden Sedimentationsraten in den Vorlandbecken sind nur unzulänglich erklärt. Im Laufe der pleistozänen alpinen Hauptvereisung scheint es, daß es in den Zentral- und Westalpen zumindest teilweise eine deutliche Reliefzunahme gab. Was jedoch im Detail in welchem Zeitraum und zu welchem Zeitpunkt die dominierende Kraft, Tektonik oder Klimaveränderung, für die verstärkten Sedimentationsraten oder erhöhte Reliefbildung waren, ist Gegenstand der derzeitigen alpinen Forschung. Die Ergebnisse thermochronologischer Studien sind dahingehend widersprüchlich, als daß sie auf steigende aber auch auf konstant bleibende Exhumierungsraten innerhalb des vermuteten Zeitraumes einer erhöhten Reliefbildung im zentral- und westalpinen Raum verweisen.

Zwei Methoden aus der Niedrig-Temperaturthermochronologie, die Apatit Spaltspur (AFT) und die (U-Th-Sm)/He Datierung (AHe), liefern Abkühlalter und werden dazu genutzt, um die Abkühlgeschichte der obersten Erdkruste zu rekonstruieren. Anhand der thermischen Rekonstruktion können Prozesse identifiziert werden, welche die oberste Erdkruste beeinflussen. Durch den Ansatz der detritischen Thermochronologie kann mittels der Analyse von Vorlandsedimenten und den daraus resultierenden thermischen Signaturen auf die einzelnen Quellgebiete eines Einzugsgebietes zurückgeschlossen werden. Dies erlaubt, eine Rekonstruktion der synsedimentären Paläo-Exhumierungsgeschichte des Hinterlandes vorzunehmen. Da Sedimentbecken häufig auch hochauflösende Klimaarchive darstellen, können die beobachteten Veränderungen der Exhumierungsraten mit den klimatischen Bedingungen zum Ablagerungszeitpunkt in Verbindung gebracht werden. Aufgrund dieser Verbindung können die Folgen einer Klimaveränderung auf Gebirge studiert werden.

Im Zuge dieser Studie wurden miozäne bis rezente Ablagerungen aus dem nordwestlichen Alpenraum mit thermochronologischen Methoden untersucht. Die Sedimente umfassen Ablagerungen des Oberrheingrabens, des westalpinen Chambaran-Beckens, die (glazio-)fluvialen Ablagerungen der Sundgau Schotter und Höheren Deckenschotter, sowie rezente Sedimente aus den Flüssen Aare, Reuss und Isère. Die Ziele dieser Studie sind: (a) die Identifizierung der Hauptliefergebiete der sedimentären Ablagerungen, um damit das alpine Flußnetz nordwestlich der Alpen seit dem Pliozän rekonstruieren zu können; (b) die Rekonstruktion der Paläo-Exhumierungsgeschichte des Hinterlandes, um dadurch den möglichen klimatischen Einfluss auf die Exhumierungsraten eines Gebirges untersuchen zu können, und (c) Grenzen und evtl. Verfeinerungen thermochronologischer Datierungsansätze an detritischen Sedimenten testen zu können.

Die in den Zentralalpen gelegenen Externmassive (Aar-Gotthard) und der Lepontin-Dom wurden als hauptsächliche Sedimentquellen für die mittelmiozänen Sedimente des Chambaran-Beckens, der pliozänen Sundgau Schotter, der pleistozänen Höheren Deckenschotter, als auch für die pliozänen bis rezenten Sedimente des Oberen Rheingrabens identifiziert. In der Gegenwart versorgt alleinig das Aar-Gotthard Massiv die in Richtung Rheingraben entwässernden Flüsse Aare

und Reuss mit Detritus. Die nord-/östlich an die Zentralalpen angrenzenden Gebiete der austroalpinen Silvrettadecke und Rhenodanubischer Flysch waren untergeordnete potentielle Liefergebiete für die Höheren Deckenschotter. Die Vulkangebiete des Oberen Rheingrabens als auch des Massif Central sind zusätzliche Sedimentquellen für das Chambaran-Becken während des Mittelmiozäns, und der pleistozänen Sedimente des Oberen Rheingrabens (nur das Vulkangebiet Hegau). Die Schweizer Molasse stellt ein untergeordnetes Liefergebiet für die Sundgau Schotter und die der frühpleistozänen Ablagerungen des Oberen Rheingrabens dar. Die Externmassive in Verbindung mit der Houillère-Zone (Mittelpenninikum) der Westalpen sind Hauptliefergebiete für die pliozänen bis rezenten Sedimente des Chambaran-Beckens.

Die Interpretation der thermochronologischen Daten unter Berücksichtigung vorhandener sedimentären Studien zeigt, daß das pliozäne Flußnetz der nordwestlichen Zentralalpen mit zwei Flusssystemen komplexer war als bisher angenommen und ließ folgende präzisierte Rekonstruktion der Flussentwicklung zu: Im Laufe des Plio- und Pleistozäns verschiebt sich die zentralalpine Hauptwasserscheide vom nördlichen Lepontin nordwärts in Richtung des Aar-Gotthard Massives; zusätzlich zum bekannten Flusssystem der Aare-Doubs, welches die Zentralalpen in Richtung Mittelmeer entwässerte, wurde im Pliozän der nordalpine Rand vom Proto-Rhein durch den Oberen Rheingraben in Richtung Nordsee entwässert.

Die neugewonnenen Thermochronologie-Daten widersprechen einem großräumigen langzeitlichen Hebungsgleichgewicht der Zentral- und Westalpen, wie es häufig in der Literatur postuliert wird. Stattdessen konnten lokale Unterschiede der Hebungsgeschichte in unterschiedlichen Bereichen der Alpen beobachtet werden: Das zentralalpine Aar-Gotthard Massiv zeigt eine konstante Exhumierungsgeschichte von ~4.2 bis 1.2 Ma, welche auch nicht durch einsetzende alpine Vergletscherungen im Frühpleistozän wesentlich unterbrochen wurde. Im Zuge der einsetzenden Hauptvergletscherung der Alpen zwischen ~ 1.2 und 1.0 Ma wurde das Aar-Gotthard Massiv temporär versiegelt, d.h. keine erosive Tätigkeit aus diesem Gebiet konnte nachgewiesen werden. Eine verstärkte Erosion der (subalpinen) Molasse war die Folge. Die heutige Erosion des Aar-Gotthard Massives scheint von Bergstürzen in höhergelegenen Bereichen dominiert zu sein, und wird begleitet von einer leicht gesunkenen Exhumierungsrate im Vergleich zum plio-pleistozänen Zeitraum. Der Lepontin-Dom wird bis ~13 Ma konstant exhumiert, und zeigt mit leicht steigenden Exhumierungsraten zwischen ~4.2 und ~1.8 Ma eine andersverlaufende Entwicklung im Vergleich zum benachbarten Aar-Gotthard Massiv. Desweiteren zeigen die modellierten Abkühlpfade der westalpinen Belledonne und Pelvoux Massive zwischen ~12 und 7 Ma zueinander unterschiedliche Abkühlpfade, gefolgt von konstanter Exhumierung bis in die Gegenwart. Und zuletzt ist eine unterschiedliche Abkühlgeschichte der nördlichen als auch südlichen Houillère-Zone zwischen ~22 und 15 Ma erkennbar. Ab ~15 Ma wird die Houillère-Zone konstant exhumiert. Die in dieser Arbeit benannten Abkühlpfade und Exhumierungs- bzw. Abkühlraten widersprechen einem generell vermuteten Hebungsgleichgewicht der Zentral- und Westalpen, da sie in ihrer Form und Weise der Exhumierung weder konstant noch einheitlich sind.

AHe-Studien mittels detritischer Thermochronologie sind stark begrenzt durch die Anzahl der datierbaren Mineralkörner. Durch die neue Kombination aus statistischen Techniken in Verbindung mit der Annahme, daß der Mittelwert von AHe-Altern zur nächstälteren AFT-Altersgruppe gehört, lassen sich auch Datensätze mit einer kleineren Anzahl von datierten Apatitkörnern für detritische Studien nützen. Mittels der thermischen Modellierung lassen sich die Bestimmung der Quellgebiete von Sedimenten verfeinern, als auch Hypothesen über mögliche Hebungsgleichgewichte von Gebirgsmassiven überprüfen.

Summary

The relations between climate, tectonics and topographic changes are still not fully understood. Strongly increased late Cenozoic sedimentation rates are observed worldwide, but a suggested relation with an enhanced climatic variability is, despite intense research, still under discussion. There are indications that these strongly increased sedimentation rates could be related to a rapidly developing relief of the associated mountainous area. Similar observations, i.e., increasing sedimentation rates or enhanced relief development, are reported from distinct periods within the development of the Central and Western European Alps. During the Early Pliocene, a strong increase in the sedimentation rates of the circum-Alpine foreland basins is observed but the cause(s) are still poorly understood. Additionally, Pleistocene glaciations affecting the Central and Western Alps are, at least partially, held responsible for a strongly enhanced Alpine relief. A detailed understanding of which force, i.e., tectonics or climate change, has essentially triggered the increase of sedimentation rates or relief development is subject of current Alpine research. Thermochronological investigations in the central- and west-Alpine realm show a contradicting pattern, where strongly increased as well as constant exhumation rates are observed for the Pleistocene, i.e., the time when enhanced relief development is assumed.

For this thesis, two low-temperature thermochronological methods, namely apatite fission-track (AFT) and (U-Th-Sm)/He dating, were applied. The yielded cooling ages are used to reconstruct the thermal history of the uppermost Earth`s crust. The two dating methods were applied to foreland sediments of the north-Alpine realm. Age groups contained in the sediments can be allocated to distinct source areas within the catchment, and thus yielding information on the provenance of the detritus. The thermochronological data additionally allow reconstructing the synsedimentary paleo-exhumation history of the source areas. As basin fills frequently store high-resolution climate information, observed changes in exhumation rates can be correlated with synsedimentary climate conditions. Based on this relation, it is possible to study the effect of climate change on a mountain belt.

Miocene to present-day sediments from the northwest-Alpine realm were analysed with thermochronological methods. The studied sediment layers comprise deposits of the Upper Rhine Graben, the west-Alpine Chambaran basin, the (glacio-)fluvial Sundgau gravel and the Höhere Deckenschotter, as well as present-day sediments from the Aare, Reuss, and Isère rivers. The goals of this thesis are: (i) to identify the major source areas of sedimentary deposits, and hence to reconstruct the evolution of the northwest-Alpine drainage system since the Pliocene; (ii) to reconstruct the paleo-exhumation history of the hinterland, and therefore to study the possible effect of climate change on Alpine exhumation rates; and (iii) to test limits and potential refinements of detrital thermochronological approaches on clastic sediments.

The central-Alpine external massifs (Aar-Gotthard) and the Lepontine Dome are identified as the major source areas for the mid-Miocene deposits of the Chambaran basin, the Pliocene Sundgau gravel, the Pleistocene Höhere Deckenschotter, and the Pliocene to recent sediments of the Upper Rhine Graben. The Austroalpine Silvretta nappe and the Rhenodanubian Flysch, both located north-east of the Central Alps, also contributed to the deposits of the Höhere Deckenschotter. The volcanic complexes of the Upper Rhine Graben and the Massif Central are additional minor sources for the mid-Miocene Chambaran basin as well as for the Pleistocene Upper Rhine Graben fill (only Hegau volcanics). The west-Alpine external massifs and the Houillère zone (Middle Penninic units) are major source areas for Pliocene to modern sediments of the Chambaran basin.

The provenance information derived from the thermochronological data, combined with already published sedimentary studies, allows reconstructing the Pliocene to present drainage

evolution. The drainage pattern was more complex and comprised more river systems than previously assumed: During the Plio- and Pleistocene, the central-Alpine water divide shifted north toward the Aar-Gotthard massif. The Central Alps were drained by the Aare-Doubs river system toward the Mediterranean Sea. Additionally, a second river system, the proto-Rhine, drained the southern Molasse basin or the northern rim of the Central Alps via the Upper Rhine Graben toward the North Sea.

The new thermochronological data of this study contradict a long-term exhumational equilibrium for the Central and Western Alps, as frequently postulated in the Alpine literature. In fact, distinct Alpine regions differ severely in their exhumation pattern: The central-Alpine Aar-Gotthard massif shows constant exhumation rates between ~4.2 and 1.2 Ma, and this constant trend was also not disturbed by the onset of first glaciations affecting the Central Alps during the Early Pleistocene. During the onset of the major Alpine glaciations between ~1.2 and 1.0 Ma, the Aar-Gotthard massif was temporarily sealed, i.e., no significant erosional activity was observed during this period. This sealing process led to intensified erosion of the Subalpine Molasse. Recent erosion of the Aar-Gotthard massif seems to be dominated by mass wasting processes such as landsliding, and is associated with lower rates compared to the Plio-Pleistocene period. The Lepontine Dome is constantly exhumed until ~13 Ma, but shows slightly increasing exhumation rates between ~4.2 and 1.8 Ma, and thus a distinct development of the exhumation pattern in comparison with the adjacent Aar-Gotthard massif. Furthermore, between ~12 and 7 Ma, modeling of the cooling histories for the west-Alpine Belledonne and Pelvoux massifs show diverging cooling paths, which are followed by constant cooling thereafter until the present day. Between ~22 and 15 Ma, different cooling histories for the northern part of the Houillère zone compared to its southern part were obtained. Only after ~15 Ma, a constant and uniform exhumation rate is observed for the whole Houillère zone. The cooling paths and exhumation/cooling rates named in this thesis contradict a generally suggested steady-state exhumation for the Central and Western Alps as cooling styles observed are neither constant nor uniform.

AHe studies using detrital thermochronology are strongly limited by the number of datable mineral grains. However, the new combination of statistical techniques, linked with the assumption that the mean value of AHe ages was derived from the same source as the next oldest AFT age group, allows to interpret smaller AHe data sets for detrital studies. Thermal modeling can be efficiently used to refine the allocation of the source area as well as to test hypotheses about potential exhumation equilibria of mountain ranges.

Table of contents

1 Introduction

The European Alps are probably the most intensely studied mountain belt in the world. Since the beginning of Alpine research (e.g. Suess, 1875), it becomes clear that the orogenic evolution is more complex than originally thought. Decades of research using structural, geophysical, petrological, thermochronological, and sedimentary methods (e.g., Merle *et al.*, 1989; Glotzbach *et al.*, 2010) form a detailed picture about the convergence of the European and African plates and the resulting Alpine orogeny (e.g., Frisch, 1979; Schmid *et al.*, 2004). In the course of time, the principal evolution of the Alps was understood and along with the further development of dating methods, Alpine research proceeded to study the challenging latest-stage evolution of Alpine topography. Strongly increased Late Cenozoic sedimentation rates, as observed globally and also for the European Alps (Kuhlemann *et al.*, 2000), may result from global climate change, although this assumption and also the applied methods to obtain the data, are controversially discussed (e.g., Molnar & England, 1990; Raymo & Ruddiman, 1992; Zhang *et al.*, 2001; Willet *et al.*, 2006; Willenbring & von Blanckenburg, 2010). Climate change is also assumed to be responsible for the development of Alpine topography where recent studies identified a strong relation of Middle Pleistocene Alpine glaciations and a significant increase in relief (e.g., Muttoni *et al.*, 2003; Haeuselmann *et al.*, 2007; Valla *et al.*, 2011, 2012). In addition, this observation implies that the eroded areas should have experienced a significant increase in exhumation rates due to isostatic uplift (e.g., Champagnac *et al.*, 2009). By contrast, recent thermochronological studies on Alpine massifs or Alpine-derived sediments suggest an exhumational equilibrium for the Central and Western Alps since the Late Miocene (e.g., Glotzbach *et al.*, 2010, 2011). The ESF EUROCORES Project *"Coupled climatic/tectonic forcing of European topography revealed through thermochronometry – THERMO-EUROPE"* was initiated to investigate the latest-stage Alpine evolution by means of low-temperature thermochronology. This PhD thesis is part of the individual project IP2 contribution to the Thermo-Europe project "*Sources and Sinks of Pliocene erosion: Investigating the latest-stage exhumation history of the Alps*", aiming to:

(i) identify major source areas of circum-Alpine depocenters (Upper Rhine Graben & Chambaran basin) and fluvio-(glacial) deposits (Sundgau gravel & Höhere Deckenschotter);
(ii) reconstruct the evolution of the northwest-Alpine drainage system;
(iii) reconstruct the paleo-exhumation histories of the hinterland, and therefore to study the potential impact of climate change on the exhumation pattern of the Central and Western Alps.

2 Geological setting

2.1 Late Cenozoic evolution of potential source areas

The European Alps are the result of the convergence between the European and African plates which resulted in the closure of the Penninic Ocean (e.g., Trümpy, 1960; Frisch, 1979). The African margin overthrust the European plate resulting in a pile of northward advancing nappes (Steck & Hunziker, 1994). The present exposures of the Central and Western Alps comprise the External Crystalline Massifs (Helvetic realm, European crust), and the (Sub-)Penninic nappes (Penninic realm, European continental and oceanic crust), whereas the African margin is almost exclusively preserved in the Southern and Eastern Alps (Southalpine and Austroalpine nappes; e.g., Schmid *et al.*, 2004). Circum-Alpine foreland basins were formed as a result of crustal thickening and associated crustal flexure. They mostly contain Alpine-derived detritus, thus storing the early record of Alpine evolution. The north-Alpine foreland was also influenced by the development of the European Cenozoic Rift System which experienced main activity during the Late Eocene/Oligocene (Dèzes *et al.*, 2004). As a result of intra-continental rifting, the Rhine, Bresse and Rhône Graben were formed, accompanied by volcanic activity adjacent to the Upper Rhine Graben and Massiv Central (Sissingh, 1998, 2001, and references therein; Dèzes *et al.*, 2004). In the following, I briefly outline the evolution of potential major source areas of the sedimentary deposits investigated for this thesis.

2.1.1 External crystalline massifs

The external massifs are composed of Hercynian European basement. Their tectonic evolution comprises collision-related overthrusting during the major phase of the Alpine orogeny with subsequent uplift (Figs. 2.1 & 2.2; e.g., Schmid *et al.*, 2004). The external massifs of the Central Alps, namely the Aar and Gotthard massifs, generally show steady exhumation since the late Miocene (Glotzbach *et al.*, 2010 and references therein), except for the southwestern Aar massif, which experienced a strong increase in exhumation since ~3.5 Ma (Reinecker *et al.*, 2008). This enhanced exhumation may be caused by tectonic denudation along the Rhône-Simplon fault zone (Reinecker *et al.*, 2008), which was active since the early Miocene (e.g., Soom, 1990; Campani *et al.*, 2010). AFT cooling ages of the Aar and Gotthard massifs range between 3 and 14 Ma (Reinecker *et al.*, 2008; Glotzbach *et al.*, 2010 and references therein) with most AFT ages ranging between 6 and 10 Ma. AHe ages of this area range between 2.3 and 9 Ma (Reinecker *et al.*, 2008; Vernon *et al.*, 2009; Glotzbach *et al.*, 2010).

The external massifs of the Western Alps show a distinct exhumation pattern: *(i)* the Mont Blanc massif underwent fast exhumation from the Early Miocene until the present, only interrupted by strongly decelerating exhumation rates between ~6 and ~2 Ma. Modern exposures of the Mont Blanc show AFT ages ranging between 2.6 and 7.7 Ma, and AHe ages between 1.4 and 6.4 Ma (Glotzbach *et al.*, 2008; Vernon *et al.*, 2008); *(ii)* the Belledonne massif shows constant exhumation since the Late Miocene with a probable increase during the Quaternary as suggested by Lelarge (1993). AFT ages range between 3.2 and 6.8 Ma (Lelarge, 1993; Vernon *et al.*, 2008); and *(iii)* the exhumation history of the Pelvoux massif shows constant exhumation until the present day, only

interrupted by two pulses of increased exhumation at 6 and 5.5 Ma. AFT ages range between 3.2 and 8.0 Ma, and AHe ages between 4.0 and 6.2 Ma (van der Beek *et al.*, 2010).

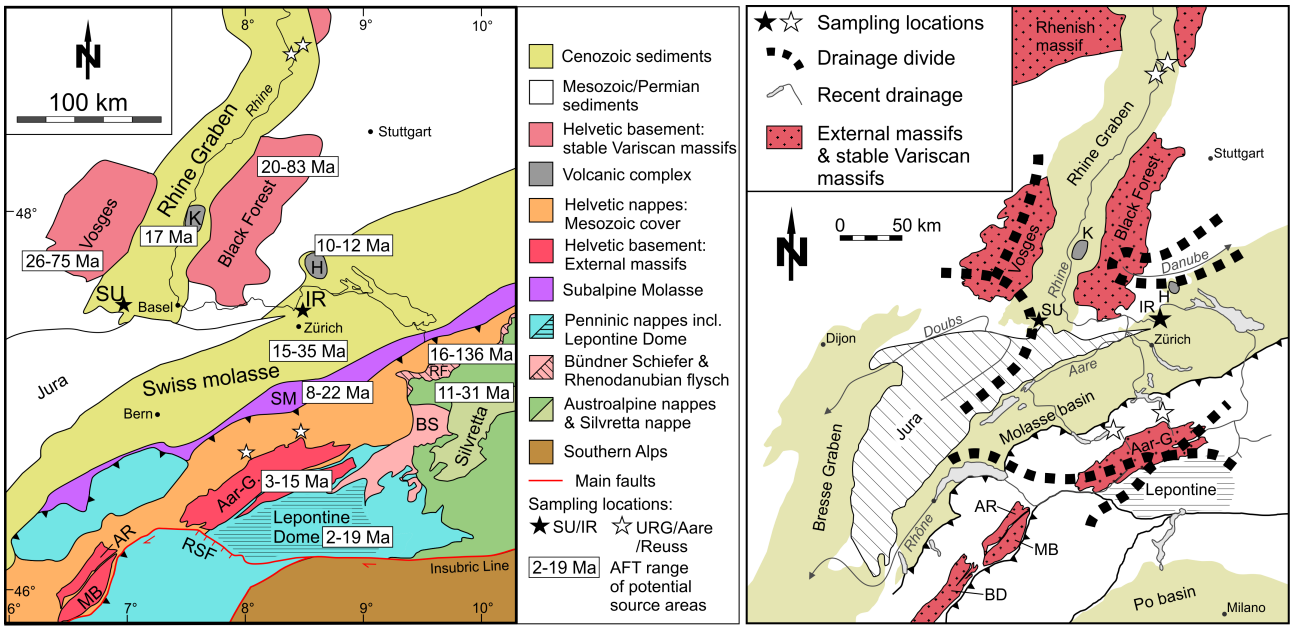

Fig. 2.1: Simplified geological map (modified after Schmid *et al.*, 2004) of potential source areas with their AFT ranges (Hurford *et al.*, 1989; Trautwein *et al.*, 2001; Timar-Geng *et al.*, 2006; Rahn & Selbekk, 2007; Reinecker *et al.*, 2008; Vernon *et al.*, 2008 and references therein; Danišik *et al.*, 2010; Glotzbach *et al.*, 2010; Link, 2010; Elfert *et al.*, 2011). SM, Subalpine Molasse; RF, Rhenodanubian Flysch; BS, Bündner Schiefer; Aar-G., Aar-Gotthard massif; AR, Aiguilles Rouge; MB, Mont Blanc. Black-filled stars, sampling locations of the Sundgau gravel (SU), Höhere Deckenschotter (IR), borehole sites of Parkinsel (P) and Viernheim (VH), and the modern Aare (A) and Reuss (R) rivers.

2.1.2 Lepontine Dome

The Lepontine Dome is located south of the Aar and Gotthard massifs, flanked by the Rhône-Simplon fault to the west and the Insubric Line to the south. It consists of Lower Penninic units which underwent late Paleogene to early Neogene regional metamorphism and a major phase of updoming during the late Oligocene and early Miocene (Merle *et al.*, 1989; Steck & Hunziker, 1994). Exhumation of the Lepontine area is linked to the post-collisional lateral extrusion of the Alps from the Oligocene-Miocene boundary onward (Frisch *et al.*, 2000). AFT cooling ages of the Lepontine Dome range between 2 and 19 Ma (Vernon *et al.*, 2008 and references therein; Elfert *et al.*, 2011) with the oldest ages occurring at the northern and southern periphery of the Lepontine area. AHe ages range between ~3 and 5 Ma (Vernon *et al.*, 2009).

2.1.3 European basement and volcanic centers adjacent to the European Cenozoic Rift System

The Upper Rhine Graben is flanked by Variscan basement rocks of the Black Forest and Vosges. These basement rocks were tectonically affected by the development of the European rift

system resulting in various Miocene and Pliocene phases of surface uplift (Ziegler & Dèzes, 2007; Rotstein & Schaming, 2011). AFT cooling ages range between 20 and 83 Ma, but most are of Paleogene age or older. AHe ages range between ~8 and 190 Ma and are mostly between 20 and 50 Ma (Timar-Geng *et al.*, 2006; Danišik *et al.*, 2010; Link, 2010). Rifting was accompanied by volcanic activity in the Upper Rhine Graben. Two of those Miocene volcanic centers are the Kaiserstuhl and Hegau complex. Volcanism of the Kaiserstuhl area (southern Upper Rhine Graben) was active at ~18-15 Ma (Lippolt *et al.*, 1963; Keller *et al.*, 2002). After short quiescence, emplacement of the alkaline Hegau volcanic complex took place at ~14-9 Ma (Schreiner, 1992; Rahn & Selbekk, 2007). Hegau apatites typically show Dpar values up to 6 µm and characteristic crystal defects (Rahn & Selbeck, 2007; Rahn, pers. comm. 2011).

The Variscan Massif Central is located at the western flank of the Bresse and Rhône Graben. This part of the European basement was uplifted and tilted northward during Burdigalian time (Dèzes *et al.*, 2004, and references therein). The Massif Central mostly show Cretaceous AFT ages but also ages down to 25 Ma (Barbarand *et al.*, 2001). It was affected by volcanism which is associated with the Cenozoic European Rift System (Nehlig *et al.*, 2003; Dèzes *et al.*, 2004). Between ~15 and 1 Ma, the most important volcanic complexes at the eastern part of this massif are the Forez, Limagne, and Velay areas, and especially at ~16 Ma the Limagne complex was very active (compilation by Nehlig *et al.*, 2003).

2.1.4 Austroalpine units in close vicinity of the Central Alps

The Central Alps are bordered by the Silvretta nappe of the Eastern Alps (Austroalpine realm, African plate). Its AFT ages are between 11 and 31 Ma, but are mostly older than 20 Ma (Hurford *et al.*, 1989). To the north, the Eastern Alps are bordered by the Rhenodanubian Flysch, whose western part also extends into the area west of Lake Constance. Its AFT ages range between 17 and 136 Ma (Trautwein *et al.*, 2001).

2.2 Evolution of the NW-Alpine depocenters since the Miocene

2.2.1 Swiss Molasse Basin

The Swiss Molasse Basin forms the western part of the north-Alpine foreland basin (Fig. 2.1). During the Neogene, it acts as both, a depocenter for Alpine-derived sediments as well as a source area for other circum-Alpine basins through sediment recycling. Evolution of the Swiss Molasse Basin was directly influenced by Alpine tectonic processes (Kuhlemann & Kempf, 2002). These orogenic processes caused opening and closing of seaways connecting the northern Alpine foreland basin with the North Sea, Paratethys and Mediterranean Sea, and therefore influenced sediment discharge patterns. From the Oligocene to Miocene, four major deposition cycles reflect repeated changes from marine to freshwater conditions in the Molasse basin. These main cycles are called the lower marine and freshwater Molasse, and upper marine and freshwater Molasse. For the last freshwater cycle (Middle Miocene), the northern Lepontine area is a major sediment supplier (Spiegel *et al.*, 2001). Deposition may have ceased around the Tortonian, as suggested by Kuhlemann & Kempf (2002). However, by early Pliocene time, the Molasse basin was affected by erosion, driven either by climate change and/or drainage reorganisation due to tectonic activity of the hinterland (e.g., Schlunegger & Mosar, 2011). Thermochronological analysis of surface samples from the Swiss Molasse Basin revealed AFT ages between 15 and 36 Ma, with a majority of ages

around 30 Ma (Cederbom *et al.*, 2004, 2011).

2.2.2 Upper Rhine Graben

Main period of sediment deposition in the Upper Rhine Graben – with several local hiatuses – was between the middle Eocene and the Quaternary (e.g., Sissingh, 1998). Alternating Pliocene sand and clay deposits indicate a fluvio-lacustrine depositional environment (Berger *et al.*, 2005). A change of the heavy mineral composition from the stable mineral suite zircon-rutile-tourmaline to garnet-epidote-hornblende dominance during the latest Pliocene points to a change of the sediment source areas. While the stable heavy minerals are interpreted as being derived from the Variscan Vosges and Black Forest, the Pleistocene mineral assemblage is thought to be of Alpine origin (Hagedorn & Boenigk, 2008; Hoselmann, 2008). The Pleistocene sediment succession is characterized by alternating sand-gravel and sand-clay layers.

2.2.3 Chambaran basin

The Chambaran basin is located between the Variscan Massif Central and Western Alps (Fig. 2.2), and thus belongs to the west-Alpine foreland. The basin fill comprises a ~1 km thick sediment succession that mainly contains deposits from Alpine source areas (Clauzon, 1990). The Lepontine area of the Central Alps was suggested as one of the major source areas of the middle Miocene Chambaran sediments (e.g., Glotzbach *et al.*, 2011). As other sources, the Variscan massifs of the Massif Central, Vosges and Black Forest were proposed (Barbarand *et al.*, 2001; Timar-Geng *et al.*, 2006). During the Miocene, marine conditions prevailed in the north- and west-Alpine foreland basins. Sediment transport across the Chambaran basin was directed southwestwards toward the Mediterranean Sea (Mortaz-Djalili & Perriaux, 1979; Kuhlemann *et al.*, 2001; Sissingh, 2001). Marine conditions ceased in the west-Alpine foreland basins around the Middle Miocene and were replaced by terrestrial sedimentation (e.g., Kuhlemann & Kempf, 2002; Ziegler & Fraefel, 2009). During Pliocene time, a marine transgression partially flooded the west-Alpine foreland basins, but never reached the Miocene extent (Sissingh, 2001). The Quaternary was dominated by a fluvio-glacial environment due to glaciations affecting the Western Alps and Massif Central (Clauzon, 1990).

2.3 Evolution of the Alpine drainage system since the Miocene

Fig. 2.1 shows the recent drainage pattern of the north-Alpine realm with the three principal drainage systems, i.e., the Danube river system draining towards the Black Sea, the Rhône river system draining towards the Mediterranean Sea, and the Rhine river system draining towards the North Sea.

Between the late Miocene and the early Pliocene, the folding of the Jura mountains (e.g., Laubscher, 1986; Madritsch *et al.* 2008) caused the division of the former southwestern sediment pathway into two drainage systems with different directions (Fig. 2.2): *(i)* the proto-Doubs river, which drained the northern Jura mountains and most of the Vosges-Black Forest arch towards the Mediterranean, and *(ii)* the Aare-Danube river system, which drained the southern Jura mountains, the eastern Black Forest, and the Alps towards the east (e.g., Liniger, 1966; Ziegler & Fraefel, 2009). Progressive subsidence of the Bresse Graben caused the separation of the paleo-Aare from

the Danube drainage system and the deflection of the paleo-Aare towards the west at ~4.2 Ma (e.g., Ziegler & Dézes, 2007; Ziegler & Fraefel, 2009). This led to the amalgamation of the paleo-Aare with the proto-Doubs resulting in the Aare-Doubs river system, which transported central-Alpine detritus towards the Mediterranean Sea via the Bresse Graben. According to Giamboni *et al.* (2004) and to Ziegler & Fraefel (2009), the main drainage divide between the North Sea and the Mediterranean Sea was situated in the central part of the southern Rhine Graben, approximately in the Kaiserstuhl area. The Aare-Doubs river deposited the Sundgau gravel at the junction between the northern Jura mountains and the southern Rhine Graben between ~4.2 and 2.9 Ma (e.g., Liniger, 1966, 1967; Petit *et al.*, 1996). Based on their clast composition, the Sundgau gravel may either represent recycled sediments from the Swiss Molasse basin as suggested, e.g., by Schlunegger & Mosar (2011) or they may predominantly be derived from a central-Alpine source, as assumed by Liniger (1966, 1967). Regarding the Alpine hinterland, Schlunegger *et al.* (2007) suggested that during the Pliocene, the main Alpine drainage divide shifted from the core region of the Central Alps, i.e., the Lepontine Dome, towards the north into the Aar-Gotthard massif.

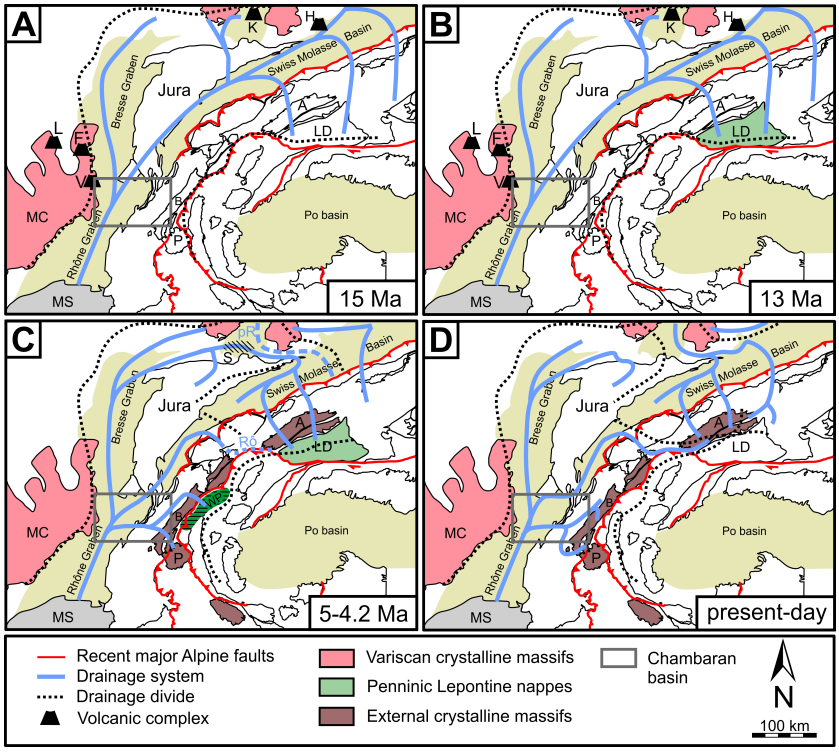

Fig. 2.2: Reconstruction of the Alpine drainage system with changing main water divides (adapted after Kuhlemann *et al.*, 2001; Schmid *et al.*, 2004; Reiter *et al.*, in prep). (a) Main drainage direction was towards the Mediterranean Sea (MS). Potential volcanic source areas for Chambaran basin fill from the Massif Central (MC) and Upper Rhine Graben are shown: F, Forez; H, Hegau; K, Kaiserstuhl; L, Limagne; V, Velay. (b) The crystalline Lepontine nappes (LD) are exhumed in the central-Alpine catchment area. Ongoing volcanic activity in the Massif Central and Hegau area. (c) During deposition of the Sundgau gravel (S, diagonal hachured area) the Isère river presumably drain the west-Alpine External Crystalline Massifs (Belledonne, B, and Pelvoux-Ecrins massif, P). It is speculated that the Rhône river system begins to drain the SW-Aar-Gotthard massif area (Rô, dotted blue line; Reinecker *et al.*, 2008). WP (horizontal hachured area) representing parts of the west-Alpine Penninic units which acted as major sediment supplier for the Chambaran basin as implied by Fügenschuh and Schmid (2003). pR, potential course of the proto-Rhine river as implied by AFT data from Upper Rhine sediments (dotted blue line in the Molasse and Upper Rhine area). (d) Present-day situation where most of the detritus is delivered by the Belledonne and Pelvoux-Ecrins massifs.

Around the Plio-Pleistocene boundary (~2.59 Ma), uplift of the Bresse Graben and coeval subsidence of the southern Rhine Graben led to the deflection of the paleo-Aare to the north into the Rhine Graben and finally to the amalgamation with the proto-Rhine. The drainage divide between the North Sea and the Mediterranean Sea shifted towards the south, now being situated at the southern end of the Rhine Graben and the northern Jura mountains. The Central Alps were drained by the Aare-Rhine river towards the North Sea and by the Rhône river towards the Mediterranean Sea. At about the same time, the drainage system of the Central Alpine hinterland may have changed from orogen-perpendicular to orogen-parallel (Berger *et al.*, 2005). In the Early Pleistocene, first glacial cycles affected the Alpine realm leaving fluvio-glacial deposits behind. One of the earliest preserved fluvio-glacial deposits are the Höhere Deckenschotter of the Swiss Molasse basin, which were delivered by the glacier system of the Central Alps (Bolliger *et al.*, 1996; Graf, 2009). At ~1.7 Ma, ongoing subsidence of the Upper Rhine Graben caused eastwards directed incision of the Aare-Rhine tributaries towards the Danube system (Ziegler & Fraefel, 2009). The separation process of the Alpine Rhine from the Danube system and its deflection towards the Upper Rhine Graben was either largely finished with the Günz glacial at ~0.8 Ma (Villinger, 2003; Litt *et al.*, 2005; Habbe *et al.*, 2007), or at the end of the Rissian glacial at ~0.2 Ma (Ellwanger *et al.*, 2011).

2.4 Climate evolution and glaciations since the Pliocene

The warm Pliocene period became colder toward its end (Ehlers & Gibbard, 2007, and references therein). Minor ice advances occurred in the Northern Hemisphere mainly affecting Canada, Greenland, Eurasia, and NW-Europe. Glaciations significantly increased in these areas after the Plio-Pleistocene boundary (2.59 Ma), with the largest ice extent presumably at ~0.4 Ma during the Pleistocene glacial maximum (Ehlers & Gibbard, 2007). However, glacial cycles did not affect the Alpine realm before the Late Pliocene. A first indication of Alpine glaciation is deposition of the Pleistocene Deckenschotter series in the Alpine foreland (Graf, 2009). This deposition is most likely related to Biber (/Praetiglian) and Günz (/Eburonian) glaciations (e.g., Litt *et al.*, 2005; Habbe *et al.*, 2007). The climax of Pleistocene Alpine glaciation lasted from ~1 to ~0.4 Ma, and was accompanied by accelerated valley incision and enhanced relief formation (Muttoni *et al.*, 2003; Haeuselmann *et al.*, 2007; Glotzbach *et al.*, 2011; Valla *et al.*, 2011, 2012). According to Preusser *et al.* (2011), maximum ice advances of this period reached as far north as the Jura mountains and southern Black Forest. The decline of Alpine glaciation started with the Holsteinian Interglacial at ~0.4 Ma. A final glacial peak occurred during the Last Glacial Maximum around 20 ka ago (Litt *et al.*, 2008, and references therein).

3 Methods and sampling

3.1 Sampling strategy

In terms of lithology, the sampling campaign of this study focused on coarse-grained sand and/or crystalline pebbles, such as granite or gneiss, because these usually contain a sufficient amount of apatites for thermochronological analysis. Sampling sites with a good stratigraphic control were preferred. During this study, samples were taken from fluvial sandy to conglomeratic deposits of the Upper Rhine Graben, Sundgau gravel, Höhere Deckenschotter, and Chambaran basin. Furthermore, sand deposits from the modern Aare, Reuss, and Isère rivers were collected (for more details see section 6.3.1, 7.4.1, & 8.4.1). These deposits span the period between the Middle Miocene and present day, and therefore stored the latest-stage exhumation history of the Western and Central Alps.

3.2 Low-temperature thermochronology

The samples were analysed by apatite fission-track and – if possible – by (U-Th-Sm)/He thermochronology. Fission-track analysis is based on the spontaneous fissioning of ^{238}U causing radiation damage (fission tracks) in the crystal lattice. By contrast, (U-Th-Sm)/He dating is based on the α-decay of ^{238}U, ^{235}U, ^{232}Th and ^{148}Sm, leading to ^{4}He accumulation in the apatite grain. Both, the amount of crystal damages/fission tracks and ^{4}He accumulation is a function of the thermal history experienced by the rock during exhumation. Both dating methods are sensitive to temperature, i.e., fission tracks/^{4}He only start to accumulate in apatite after the rock has passed through a specific temperature range.

3.2.1 Apatite fission-track dating

The AFT method is sensitive to temperatures between ~110 and 60°C (Gleadow & Duddy, 1981). While at temperatures above ~110°C, most of the tracks are fully annealed, tracks are partially annealed in the temperature range between ~110 and 60°C (Partial Annealing Zone, PAZ). Fission tracks are nearly stable at temperatures below 60°C, and accumulate with time. Under the assumption that subsidence and exhumation are usually associated with heating and cooling, apatite fission-track thermochronology is thus sensitive to crustal movements in a depth of ~5 to ~2 km of the upper crust, depending on the geothermal gradient.

Samples were processed using standard separation techniques, such as crushing, sieving, Wilfley table, followed by magnetic and heavy liquid separation methods. Apatite concentrates were mounted in epoxy resin on a glass slide, ground, and polished to reveal inner surfaces. For revealing spontaneous tracks, the mounts were etched in 5 M HNO 3 at 20°C for 20 seconds. After irradiation at the reactor facility Garching FRM II (Germany), micas were etched using 40% HF at 22 ±1°C for 30 minutes to reveal induced tracks. Single grain ages were calculated using Trackkey software of Dunkl (2002). Errors of AFT ages are given at the 1σ confidence level. I tried to analyse at least 60 grains per sample, corresponding to 95% confidence that no fraction ≥0.085 is missed

(Vermeesch, 2004). To identify different grain age populations (peak ages/age groups) indicative of different source areas, binomial peak fitting (program Binomfit by Stewart & Brandon, 2004) was used. The distribution of fission track lengths reflects the residence history of the apatite within the PAZ, and therefore display the thermal history of the source rock. For ensuring reproducible and comparable results, track lengths are only measured if the grain's surface is parallel to the crystallographic c-axis. Length reduction is represented by the mean track length (MTL) and its standard deviation. The exact temperature sensitivity of apatite depends on its chemical composition (Green *et al.*, 1986). It is assumed that the chemical composition is related to the etching velocity. A kinetic parameter for the annealing behaviour of apatites is thus the Dpar value, i.e., the arithmetic mean of etch figures (from fission tracks) which are parallel to the crystallographic c-axis (e.g., Burtner *et al.*, 1994; Donelick *et al.*, 1999). The distribution of track lengths and Dpar values are used to reconstruct the time-temperature paths of studied rock units through thermal modeling.

3.2.2 Apatite (U-Th-Sm)/He dating

The AHe method is sensitive to temperatures between ~85 and 40°C (Wolf *et al.*, 1998) therefore AHe analysis has the potential to reflect crustal processes closer to the surface than the AFT method. The AHe method is based on the accumulation of ^{4}He in the apatite crystals during cooling of the source rock. ^{4}He is produced by α decay of ^{238}U, ^{235}U, ^{232}Th, and ^{148}Sm in the apatite crystal. At temperatures above ~85°C, ^{4}He diffuses out of the grain. Between ~85 and 40°C (Partial Retention Zone / PRZ), ^{4}He is partially retained in the apatite crystal. Below the temperatures of the PRZ, nearly all ^{4}He remains within the apatite crystal, allowing to quantify the time elapsed since the sample has reached shallow crustal levels.

Suitable grains, i.e., apatites without cracks or U-bearing inclusions, were put into Pt tubes. The tubes were cleaned with 37% HCl at 35-40°C for 48 hours in advance, to avoid contamination. ^{4}He was extracted by laser heating and measured with a Balzers quadrupole mass spectrometer using the ^{3}He isotope dilution method. The contents of U, Th, and Sm were detected by mass spectrometry using a second-generation Varian quadrupole ICP-MS. Both analyses were performed at the University of Melbourne (Australia). Most apatites were corrected for ^{4}He loss at grain margins following the alpha correction approach of Farley *et al.* (1996). However, it is not known how much of the He-depleted rim was removed during sediment transport. To avoid potential overcorrection, mechanical grain abrasion (Spiegel *et al.*, 2009) was used instead of alpha correction for appropriate grains with diameters of ≥90 µm. During my laboratory work, I introduced mechanical grain abrasion (Krogh, 1982) in the working group, installed and tested an abrasion cell ready for standard operational application. Test runs with grain abrasion showed that repeated abrasion runs with an air pressure of ~1.5 bar for ~20 seconds efficiently removed the required ~30 µm of the grain´s rim. For hard rocks, the reproducibility of single grain AHe ages provides a measure for the analytical quality. However, since detrital samples can have various sources with different AHe age signatures, this criteria no longer applies. Hence, generally more grains are necessary for a reliable analysis, as compared to hard rock analyses. Potential statistical outliers of an AHe data set can be identified with the program Outlier by István Dunkl (for details see personal download section at URL: http://www.sediment.uni-goettingen.de). Also calculation of a central age as introduced by Vermeesch (2008) can be useful for further interpretation (see section 9.1). Possible factors biasing AHe ages are: *(i)* ^{4}He injection into the crystal from neighboring uranium-bearing minerals or (helium-)saturated fluids (Spiegel *et al.*, 2009), *(ii)* ^{4}He accumulation through radiation damage (e.g., Gautheron *et al.*, 2009), or *(iii)* enhanced ^{4}He diffusion along cracks

within the crystal.

3.2.3 Reconstructing time-temperature paths by thermal history modeling

From the AFT and/or AHe data, cooling paths can be extracted by thermal history modeling. One tool for reconstructing thermal histories is the program HeFTy (Ketcham, 2005). HeFTy offers two ways of thermal modeling, forward and inverse. For both approaches, assumed thermal histories are tested against their fit with the thermochronological data observed. Forward modeling means that a thermal history can be tested by manually proposing a time-temperature path, for which the program calculates the resulting AFT age, length distribution, and/or AHe age, according to a certain annealing and/or diffusion model. After forward modeling, the user is able to compare the thermochronology data predicted by the model to the data observed. For inverse modeling, only constraints such as starting and end temperature are given by the operator. HeFTy then randomly tests a certain number of time-temperature paths, and statistically compares the resulting AFT age, track lengths, and/or AHe data against those actually observed. According to the goodness of fit, the single paths are either rejected, or classified as acceptable or good. In the end, inverse modeling provides envelopes with possible, but not necessarily unique solutions for the thermal history of the investigated sample. For this thesis, forward modeling of AFT and AHe data from sediments of the Chambaran basin was performed. Regarding forward modeling, HeFTy was instructed to use the annealing model after Ketcham *et al.* (2007) and the diffusion model after Farley (2000).

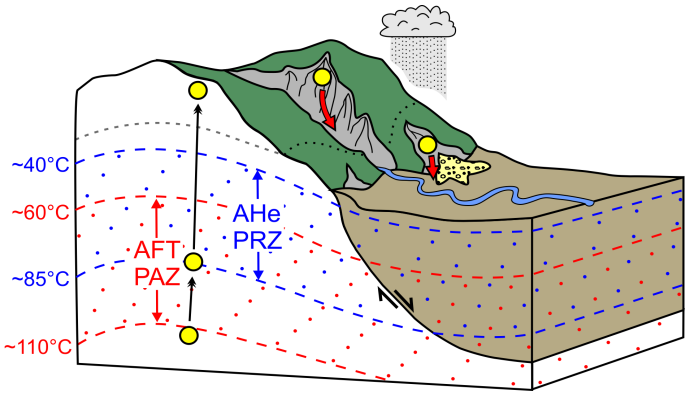

Fig. 3.1: The exhumation of an apatite-bearing rock unit, and its sediment pathways into the foreland basin (modified after Ehlers & Farley, 2003). Isotherms (dashed lines) show the AFT Partial Annealing Zone and the AHe Partial Retention Zone with associated temperature ranges. Yellow circles display the cooling path of an apatite grain toward the surface as well as the erosion and transport of material into the adjacent foreland basin.

3.3 Detrital thermochronology

Detrital thermochronology is used to identify the potential source areas by analysing foreland sediments, and to reconstruct the paleo-exhumation history of the hinterland (Fig 3.1). Preconditions for the applicability of this approach are: *(i)* no reheating to temperatures above the thermal sensitivity of the used thermochronometer has occurred after deposition; *(ii)* a reliable stratigraphic allocation of the sampled sediment layers; and *(iii)* potential source areas should differ significantly regarding their cooling age patterns. It is important to keep in mind that detrital

thermochronology on apatites can only record the denudation and exhumation history of apatite bearing lithologies (e.g., Attal & Lavé, 2009). For AHe analysis, individual grain abrasion during sediment transport towards the depocenters can additionally influence single grain ages (e.g., Nesbitt & Young, 1996). The influence of grain abrasion and mineral coating is reducible to a minimum through mechanical grain abrasion of well-suited grains (diameter ≥90 μm).

Usually AFT data sets are used for thermal reconstructions of present-day hard rock exposures. As mentioned above, inversion of AFT data requires analysing the fission track lengths distribution. However, measuring track lengths in detrital samples is somewhat a Sisyphean challenge as most samples contain more than one source area, and length distributions are only useful if they can be attributed to a certain AFT age group. The most reliable way extracting data from apatites is AFT/AHe double dating, i.e., using the same apatite grain for AFT and AHe analyses. Since this approach requires large and pristine apatites, its application in detrital studies is strongly limited. As described in section 3.2.1, the usual necessary precondition for a reliable identification of major source areas within a detrital study is to analyse at least 60 grains per sample (Vermeesch, 2004). However, a different way to tackle this challenge was recently described by Avdeev *et al.* (2011) who introduced a new method for inverse modeling detrital AHe data sets based on a Bayesian estimation approach. One main conclusion of this study was that also with a relatively low number of AHe ages (≤20) thermal modeling yield reliable thermal reconstructions. Alternatively, as described in section 9, the combination of well-known techniques to identify statistical outliers of a AHe data set, calculation of central AHe ages (up to 8), and forward modeling of a combined detrital AHe/AFT data set can be also successfully used to significantly refine provenance analysis which is solely based on AFT data.

3.3.1 Provenance analysis and reconstructing paleo-exhumation histories

The provenance of a clastic sediment is identified by comparing lag time values of the sediment with the thermal signature of potential source areas. The lag time is defined as the difference between the cooling age of a detrital mineral and its stratigraphic age, and covers the time of exhumation from closure depth to the surface, sediment transport and deposition, with the two latter processes being negligible compared to the time needed for exhumation (Garver *et al.*, 1999). The thermal signature of a source area can consist of a relatively wide range of cooling ages, e.g. as observable in Molasse deposits, which experienced a variable degree of thermal overprint post-deposition. Therefore, probability-density plots reflecting interpolated surface AFT age distribution of potential source areas are used for provenance analysis (see also section 5 & 6).

Lag time is additionally used for inferring paleo-cooling and paleo-exhumation rates of potential source areas. The comparison of lag times across a stratigraphic section (e.g., a drill core) provides information on changes in paleo-exhumation rates: decreasing lag times upsection toward stratigraphically younger deposits generally indicate accelerated denudation of the source area, whereas increasing lag times upsection indicate slower denudation, and constant lag times are indicative for an exhumational equilibrium of the source area. Additionally, a lag time can be converted into a long-term exhumation rate $\dot{\varepsilon}_m$ as introduced by Garver *et al.* (1999):

$$\dot{\varepsilon}_m = [(T_c - T_s) / G] / \Delta t$$

where T_c, closure temperature; T_s, average temperature of the surface (assumed to be 10°C for the Alps); G, paleo-geothermal gradient (assumed for this study: 25 ±5°C km^{-1}); and Δt, lag time.

4 Interpretation and discussion

For detailed results of this study, I refer to section 6.5, 7.6, and 8.5. For the Chambaran data, the youngest associated AFT/AHe age pair of a time slice is abbreviated to facilitate the interpretation of the lag time plot (Fig. 4.1), e.g., youngest AFT/AHe pair at 15 Ma depositional age is equal to sample pair 15-1, second youngest age pair at 15 Ma is 15-2 and so forth. Outlier and "age groups" consisting of only one single AHe age are excluded from interpretation.

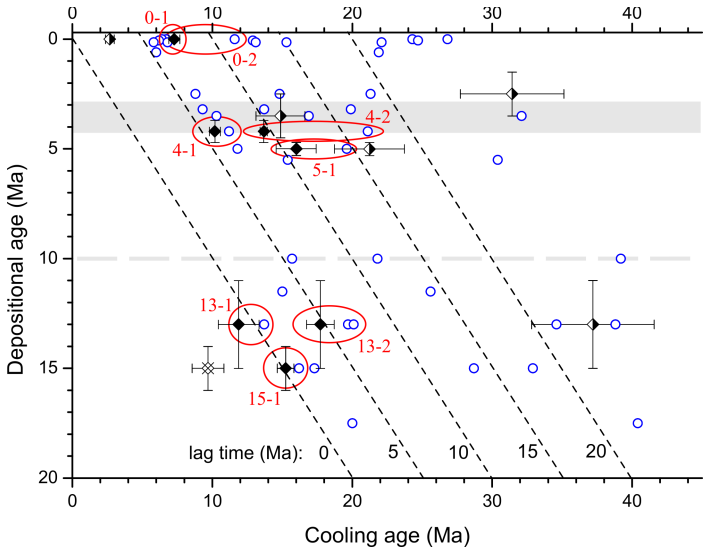

Fig. 4.1: AHe data and AFT peak ages plotted against depositional ages with lines of equal lag times (broken lines). Dotted, horizontal line represents timing of drainage reorganisation at ~10 Ma. Grey-highlighted area indicates deposition time of the Sundgau gravel (~4.2-2.9 Ma). White-filled (crossed) diamonds represents the statistical outlier. Half-white/half-black-filled diamonds represent single AHe ages. Black diamonds represent central AHe ages. Blue circles represent AFT age groups from Glotzbach *et al.* (2011); for reason of clarity AFT errors are not shown. Red ellipses represent AHe/AFT pairs used for modeling cooling histories of major source areas.

4.1 Provenance of circum-Alpine deposits

Deposition from 15 until 13 Ma

Glotzbach *et al.* (2011) suggested from their AFT data set that the main sediment contributor to the Chambaran basin were the Penninic units of the Lepontine area. This interpretation is based on the very short lag times of sediments with 15 and 13 Ma deposition age (Fig. 4.1), and on the fact that the Lepontine area experienced rapid exhumation at that time (e.g., Schlunegger & Willet, 1999). Spiegel *et al.* (2000), however, showed that first large exposures of Penninic units were not recorded in the Swiss Molasse sediments before ~14 Ma. Hence, the provenance of the Chambaran sediments has to be reconsidered, particularly for the oldest, 15 Ma sample. The zero lag times (within error) of sample pairs 15-1 & 13-1 can be alternatively explained by *(i)* thermal resetting of the AHe(/AFT) system or *(ii)* substantial input of volcanic material into the basin. Regarding *(i)*,

thermal resetting seems unlikely as the sampled Miocene sediments are lacking severe compaction, and maximum burial temperatures are estimated at ~25°C (vitrinite reflectance: 0.21, Moss, 1992; temperature calculation after Barker & Pawlewicz, 1986). Also, sampled sediments showed no signs of hydrothermal activity, as reported from the present-day Rhône Graben (Garibaldi *et al.*, 2010). Regarding *(ii)*, the explanation of volcanic input is supported by the occurrence of plastic clay layers (benthonite?) in Burdigalian sediments of the Chambaran basin (BRGM borehole St. Lattier-2), and the morphology of analysed apatite grains (length up to 300 µm, flat, angular to subangular) which may indicate volcanic origin and short sediment transport. Potential source areas are volcanic complexes located in the Massif Central and/or Upper Rhine Graben (Fig. 2.2a), which were active at that time. Thus, the youngest age groups contained in the two middle Miocene samples are interpreted as being sourced from synsedimentary volcanism. However, the 13 Ma sample also contains an older age group (13-2), which was likely derived from the Lepontine area. This interpretation is based on *(i)* the AFT lag time of ~7 Ma which coincides with the thermal signature of modern Lepontine exposures (Vernon *et al.*, 2008, and references therein; Elfert *et al.*, 2011), and *(ii)* the calculated cooling rate of ~12°C Ma^{-1} which agrees with thermal reconstructions of the Lepontine area (Hurford *et al.*, 1986; Pignalosa *et al.*, 2011).

Deposition from 5 until 2.59 Ma

For this time slice, I sampled sedimentary deposits of the Sundgau gravel, Chambaran basin, and Upper Rhine Graben, all three of a similar depositional age of 4 ±1 Ma. Regarding the Sundgau gravel, the analysis of whitish granitic pebbles yielded single AFT and AHe age groups of ~10 Ma, suggesting that the pebbles were all derived from the same source. With the resulting AFT lag times from 7 to 6 Ma (Fig. 4.2), the most likely source is the Aar-Gotthard massif, where similar AFT and AHe ages and lithologies frequently occur in the present-day exposures. A sand sample of the Sundgau gravel also contains a ~10 Ma AFT age group, but additionally an older age group of ~15 Ma (11-12 Ma lag time). The single apatite grain dated by AHe analysis from this sample yielded an age of ~13 Ma and thus seems to belong to this older age group. Schlunegger & Mosar (2011) suggested that the Sundgau gravel contain reworked material from the Swiss Molasse Basin. However, the AFT signature, even of the older age group, is slightly too young to be derived from the Molasse basin. Furthermore, the heavy mineral composition of the Sundgau deposits also argues against a major contribution from the Swiss Molasse basin (Liniger, 1966, 1967). Instead, because of the slightly older AFT ages of the present-day exposures (compared to the Aar-Gotthard massif), and in accordance with the interpretation of AFT ages from the Rhine Graben sediments (see text below), the older age group is assigned to the erosion of the Lepontine area, although this assumption may be speculative.

Until ~2.9 Ma, the Central Alps were drained via the Sundgau gravel and the west-Alpine foreland toward the Mediterranean Sea. Thus, the ~6 Ma lag time of sample pair 4-1 from the Chambaran basin may indicate a provenance from the central-Alpine Aar-Gotthard massif. This would be in line with the provenance of the Sundgau samples, and thus with the postulated drainage pattern at that time. In addition, the modeled constant exhumation rate of ~0.5 km Ma^{-1} for sample pair 4-1 is in agreement with the exhumation history of the Aar-Gotthard massif as reported by Glotzbach *et al.* (2010). Based on these observations, I favour the interpretation that the Aar-Gotthard massif is a major source area for the Pliocene Chambaran deposits. Furthermore, sample pairs 5-1 and 4-2 yield similar lag times of ~15 and 17 Ma. These lag times suggest a provenance from the middle Penninic domain (Houillère zone) in the Western Alps, which shows comparable age signatures and cooling rates for their present-day exposures (Fügenschuh & Schmid, 2003; Vernon *et al.*, 2008).

With a lag time of ~15 Ma, AFT ages of Pliocene strata of the Upper Rhine Graben are too young to be derived from Variscan graben shoulders and too old to be derived from the basement of the Aar-Gotthard massif. However, along the northern margin of the Alps, i.e., in the Subalpine Molasse and/or western Rhenodanubian Flysch units (Fig. 2.1, see also section 6.6; Trautwein *et al.*, 2001; Cederbom *et al.*, 2004; Vernon *et al.*, 2008), similar AFT ages occur. Thus, unlike previous assumptions (e.g., Ziegler & Fraefel, 2009), the Pliocene Rhine river received detritus from the Alps, although this seems to be derived from the north-Alpine margin, not from the Alpine core.

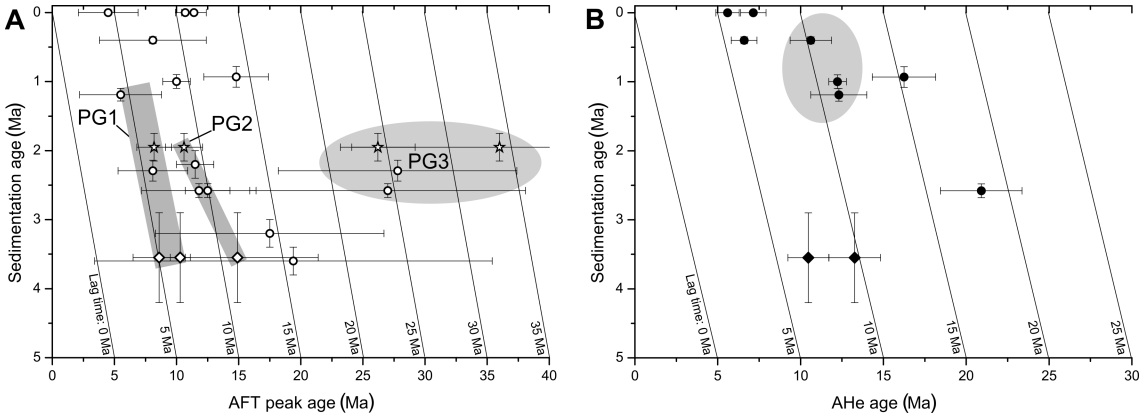

Fig. 4.2: (a) AFT age groups plotted against deposition ages with lines of equal lag times. Circles represent data from the Rhine Graben and modern Rhine tributaries (without data of Variscan sources), diamonds represent ages derived from the Sundgau samples, and stars represent ages of the Höhere Deckenschotter samples. Grey highlighted areas: PG1 most likely reflect erosion of the Aar-Gotthard massif, PG2 reflects erosion of a source area south of PG1 (presumably Lepontine Dome or southernmost external massifs), and PG3 is either derived from an east Alpine source or from erosion of the Swiss Molasse basin. (b) AHe ages plotted against deposition ages. The black-filled circles represent AHe ages of Rhine Graben samples and from modern Rhine tributaries, and black-filled diamonds represent AHe ages yielded by Sundgau samples. The grey highlighted area contains AHe ages associated with erosion of Hegau volcanics.

Deposition from 2.59 until 1.2 Ma

After the Plio-Pleistocene boundary, AFT age groups with 6 to 9 Myr lag times occur in the Upper Rhine Graben, coeval with a change in the heavy mineral composition from stable minerals to garnet-epidote dominance (for details see section 6.4.2). The young AFT ages are most likely derived from the Central Alpine core region (i.e., Aar-Gotthard massif and Lepontine Dome). Thus, after ~2.6 Ma, the north-Alpine drainage system experienced a significant change, with the catchment of the paleo-Rhine river now reaching the Alpine core region. Temporally, this change approximately coincides with a change of the Alpine stress field (Sue *et al.*, 2007), and possibly with the change from an orogen-perpendicular to an orogen-parallel drainage network (Reinecker & Kuhlemann, 2008). A causal relationship to the observed change of the paleo-Rhine catchment, however, remains speculative. Rhine Graben sediments of this time slice contain two relatively similar age groups which can nevertheless be statistically distinguished from each other; a young age group with ~5 Ma lag time (~2.3 to 1.2 Ma depositional age) and a slightly older age group with ~9 Ma lag time (~2.6 to 2.2 Ma depositional age; Fig. 4.2a). The sand samples of the Höhere Deckenschotter also show the same distinction between lag times of a youngest (~6 Ma) and a second youngest (~9 Ma) age group. I tentatively assign the younger AFT age groups to the Aar-Gotthard massif and older AFT age groups to the Lepontine Dome, in agreement with slightly older

ages observed in present exposures of the Lepontine Dome. If true, this would mean that parts of the Lepontine Dome were drained northward until at least 2.2 Ma, in agreement with the suggestion of Schlunegger *et al.* (2007). The oldest Pleistocene Rhine Graben deposits also contain AFT age groups of ~30 Ma. Similar AFT ages were reported from the Swiss Molasse Basin (Cederbom *et al.*, 2011). This indicates that, after changing its course, the paleo-Rhine incised into the Swiss Molasse Basin.

The sand samples from the Höhere Deckenschotter also contain an older AFT age group (~26 and 36 Ma). These two older AFT age groups are too old to be derived from the Central Alps. Similar AFT ages also occur in the early Pleistocene sediments of the Upper Rhine Graben (PG3 in Fig. 4.2a). They may either represent erosion of the Rhenodanubian Flysch and/or Silvretta nappe of the Eastern Alps, or they reflect reworking of molasse sediments. The first interpretation is preferred, because particularly the ~36 Ma age group is a bit too old to be derived from the Swiss Molasse Basin, and because the PG3 age group does not display a "recycling trend" (i.e., increasing AFT ages upsection, assuming that the PG3 ages from the Rhine Graben and from the Höhere Deckenschotter were derived from the same source).

Deposition after 1.2 Ma

At 1.2 Ma, only one age group yielding a lag time of ~5 Ma is still present in the samples from the Upper Rhine Graben. If the assumption that the ~9 Ma lag times were derived from the Lepontine Dome is correct, then the disappearance of detritus from the Lepontine Dome would indicate a shift of the main drainage divide to the north, in a similar position as today. This would agree with the drainage pattern described by Schlunegger *et al.* (2007). Between 1.2 and 0.9 Ma, the increasing AFT ages upsection (Fig. 4.2) are contrary to what is expected for incision into crystalline basement but typical for sediment recycling. Below I discuss this topic in relation with hinterland exhumation. Interestingly, euhedral and elongated apatites occur in the Rhine Graben samples between ~1.2 and 0.4 Ma depositional age. They yield an AHe age of ~12 Ma, show large Dpar values, and high amount of lattice defects, similar to what is described for the Hegau volcanics (Rahn & Selbekk, 2007; Meinert Rahn, pers. comm.). Thus, after 1.2 Ma the paleo-Rhine drained the Hegau area (Fig. 2.1), which indicates that the Rhine River followed essentially the same course as it does today.

Present day situation

The sample pairs 0-1 and 0-2 of the present-day Chambaran samples show predominantly AHe ages of ~7 Ma and AFT ages of ~12 Ma (Glotzbach *et al.*, 2011), comparable to what is reported from the Pelvoux and Belledonne massifs (Vernon *et al.*, 2008; van der Beek *et al.*, 2010). Additionally, modeled cooling histories of 0-1 and 0-2 revealed constant exhumation rates since the Late Miocene (~7 Ma) consistent with thermal reconstructions from modern rock exposures of the Belledonne and Pelvoux massifs (Lelarge, 1993; van der Beek *et al.,* 2010).

The present-day sediments of the Aare and Reuss rivers at the foot of the Aar-Gotthard massif contain predominantly AFT ages of ~11 Ma and AHe ages of ~5 Ma. The AFT ages are in apparent contrast to the age pattern of the source area (Aar-Gotthard massif), where similar old ages are only observed on the top of the mountains, while the valleys display younger AFT ages around 5 to 7 Ma (Reinecker *et al.*, 2008; Glotzbach *et al.*, 2010). This may indicate that the majority of detritus is derived from the mountain tops and thus transported to the rivers by mass wasting processes such as landsliding (Larsen & Montgomery, 2012). This interpretation is in agreement with the pronounced relief and the oversteepened valleys of the source areas. An additional trend observed in the data set is a change toward slightly increasing of apatite Dpar values of the Sundgau gravel (deposition 4.2 – 2.9 Ma), the Höhere Deckenschotter (deposition 2.1 – 1.8 Ma), and the

modern Aare and Reuss river sediments (see section 6.5 for further details). For all three areas, the Aar-Gotthard massif is assumed as the main sediment source. While a large part of the apatites from the Sundgau gravel shows Dpar values <1.5 µm, the majority of apatites from the Höhere Deckenschotter has Dpar values between 1.5 and 2 µm. Apatites with Dpar values >2 µm mainly occur in the modern river sands. Thus, erosion of the Aar-Gotthard massif seems to have gradually exposed rocks containing apatite with increasingly higher Dpar values. Dpar is a proxy for the chemical composition of apatite. Systematic relations between Dpar value and source rock geochemistry have not been studied so far, and to my knowledge, no similar Dpar-trend was described in provenance analysis before. The shift in Dpar values may reflect the geochemical evolution and/or differentiation of the (meta-)magmatic source rocks exposed in the Aar-Gotthard massif, although of course further investigations are required here.

4.2 Evolution of the north-Alpine drainage system since the Miocene

Based on the provenance analysis and the implications of the lag time plot, I propose the following evolution of the northwest-Alpine drainage system since the middle Pliocene:

Drainage system between 15 and 13 Ma

The northwestern Alps were drained toward the Mediterranean Sea during the Middle Miocene (Kuhlemann *et al.*, 2001). Between 15 and 13 Ma, this drainage system transported volcanic material from active volcanic complexes of the western Massif Central and/or Upper Rhine Graben via the Chambaran area toward the Mediterranean Sea. At ~13 Ma, the sediments also contained detritus from the Lepontine area (Fig. 2.2).

Drainage system between 5 and 2.9 Ma

The drainage pattern of this period was more complex than previously thought. The west-Alpine middle Penninic units (Houillère zone; Fig. 2.2c) were drained towards the Chambaran basin by a paleo-Isère. Furthermore, the Sundgau gravel were part of the Aare-Doubs system, transporting Alpine debris to the west into the Bresse Graben (in agreement with previous studies, e.g., Liniger, 1966, 1967; Giamboni *et al.*, 2004). The Aare-Doubs system originated in the Aar-Gotthard massif and probably the northern Lepontine Dome, thus the main Alpine drainage divide was presumably located south of the Aar-Gotthard massif. This is in good agreement with Schlunegger *et al.* (2007), who suggested that the drainage divide was situated in the Lepontine Dome area during or prior to the Pliocene. The age signature of the Rhine Graben sediments differs from the age signature of the contemporaneously deposited Sundgau gravel. This implies that the proto-Rhine and the Aare-Doubs rivers were not connected with each other. The proto-Rhine most likely received detritus from the southern Molasse basin or northern Central Alps, and thus the proto-Rhine headwaters reached further south than previously assumed (e.g., Ziegler & Fraefel, 2009). Accordingly, the drainage divide between the North Sea and the Mediterranean Sea was not situated in the Kaiserstuhl area, as previously suggested, and the Alpine realm was at least partly drained towards the North Sea. The two river systems, the Aare-Doubs and the proto-Rhine were flowing more or less parallel to each other while passing the northern Jura mountains. After leaving behind the passage between the northern Jura and the Black Forest, the proto-Rhine headed northwards into the Rhine Graben and eventually toward the North Sea (Fig. 4.3a).

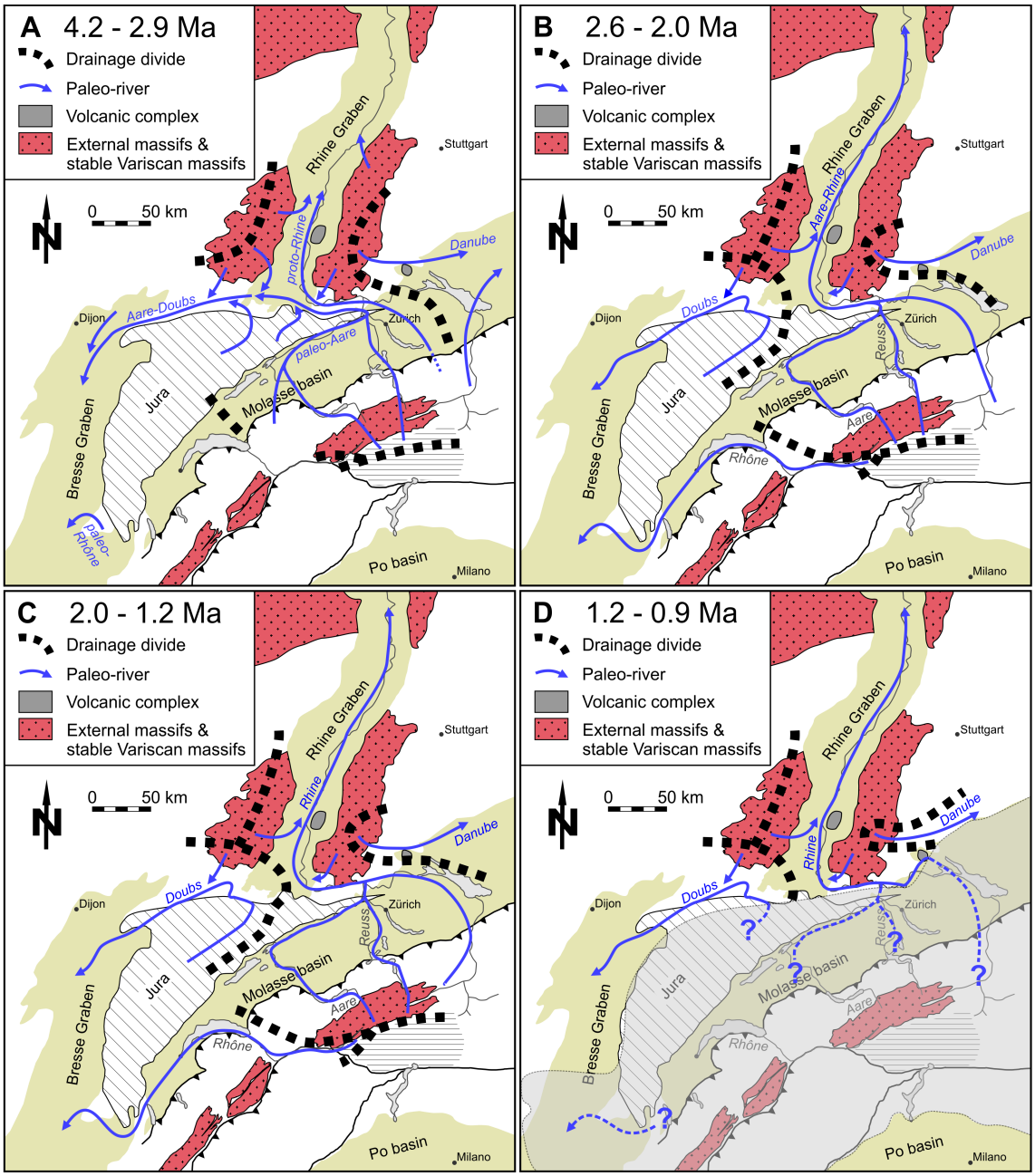

Fig. 4.3: Changes in the northwestern Alpine drainage system (modified from Giamboni et al., 2004; Berger et al., 2005; Ziegler & Fraefel, 2009). (a) During deposition of the Sundgau gravel, the Aare-Doubs and the proto-Rhine were flowing parallel to each other towards the northwest. After passing the passage between the Jura mountains and the Black Forest, the Aare-Doubs headed southwestwards to the Mediterranean Sea and the proto-Rhine northwards in the Upper Rhine Graben. The central-Alpine main water divide was most likely located in the northern Lepontine Dome. (b) The Aare-Rhine river drained the Central Alps and a more easterly located source area. (c) The Rhine river drained the Central Alps with a northward moving main Alpine water divide. (d) Prior and during the most intense glaciation of the Alps (grey-highlighted area reflects the assumed glacial extent and was adapted from Preusser et al., 2010, 2011). The Alpine source areas were most likely sealed due to the glaciation, and the Rhine catchment now additionally includes the Hegau volcanic complex.

Drainage system between ~2.6 and 2.0 Ma

After the Plio-Pleistocene boundary, the AFT age signature of the Rhine Graben deposits has changed significantly, indicating that the Aare-Rhine river now received debris from the external massifs of the Central Alps and presumably from an Eastern Alpine source (Fig. 4.3b). This corroborates previous reconstructions describing a deflection of the Aare river towards the north into the Rhine Graben (e.g., Petit *et al.*, 1996). The Höhere Deckenschotter and the – slightly older – Rhine Graben sediments show similar age signatures, implying that *(i)* they belonged to the same river system, and *(ii)* that the drainage network was unchanged by first glaciation of the Alpine foreland, that resulted in the deposition of the Höhere Deckenschotter. The main Alpine drainage divide was still situated either in the southernmost Aar massif or in the Lepontine Dome (source area of the PG2 age group, Fig. 4.3a). This southern rim of the Aare-Rhine catchment shows constantly increasing exhumation. In accordance with previous studies, the drainage change between 2.9 and 2.6 Ma is explained with tectonic reasons, namely the uplift of the Bresse Graben and the subsidence of the southern Rhine Graben (e.g., Dèzes *et al.*, 2004), probably related to the change from thin-skinned to thick-skinned deformation in the Jura fold belt (Ustaszewski & Schmid, 2007; Ziegler & Fraefel, 2009).

Drainage system between ~2.0 and 1.2 Ma

After 2.0 Ma, the age signature of the Rhine Graben sediments changed again, with the PG2 and PG3 age groups disappearing and only the PG1 age group still present. This implies another change of the drainage system, associated with a northward shift of the main Alpine drainage divide (Fig. 4.3c). Different tectonic changes, which may explain the changes of the drainage system, were suggested to have taken place during or since the Pliocene. The detailed timing of the latest stage Alpine evolution, however, is poorly constrained, thus making a temporal correlation with the drainage evolution difficult. Based on the literature data and my own thermochronological data, the following scenario is proposed: Since ~3.5 Ma (Reinecker *et al.*, 2008), the central-Alpine core region was affected by orogen-perpendicular extension caused by a decrease or cessation of convergence (Sue *et al.,* 2007). Extension led to normal faulting along the Rhône valley, resulting in accelerated exhumation of the southwestern Aar massif (as reflected in the lag time trend of the PG2 age group), and finally southward migration of the Rhône river down the normal fault and the change towards an orogen-parallel drainage system (Reinecker *et al.*, 2008; Reinecker & Kuhlemann, 2008). Extension normally causes decreasing topography, thus a reduced topography in the area of the southwestern Aar massif may have triggered the shift of the main Alpine drainage divide towards the north (cf. Schlunegger *et al.*, 2007). After this shift, the southwestern Aar massif and the Lepontine Dome were drained towards the west and south, reflected by the disappearence of the PG2 age group in the basin deposits. If this scenario is true, then the establishment of an orogen-parallel river network and the associated northward shift of the main drainage divide can be dated as having occurred between 2.0 and 1.2 Ma, and was the result of a change in the Alpine stress field, as described by Sue *et al.* (2007).

Drainage system between ~1.2 and 0.9 Ma

According to Muttoni *et al.* (2003), Litt *et al.* (2005), Haeuselmann *et al.* (2007), Valla *et al.* (2011, 2012), most intense Alpine glaciation was reached at ~1.0 Ma. I therefore adopted the maximum ice extent as reconstructed by Preusser *et al.* (2010, 2011) for that time slice (Fig. 4.3d). The age signature of the Rhine Graben sediments again strongly changed, now indicating sediment recycling instead of crustal incision. Glaciation seems to have effectively sealed the Alpine landscape, thus causing strong reduction of the catchment size of the Rhine river, a shift of the sediment source area towards the north into the north-Alpine foreland, and a cut-off of the

connection between the Alps and the Rhine Graben/North Sea. Also at that time, debris from the Hegau volcanics started to occur in the Rhine Graben deposits, indicating that the course of the Rhine river across the north-Alpine foreland was now essentially the same as it is today, i.e., crossing the area of the Hegau volcanics.

Drainage system between 0.4 Ma to recent

After the end of main glaciation, the connection of the Rhine river with the Alpine source areas was re-established. Erosion of the Hegau volcanics went on. During this period the modern drainage system has been fully established.

4.3 Late Cenozoic paleo-exhumation history of the Central and Western Alps

Here I extract the paleo-exhumation history of the sediment source areas from detrital ages of north- and west-Alpine depocenters from the Middle Miocene to the present day. From the Plio-Pleistocene boundary on, climatic information stored in the Upper Rhine Graben basin fill is available and will be linked to paleo-exhumation trends. Generally, a trend of decreasing AFT lag times associated with erosion of the Variscan basement is observed for the Rhine Graben sedimentary section. Although age uncertainties are rather high, such a trend is in agreement with continuous and increasing incision into basement rocks and may indicate relief rejuvenation of the Black Forest and Vosges during Plio-Pleistocene glaciations. The following discussion, however, focuses on the younger age groups thought to be of Alpine origin. Fig. 4.4 shows the relation between the youngest AFT age groups and Plio-Pleistocene glacial-interglacial cycles.

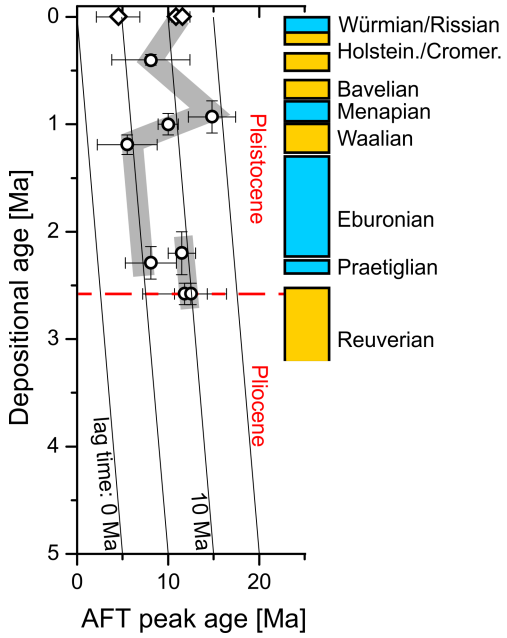

Fig. 4.4: AFT lag times for assumed Alpine source areas correlated with glacial cycles. Major trends of AFT peak ages from samples VH/P34 and Aare/Reuss are highlighted in grey.

Aar-Gotthard massif

The AFT lag times of ~6 Ma, extracted from the sediment deposits of the Upper Rhine Graben, Sundgau gravel, and Höhere Deckenschotter point to constant exhumation of the Aar-Gotthard massif between 4.2 and 1.2 Ma (PG1 in Fig. 4.2). The calculated paleo-exhumation rate of 0.7 ±0.2 km Ma^{-1} is also in good agreement with modeled exhumation rates of modern hard rock exposures from this area (Reinecker *et al.*, 2008; Glotzbach *et al.*, 2010). Between ~2.6 and 1.2 Ma, the Alps experienced their first major glaciation cycles, the Biber (/Praetiglian) and Günz (/Eburonian) glaciations (Fig. 4.4). The constant AFT lag times, however, show that this shift to a glacial erosion regime was not sufficient to disturb the long-term exhumational equilibrium of the Aar-Gotthard massif, at least within the sensitivity of the AFT system. From ~1.2 to ~0.9 Ma, a trend to strongly increasing AFT peak ages and lag times is observed, temporally coeval with the main glaciation period of the Alps (~Haslach-Mindel/Menapian). This seems contradictory, because enhanced valley incision and relief formation, interpreted as the erosional response to main Alpine glaciation, is assumed around ~1 Ma. Accordingly, a glacially induced increase of erosion rates was expected, opposite to the trend observed. The upsection trend of increasing AFT ages is typical for recycling of (unreset) sediment (e.g., Spiegel *et al.*, 2000), and may be explained by three scenarios:

(i) the previous glacial cycles may have deposited glacial till that shields underlying bedrock from further incision. The age trend would then reflect removal of this glacial sediment (see Koppes & Montgomery, 2009); *(ii)* glaciers covering the Central Alps were frozen to their beds thus impeding significant subglacial erosion (see Miller *et al.*, 2006). As a result, the locus of headwater erosion would shift to the north causing erosion and recycling of (subalpine) Molasse sediment; and *(iii)* following the reconstruction of Preusser *et al.* (2011) for the maximum ice extent, Alpine glaciers may have reached the southern border of the Black Forest. Again assuming that main erosion took place in front of the glaciers, the age trend may reflect reworking of sediment deposited in the southern Upper Rhine Graben. For the first and third scenario, reworked sediment would be recently deposited and the original source areas were presumably also situated in the Central Alps. Thus, I would expect younger AFT ages than those observed (Fig. 4.2). Accordingly, scenario two is considered as the most likely, but a combined effect of all three scenarios is not excluded. Between ~0.9 and ~0.4 Ma, both, AFT peak ages and lag times decrease once again, indicating an increase in denudation of the Aar-Gotthard massif. The increase occurs after the most extensive Alpine glaciation (Muttoni *et al.*, 2003; Ehlers & Gibbard, 2007; Preusser *et al.*, 2011). Enhanced hinterland denudation is interpreted as a delayed response to intense glaciation, resulting from warmer basal temperatures and thus enhanced erosive force of the retreating glaciers, similar to what is described for Patagonia and Greenland (Rignot *et al.*, 2003; Howat *et al.*, 2005; Koppes & Montgomery, 2009). Furthermore, exhumation likely accelerates due to isostatic adjustments of the Alps after glacial retreat. Present-day sediments from the Aar-Gotthard massif draining Reuss and Aare rivers predominantly contain AFT ages around ~11 Ma. Similar ages mainly occur on mountain tops of the Aar-Gotthard massif, whereas in the valleys, rocks with AFT ages around ~5 Ma are exposed. Similar young 5 Ma ages also occur in Reuss sediments, but their contribution is minor compared to the older 11 Ma AFT age group. Thus, while glacial erosion obviously causes valley incision, the present interglacial period is related to erosion of more elevated areas. The most effective process for removing material from mountain tops and transporting it to the valleys/rivers is landsliding. Landsliding is known to become more frequent at the transition between glacial and interglacial periods (e.g., Ivy-Ochs *et al.*, 2009), and also during recent warming of the last decades, and may thus explain the AFT signal observed in recent sediments of central-Alpine origin. The modern exhumation rate of the Aar-Gotthard massif has slowed down to 0.4 ±0.2 km Ma^{-1} compared to the rates between 4.2 and 1.2 Ma.

Lepontine Dome

First evidence of Lepontine-derived detritus in the Chambaran basin is observed in middle Miocene sediments with ~13 Ma deposition age (sample pair 13-2). Thermal modeling of 13-2 yielded constant cooling at a rate of ~12°C Ma^{-1} (may be comparable to an exhumation rate of about 0.5 km Ma^{-1}; Fig. 4.5, Table 4.1) between ~22 and 13 Ma which coincides with thermal reconstructions from present-day exposures of the Lepontine area (Hurford *et al.*, 1986; Pignalosa *et al.*, 2011). Between ~4.2 and ~1.8 Ma, the decreasing AFT lag times of the sampled Sundgau gravel, Upper Rhine Graben, and Höhere Deckenschotter reflect slightly increasing exhumation rates of the Lepontine area from 0.4 ±0.1 to 0.5 ±0.1 km Ma^{-1}.

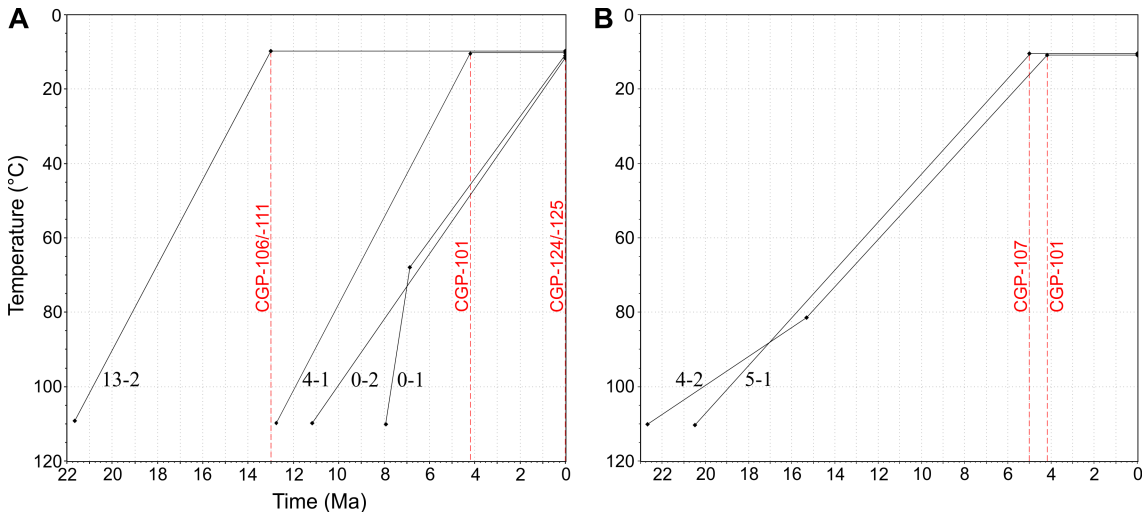

Fig. 4.5: (a) Modeled time-temperature paths of the AHe/AFT pairs 13-2, 4-1, 0-1, and 0-2 used for refinement of provenance analysis and testing the hypothesis of steady-state exhumation for the Western Alps. (b) Modeled thermal histories for AHe/AFT pairs 5-1 and 4-2.

AHe/AFT pair	Depositional age (Ma)	Cooling rate (°C Ma^{-1})	Exhumation rate (km Ma^{-1})
0-1	recent	40 → 9	1.6 → 0.4
0-2	recent	9	0.4
4-1	4.2 ±0.5	12	0.5
4-2	4.2 ±0.5	3 → 7	0.1 → 0.3
5-1	5.0 ±0.3	7	0.3
13-2	13 ±2	12	0.5

Table 4.1: Calculated cooling and exhumation rates. Cooling rates are extracted from modeled cooling paths. For calculating exhumation rates, a geothermal gradient of 25°C km^{-1} was assumed. Modeling of 0-1 and 4-2 yielded changing cooling rates through time.

Middle Penninic Houillère zone

The west-Alpine Middle Penninic Houillère zone shed detritus to the Chambaran basin during the Pliocene (sample pairs 5-1 and 4-2). Thermal modeling of sample pair 5-1 shows that the Houillère zone must have experienced constant cooling at a rate of ~7°C Ma^{-1} since the Early Miocene (Table 4.1). This observation is in good agreement with the thermal reconstruction from the northern part of this area (Fügenschuh & Schmid, 2003). Thermal modeling revealed that sample pair 4-2 shows a slower cooling rate in comparison to sample pair 5-1 until ~15 Ma, but after after ~15 Ma both cooling rates harmonize to ~7°C Ma^{-1} (Fig. 4.5). A similar cooling history is described for the southern Houillère area, where tilting of this area is assumed to have started at ~17 Ma (Fügenschuh & Schmid, 2003). Both cooling paths show constant cooling of the whole Houillère area from ~15 Ma until at least ~4 Ma.

Belledonne and Pelvoux massifs

The Belledonne and Pelvoux massifs underwent constant exhumation since ~7 Ma, as reflected by the modeled cooling paths of samples from recent river sands of the Chambaran basin (sample pairs 0-1 and 0-2). Sample pair 0-1 yielded a strongly increased exhumation rate of ~40°C Ma^{-1} prior ~7 Ma, which has not been reported previously for these two massifs. As the modern Isère river drains both massifs, the Belledonne and the Pelvoux, a further allocation of this thermal history (0-1) to a specific massif is not possible.

4.4 Limits and potential refinements of detrital thermochronology

For hard rock samples, one of the great advantages of using AFT thermochronology is that this technique not only provides cooling ages but also, through length measurements and thermal history modeling, thermal evolutions covering the temperature range between ~110 and 60°C. As described previously, length measurements are not routinely applied for detrital samples as these contain several age groups and thus, for assigning track length values to certain age groups, only length measurements on grains that were also dated, can be used. Particularly for young age groups, it is thus nearly impossible to measure statistically meaningful numbers of track lengths for these age groups.

Combining AFT with AHe data would provide better constraints for the thermal history of the source area, but again, particularly for detrital samples, where apatite grains were transported over larger distances, it is close to impossible to extract the high number of pristine grains required for reliable AHe dates. Accordingly, for detrital samples, usually no thermal history modeling is used and instead, thermal histories of the source areas are solely resolved by applying the lag time concept.

I used the example of the west-Alpine Chambaran basin to test how, despite the given limitations, a refined reconstruction of source area exhumation history may nevertheless be possible. A large data set of AFT ages already existed for this basin (Glotzbach *et al.*, 2011). I used the same samples (but not the same grains) for additionally dating as many apatites as possible by (U-Th)/He thermochronology (up to 11 grains per sample/time slice). From these dates, I identified outliers (Dunkl) and calculated central ages (Vermeesch, 2008). Next, I assumed that each AHe age group was derived from the same source area as the next oldest AFT age group of the same sample. These two age groups were then combined for forward thermal history modeling. The derived time-temperature path reflects the thermal history of the source area. Based on this approach, I obtained modified provenance results, compared to the previous provenance analysis solely based on AFT data and the lag time concept (Glotzbach *et al.*, 2011). The most important conclusion from the

refined analysis is that more source areas than previously assumed have contributed to the strata of the Chambaran basin, and that a long-term exhumational equilibrium of the Western Alps since ~10 Ma, as postulated from the AFT data set, cannot be corroborated.

5 Contribution to the developed scientific papers

Paper 1:	Original submission to *Basin Research*	9th March 2012
	Acceptance of 3rd revised version	1st February 2013
	(doi: 10.1111/bre.12023)	
	Concept (Idee)	30%
	Data collection (Datenerhebung)	100%
	Realization (Umsetzung)	80%
Paper 2:	Original submission to	
	International Journal of Geosciences	intended in May 2013
	Final preparations for submission	
	Concept (Idee)	30%
	Data collection (Datenerhebung)	100%
	Realization (Umsetzung)	80%
Paper 3:	Original submission to *Terra Nova*	intended in June 2013
	Final preparations for submission	
	Concept (Idee)	70%
	Data collection (Datenerhebung)	100%
	Realization (Umsetzung)	80%

6 First paper:

Relations between denudation, glaciation, and sediment deposition: implications from the Plio-Pleistocene Central Alps

Wolfgang Reiter[1*], Simon Elfert[1], Christoph Glotzbach[2], Matthias Bernet[3] and Cornelia Spiegel[1]

[1]*Department of Geosciences, University of Bremen, Germany*
[2]*Institute of Geology, Leibnitz University of Hannover, Germany*
[3]*Institute of Geosciences, Joseph Fourier University, Grenoble, France*

[*]Corresponding author: Wolfgang Reiter, Department of Geosciences, University of Bremen, Klagenfurter Strasse, 28359 Bremen, Germany. E-mail address: wreiter@uni-bremen.de

6.1 Abstract

Despite abundant data on the early evolution of the Central Alps, the latest stage exhumation history, potentially related to relief formation, is still poorly constrained. We aim for a better understanding of the relation between glaciation, erosion and sediment deposition. Addressing both topics, we analysed late Pliocene to recent deposits from the Upper Rhine Graben and two modern river sands by apatite fission-track and (U-Th-Sm)/He thermochronology. From the observed age patterns we extracted the sediment provenance and paleo-erosion history of the Alpine-derived detritus. Due to their pollen and fossil record, the Rhine Graben deposits also provide information on climatic evolution, so that the erosion history can be related to glacial evolution during the Plio-Pleistocene. Our data show that Rhine Graben deposits were derived from Variscan basement, Hegau volcanics, Swiss Molasse Basin, and the Central Alps. The relations between glaciation, Alpine erosion, and thermochronological age signals in sedimentary rocks are more complex than assumed. The first Alpine glaciation during the early Pleistocene did not disturb the long-term exhumational equilibrium of the Alps. Recent findings indicate that main Alpine glaciation occurred at ~1 Ma. If true, then main Alpine glaciation was coeval with an apparent decrease of hinterland erosion rates, contrary to the expected trend. We suggest that glaciers effectively sealed the landscape, thus reducing the surface exposed to erosion and shifting the area of main erosion north toward the Molasse basin, causing sediment recycling. At around 0.4 Ma, erosion rates increased again, which seems to be a delayed response to main glaciation. The present-day erosion regime seems to be dominated by mass-wasting processes. Generally, glacial erosion rates did not exceed the pre-glacial long-term erosion rates of the Central Alps.

6.2 Introduction

The role of glaciation in the erosion histories of orogens remains controversial. On one hand, glaciation was described as an extremely efficient process for erosion (e.g., Shuster *et al.*,

2005; Berger *et al.*, 2008; Brocklehurst, 2008). For the Alps, it was suggested that Pleistocene glaciation led to enhanced erosion, valley incision and relief formation (Muttoni *et al.*, 2003; Haeuselmann *et al.*, 2007; Valla *et al.*, 2011, 2012; Glotzbach *et al.*, 2011; Garzanti *et al.*, 2011). On the other hand, Koppes & Montgomery (2009) showed that glacial erosion is most efficient on shorter time scales whereas on longer time scales, glacial and fluvial erosion may be equally efficient. Also, glaciation may lead to the preservation of a landscape (for recent studies see, Miller *et al.*, 2006; Willenbring Staiger *et al.*, 2006; Thomson *et al.*, 2010). The exact relation between glaciation, erosion, and the sedimentary record of these processes is still unclear. For this study, the effect of glaciation on the late-stage erosion history of the Alps is investigated. The Alps are generally a well-studied area, but their youngest geological evolution is debated. As outlined above, recent studies suggest that main relief formation of the Alps was related to glaciation since ~1 Ma, whereas other studies propose that main Alpine erosion was unrelated to glaciation and started ~5 Ma (Kuhlemann *et al.*, 2002; Willet *et al.*, 2006; Cederbom *et al.*, 2011). This is in contradiction to Glotzbach *et al.* (2010) who describe a long-term steady exhumation since at least ~7 Ma for the Alps.

The erosion history of an orogen is stored in its syntectonic detritus deposited in surrounding sedimentary basins. Low-temperature thermochronology on these basins, namely apatite-fission track analysis (AFT) and (U-Th-Sm)/He dating (AHe), are suitable for monitoring geodynamic processes affecting uppermost crust of the orogen. Detrital thermochronology allows *(i)* distinguishing different source areas of the sedimentary deposits and *(ii)* reconstructing paleo-denudation history of the hinterland. Therefore, detrital thermochronology potentially provides insights into the controlling mechanisms of Alpine erosion.

As we are interested in the youngest geological evolution of the European Alps, one major Plio-Pleistocene Alpine depocenter north of the Central Alps, namely the Upper Rhine Graben, has been chosen. Heavy mineral analyses suggest that sediment fill of the Upper Rhine Graben was derived from the Central Alps at least since the Pleistocene (Boenigk, 1987; Hoselmann, 2008). Hence, information about Alpine denudation is stored in the sediment of the Upper Rhine Graben. Furthermore, the Upper Rhine Graben deposits are well studied in terms of stratigraphy (Rolf *et al.*, 2008; Wedel, 2008), and they represent a high-resolution climate archive (e.g., Knipping, 2008; Weidenfeller & Knipping, 2008), thus providing the opportunity to correlate changes in the hinterland denudation history with climatic changes during sediment deposition.

6.3 Sampling and methods

6.3.1 Details of sampling

To obtain information on the youngest cooling history of the Central Alps, Plio-Pleistocene sedimentary rocks from the Upper Rhine Graben were sampled. These were derived from two boreholes in Ludwigshafen (P34) and in Viernheim (VH). The drill sites are located in the "Heidelberger Loch" area of Germany, a major Quaternary depocenter of the Rhine Graben. Drill-hole depths are ~300 m for P34 and ~350 m for VH. Two surface samples of recent fluvial sand were collected from the Aare and Reuss rivers in Switzerland with detritus exclusively derived from the Aar and Gotthard massifs (Fig. 6.1). Depositional ages were compiled from magnetostratigraphy (Rolf *et al.*, 2008), optical stimulated luminescence data (Lauer *et al.*, 2010), biostratigraphy (Hagedorn & Boenigk, 2008, and references therein; Knipping, 2008; Wedel, 2008; Weidenfeller & Kärcher, 2008; Weidenfeller & Knipping, 2008; Gabriel *et al.*, 2010 and references therein) and biostratigraphic correlation of the Praetiglian and Reuverian for the VH drill core (pers. comm.

Georg Heumann, University of Bonn, Germany). The Plio-Pleistocene boundary is assumed at 2.59 Ma (ICS, 2010; Litt, 2007). It should be noted, however, that correlation of Alpine glacial cycles with those of NW Europe, as depicted in Fig. 6.3, is still associated with uncertainties and should be viewed with caution (e.g., Ellwanger *et al.*, 2011). From the 27 samples taken, 15 have been analysed while the rest did not yield enough apatite for AFT or AHe analyses. Apatite yield from the Pliocene Rhine sedimentary rocks was especially poor.

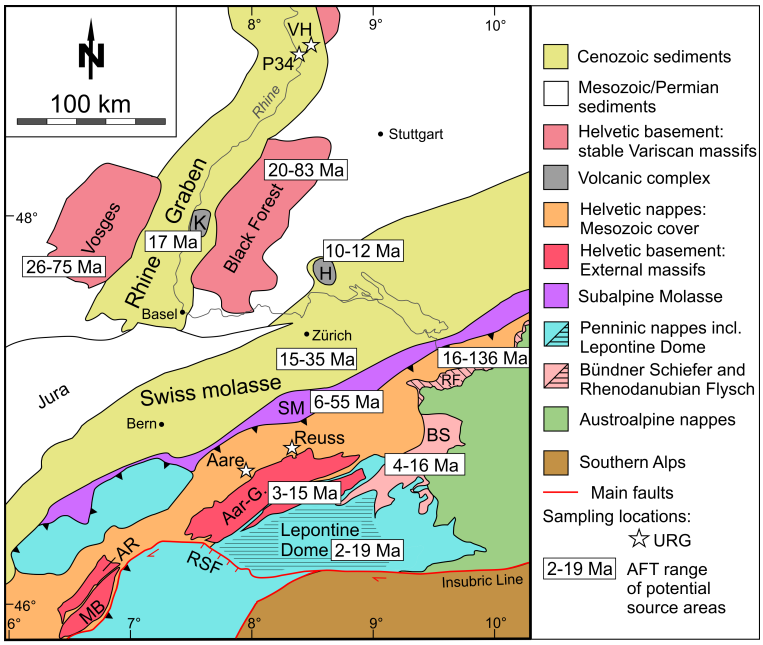

Fig. 6.1: Simplified geotectonic map of the study area (modified after Schmid *et al.*, 2004) with present-day AFT ages of potential source areas (see text for references). Aare/Reuss, location of surface samples of Aare/Reuss rivers (Switzerland); Aar-G., Aar-Gotthard massif; AR, Aiguilles Rouges massif; BS, Bündner Schiefer; G, Gotthard massif; H, Hegau volcanics; K, Kaiserstuhl volcanics; MB, Mont Blanc massif; P34, borehole Parkinsel/Ludwigshafen (Germany); RF, Rhenodanubian Flysch; RSF, Rhône-Simplon fault; SM, Subalpine Molasse; VH, borehole Viernheim (Germany).

6.3.2 Details of AFT analysis

AFT dating is sensitive to temperatures between ~110 and 60°C (Gleadow & Duddy, 1981). For AFT analysis we used the external detector method as described by Gleadow (1981) and the zeta calibration method described by Hurford & Green (1983).

Samples were processed using standard separation techniques. Apatite concentrates were mounted in epoxy resin on a glass slide, ground, and polished to reveal inner surfaces. For revealing spontaneous tracks, the mounts were etched in 5 M HNO_3 at 20°C for 20 seconds. After irradiation at the reactor facility Garching FRM II (Germany), micas were etched using 40% HF at 22 ±1°C for 30 minutes to reveal induced tracks. Single grain ages were calculated using Trackkey software of Dunkl (2002). Errors of AFT ages are given at the 1σ confidence level. We tried to analyse at least 60 grains per sample, corresponding to 95% confidence that no fraction ≥0.085 is missed (Vermeesch, 2004). However, due to poor sample quality, we were not always able to meet this criterion.

To identify different grain age populations (peak ages) indicative of different source areas, binomial peak fitting (Stewart & Brandon, 2004) was used. The mean diameter of etch figures on the apatite surface parallel to the crystallographic c-axis (Dpar) served as a proxy for the annealing kinetics of apatites (Donelick *et al.*, 1999). Three to five Dpar values were measured for each dated grain.

6.3.3 Details of AHe analysis

AHe dating is sensitive to temperatures between ~85 and 40°C (Wolf *et al.*, 1998). Grain selection criteria regarding quality, size and geometry followed the routine described by Farley (2002). Up to five single grains per sample were dated by AHe thermochronology. This amount of analysed grains is not sufficient for representing the whole age distribution of the exposed source areas; however, the goal is to provide additional information on the thermal evolution of selected source areas and thus to complement the denudation histories derived from AFT thermochronology.

Suitable grains were put into Pt tubes cleaned with 37% HCl at 35-40°C for 48 hours in advance, to avoid contamination. ^{4}He was extracted by laser heating and measured with a Balzers quadrupole mass spectrometer using the ^{3}He isotope dilution method. The contents of U, Th, and Sm were detected by mass spectrometry using a second-generation Varian quadrupole ICP-MS. Both analyses were performed at the University of Melbourne (Australia).
Most apatites were corrected for ^{4}He loss at grain margins following the alpha correction approach of Farley *et al.* (1996). However, we do not know how much of the He-depleted rim was removed during sediment transport. To avoid potential overcorrection, we used mechanical grain abrasion (Spiegel *et al.*, 2009) instead of alpha correction for appropriate grains with diameters of ≥90 µm.

6.3.4 Concept of detrital thermochronology

Provenance analysis

Prerequisites for using age signatures from detrital rocks for provenance studies are i) that potential source areas differ regarding their age patterns, and ii) that no reheating to temperatures above the thermal sensitivity of the used thermochronometer has occurred after deposition. Concerning the first prerequisite, Central Alpine sources can be distinguished from the Variscan graben shoulders, because the former yield mainly Neogene AFT ages, whereas the latter yield predominantly Cretaceous to Paleogene AFT ages. A more detailed distinction between different Alpine sources is more difficult. Present-day AFT age pattern of the Aar and Gotthard massifs and the Lepontine area largely overlap. However, for the southern and northern Lepontine Dome, AFT ages up to 19 Ma have been described (Vernon *et al.*, 2008; Elfert *et al.*, 2011). Similar old ages were not observed for the Aar and Gotthard massifs. Regarding the second prerequisite, maximum post-depositional temperatures can be estimated from vitrinite reflectance analysis. Vitrinite reflectance analyses of the Sandhausen and Harthausen boreholes ~20-30 km south/southwest from the sampled P34/VH boreholes show values of 0.2-0.3 at a maximum depth of 500 m (Teichmüller & Teichmüller, 1986). Therefore, estimated maximum post-depositional temperatures of the sampled boreholes did not exceed ~30°C (calculated after Barker & Pawlewicz, 1986), so that no reheating to temperatures of the AFT partial annealing zone or AHe partial retention zone is expected.

The results of detrital thermochronology may be biased by different erodibilities (e.g., Attal & Lave, 2009; Nie *et al.*, 2012) and apatite yields of source rocks (e.g., Spiegel *et al.*, 2004). Generally, lithologies such as mudstones, limestones, or fine-grained volcanic rocks have low apatite yields. Potential Central Alpine source areas, which are very poor in or devoid of apatite, are the Jura Mountains, most of the autochthonous Mesozoic cover of the Helvetic nappes and part of the Bündner Schiefer. It should be kept in mind that erosion of these units is not monitored by our data. In addition to AFT thermochronology, we included previously published information on heavy mineral assemblages, paleo-currents, and sediment transport in our interpretations. Moreover, Dpar values of apatites were used as further provenance indicators. These may be characteristic for the lithologies of a source area. Particularly, volcanic apatite often yields higher Dpar values than apatite derived from crystalline basement rocks (e.g., Spiegel *et al.*, 2007; Link, 2010).

Lag time concept

The lag time, defined as the difference between the cooling age of a detrital mineral and its stratigraphic age, covers the time of exhumation from closure depth to the surface, sediment transport and deposition, with the two latter processes being negligible compared to the time needed for exhumation (Garver *et al.,* 1999). Lag time can thus be used for inferring paleo-cooling and paleo-denudation rates. Also, comparing lag time across a stratigraphic section (e.g., a drill core) provides information on changes in paleo-denudation rates: decreasing lag times upsection generally indicate accelerated denudation of the source area, whereas increasing lag times upsection indicate slower denudation. Constant lag times are indicative for an exhumational equilibrium in the source area.

6.4 Geological setting

6.4.1 Evolution of potential source areas

We briefly outline the overall geological setting and the evolution of the potential source areas. AFT age ranges of the main entities are shown in Figs. 6.1 & 6.6.

External massifs

The external massifs are composed of Hercynian European basement. Their tectonic evolution comprises collision-related overthrusting during the major phase of the Alpine orogeny with subsequent uplift (e.g., Schmid *et al.*, 2004). The external massifs of the Central Alps, namely the Aar and Gotthard massifs, generally show steady exhumation since the late Miocene (Glotzbach *et al.*, 2010 and references therein), with the exception of the southwestern Aar massif, which experienced a strong increase in exhumation since ~3.5 Ma (Reinecker *et al.*, 2008). This enhanced exhumation may be caused by tectonic denudation along the Rhône-Simplon fault zone (Reinecker *et al.*, 2008), which was active since the early Miocene (e.g., Soom, 1990; Campani *et al.*, 2010). AFT cooling ages of the Aar and Gotthard massifs range between 3 and 14 Ma (Reinecker *et al.*, 2008; Glotzbach *et al.*, 2010 and references therein) with most AFT ages ranging between 6 and 10 Ma. AHe ages of this area range between 2.3 and 9 Ma (Reinecker *et al.*, 2008; Vernon *et al.*, 2009; Glotzbach *et al.*, 2010).

Lepontine Dome

The Lepontine Dome is located south of the Aar and Gotthard massifs, flanked by the Rhône-Simplon fault to the west and the Insubric Line to the south (Fig. 6.1). It consists of Lower

Penninic units which underwent Paleogene regional metamorphism and a major phase of updoming during the Oligocene (Steck & Hunziker, 1994). Exhumation of the Lepontine Dome is linked to the post-collisional lateral extrusion of the Alps from the Oligocene-Miocene boundary onward (Frisch *et al.*, 2000). AFT cooling ages of the Lepontine Dome range between 2 and 19 Ma (Vernon *et al.*, 2008 and references therein; Elfert *et al.*, 2011) with the oldest ages occurring at the northern and southern periphery of the Lepontine area. AHe ages range between ~3 and 5 Ma (Vernon *et al.*, 2009).

Swiss Molasse basin

Evolution of the Swiss Molasse basin, the western part of the northern Alpine foreland basin, was directly influenced by Alpine tectonic processes (Kuhlemann & Kempf, 2002). These orogenic processes caused opening and closing of seaways connecting the northern Alpine foreland basin with the North Sea and Paratethys, and therefore influenced sediment discharge. From the Oligocene to Miocene, four major deposition cycles reflect repeated changes from marine to freshwater conditions in the Molasse basin. These main cycles are called the lower and upper marine Molasse, and the lower and upper freshwater Molasse. For the last freshwater cycle (late Early Miocene), the northern Lepontine area is a major sediment supplier (Spiegel *et al.*, 2001). Deposition may have ceased around the Tortonian, as suggested by Kuhlemann & Kempf (2002). However, by early Pliocene time, the Molasse basin was affected by erosion, driven either by climate change and/or drainage reorganisation due to tectonic activity of the hinterland (e.g., Schlunegger & Mosar, 2011). Thermochronological analysis of surface samples from the lower marine Molasse revealed AFT ages between 15 and 36 Ma, with the majority of the ages around 30 Ma (Cederbom *et al.*, 2011).

European basement and volcanic centers adjacent to the Rhine Graben

The Upper Rhine Graben is flanked by Variscan basement rocks of the Black Forest and Vosges (Fig. 6.1). These basement rocks were tectonically affected by development of the European rift system resulting in various Miocene and Pliocene phases of surface uplift (Ziegler & Dèzes, 2007; Rotstein & Schaming, 2011). AFT cooling ages range between 20 and 83 Ma, but most are of Paleogene age or older. AHe ages range between ~8 and 190 Ma and are mostly between 20 and 50 Ma (Timar-Geng *et al.*, 2006; Danišik *et al.*, 2010; Link, 2010).

Rifting was accompanied by volcanic activity in the Upper Rhine Graben. Two of those Miocene volcanic centers are the Kaiserstuhl and Hegau complex. Carbonatitic volcanism of the Kaiserstuhl area (southern Upper Rhine Graben) was active at ~18-15 Ma (Lippolt *et al.*, 1963; Keller *et al.*, 2002). After short quiescence, emplacement of the alkaline Hegau volcanic complex took place at ~14-9 Ma (Schreiner, 1992; Rahn & Selbekk, 2007). Hegau apatites typically show Dpar values up to 6 µm and characteristic crystal defects (Rahn & Selbeck, 2007; Rahn, pers. comm. 2011).

6.4.2 Evolution of the Upper Rhine Graben basin

Most deposition in the Upper Rhine Graben, with local hiatuses, was between the middle Eocene and Quaternary (e.g., Sissingh, 1998). Alternating Pliocene sand and clay deposits indicate fluvio-lacustrine deposition (Berger *et al.*, 2005). A change in heavy mineral composition from stable zircon-rutile-tourmaline to garnet-epidote-hornblende dominance during the latest Pliocene (Fig. 6.2) points to a change in source area. While stable heavy minerals are attributed to Variscan massifs, the Pleistocene mineral assemblage is thought to be of Alpine origin (Hagedorn &

Boenigk, 2008; Hoselmann, 2008). The Pleistocene sediment succession is characterized by alternating sand-gravel (KL) and sand-clay (ZH) layers.

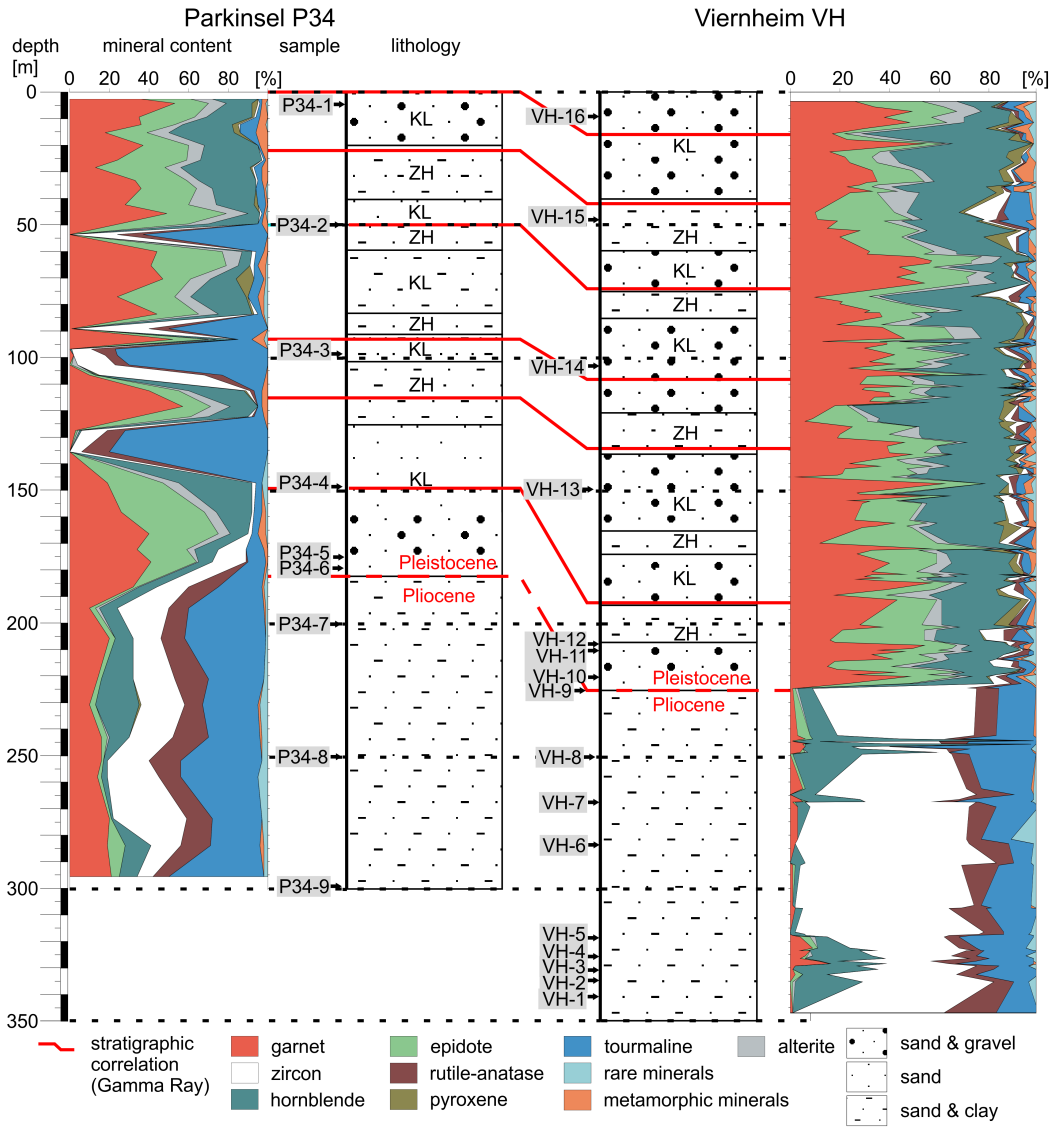

Fig. 6.2: Stratigraphic correlation of the P34 and VH wells depicting lithologies, heavy mineral content (modified after Hagedorn & Boenigk, 2008, and Hoselmann, 2008) and sample depths. Red lines mark the correlations of the sediment successions from P34 and VH drillings based on gamma ray data of Hunze & Wonik (2008). KL, sand-gravel layers; ZH, sand-clay layers.

6.4.3 Climate evolution and glaciations since the Pliocene

The warm Pliocene period became colder toward its end (Ehlers & Gibbard, 2007 and references therein). Minor ice advances occurred in the Northern Hemisphere mainly affecting Canada, Greenland, Eurasia, and NW-Europe. Glaciations significantly increased in these areas after the Plio-Pleistocene boundary (2.59 Ma), with the largest ice extent presumably at ~0.4 Ma during the Pleistocene glacial maximum (Ehlers & Gibbard, 2007).

However, glacial cycles did not affect the Alpine realm before the Late Pliocene. A first

indication of Alpine glaciation is deposition of the Pleistocene Deckenschotter series in the Alpine foreland (Graf, 2009). This deposition is most likely related to Biber (/Praetiglian) and Günz (/Eburonian) glaciations (e.g., Litt *et al.*, 2005; Habbe *et al.*, 2007; Fig. 6.3). The climax of Pleistocene Alpine glaciation lasted from ~1 to ~0.4 Ma, and was accompanied by accelerated valley incision and enhanced relief formation (Muttoni *et al.*, 2003; Haeuselmann *et al.*, 2007; Glotzbach *et al.*, 2011; Valla *et al.*, 2011, 2012). According to Preusser *et al.* (2011), maximum ice advances of this period reached as far north as the Jura mountains and southern Black Forest. The decline of Alpine glaciation began with the Holsteinian Interglacial at ~0.4 Ma, with a final peak at the Last Glacial Maximum around 20 ka ago (Litt *et al.*, 2008 and references therein).

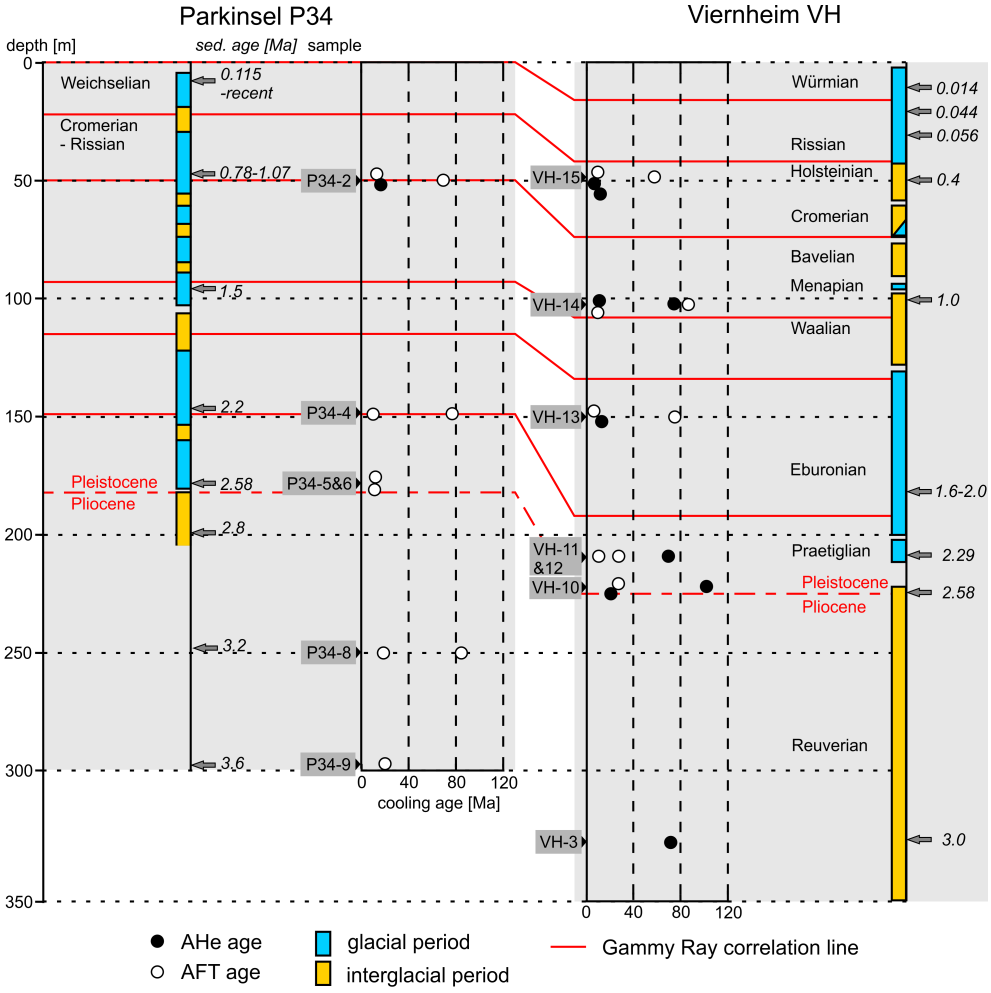

Fig. 6.3: AFT peak ages and AHe ages of the P34 and VH drilling in relation to sample depths, depositional age (sed. age) and glacial-interglacial cycles (Gabriel *et al.*, 2010; see text for details). Errors of AFT peak ages and AHe ages are shown in Tables 6.2 and 6.3.

6.5 Results

Results of AFT analysis, peak fitting, and AHe analysis are shown in Tables 6.1, 6.2, and 6.3, and in Figs. 6.4 & 6.5. The AHe results show no systematic differences between ages based on alpha-ejection corrections and those derived from mechanical abrasion. Thus, at least in this case, abrasion during sediment transport does not seem to have a significant effect on AHe ages.

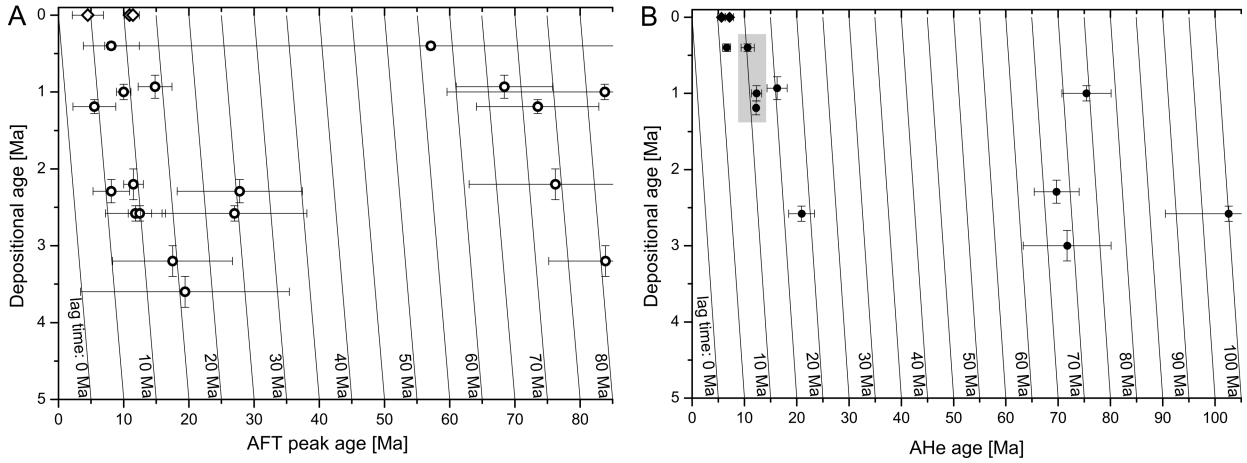

Fig. 6.4: (a) AFT peak ages plotted against depositional ages with lines of equal lag times. Circles represent peak ages from P34 and VH drill cores, and diamonds the peak ages from the Aare and Reuss rivers. (b) AHe ages plotted against depositional ages. The black-filled circles represent AHe ages from P34/VH drill cores, black-filled diamonds represent AHe ages from Aare/Reuss river samples, and grey highlighted area outlines the AHe ages presumably associated with the erosion of Hegau volcanics.

In general, most samples contain an older age group with Cretaceous to early Paleogene AFT and/or AHe ages, and a younger age group with AFT/AHe ages ≤30 Ma (Fig. 6.4). Regarding the younger age groups, we observe the following: *(i)* Rhine Graben deposits with at ~3.6-2.6 Ma depositional age contain a poorly defined AFT age group with a lag time of ~15 Myr. *(ii)* After the Plio-Pleistocene boundary (~2.6 Ma), the age signatures change. For deposition at ~2.6-1.2 Ma, two young age groups with constant lag times of ~6 and 9 Myr are present. Additionally, the earliest Pleistocene samples contain an AFT age group with a lag time of ~25 Ma and AHe ages with lag times of ~20 Ma. *(iii)* For deposition at 1.2-0.9 Ma, only one young AFT age group is present, showing a strong increase of lag times from ~5 to 15 Myr. Samples of this age, particularly sample VH-14, also contain a large number of euhedral, elongated apatites with large Dpar values up to 5.9 µm and a high amount of crystal defects (Fig. 6.5). The latter impedes AFT dating; however, AHe dating yielded an age of ~12 Ma for these grains (grey-shaded area of Fig. 6.4b). *(iv)* After 0.9 Ma, lag times again decrease. *(v)* Present-day sediments derived from the Aare and Reuss rivers (i.e., draining the Aar and Gotthard massifs) contain predominantly AFT peak ages of ~11 Ma and AHe ages of ~5 Ma.

Sample	Stratigraphic age ± error (Ma)	Latitude	Longitude	Elevation (m)	n	ρs	Ns	ρi	Ni	ρd	Nd	P(χ^2) (%)	Dispersion	Central age ± 1σ (Ma)	U (ppm)	Mean Dpar ± s.d. (µm)
Aare	recent	46.74095	8.03800	564	77	2.871	250	104.00	9057	24.68	37343	97	0.00	10.9 ± 0.8	45.6	1.9 ± 0.2
Reuss	recent	46.89721	8.60971	431	77	2.290	207	83.88	7583	24.68	37343	7	0.13	10.9 ± 0.9	40.8	1.9 ± 0.3
VH-15	0.40 ± 0.05	49.56793	8.57542	-48	10	2.189	14	41.28	264	16.43	25346	0	0.80	20.8 ± 8.0	26.6	2.6 ± 1.8
P34-2	0.93 ± 0.15	49.46815	8.45852	-50	13	3.270	37	39.41	446	18.70	27688	2	0.56	27.8 ± 6.9	23.2	2.5 ± 1.2
P34-2-2	0.93 ± 0.15	49.46815	8.45852	-50	17	6.349	139	63.12	1382	25.00	37817	0	0.78	30.5 ± 6.9	35.3	1.8 ± 0.3
VH-14	1.0 ± 0.1	49.56793	8.57542	-103	33	1.532	36	43.63	1025	16.49	25346	56	0.02	9.2 ± 1.6	32.4	2.5 ± 1.4
VH-14-3	1.0 ± 0.1	49.56793	8.57542	-103	33	1.445	78	42.80	2311	25.00	37817	0	0.86	15.9 ± 3.3	22.7	1.6 ± 0.1
VH-13	1.19 ± 0.1	49.56793	8.57542	-150	13	10.880	91	62.29	521	16.56	25346	0	1.27	19.7 ± 8.5	36.7	2.1 ± 1.3
P34-4	2.2 ± 0.2	49.46815	8.45852	-149	32	0.871	24	25.08	691	18.76	27688	91	0.00	10.4 ± 2.2	15.1	1.9 ± 0.3
P34-4-2	2.2 ± 0.2	49.46815	8.45852	-149	42	3.056	109	55.12	1966	24.93	18862	0	0.89	24.4 ± 4.4	27.1	1.9 ± 0.3
VH-12	2.29 ± 0.15	49.56793	8.57542	-210	23	1.678	26	32.71	507	16.62	25346	4	0.73	13.5 ± 3.6	23.4	1.6 ± 0.2
VH-11	2.29 ± 0.15	49.56793	8.57542	-210	12	2.397	23	45.97	441	16.69	25346	17	0.47	15.8 ± 4.3	29.9	1.8 ± 0.2
P34-5	2.58 ± 0.1	49.46815	8.45852	-174	7	0.856	4	30.81	144	18.65	27688	55	0.01	8.3 ± 4.2	20.7	2.1 ± 0.0
P34-5-2	2.58 ± 0.1	49.46815	8.45852	-174	31	1.582	50	48.24	1525	25.00	37817	96	0.00	13.1 ± 1.9	22.7	1.7 ± 0.2
P34-6	2.58 ± 0.1	49.46815	8.45852	-177	3	2.371	7	59.28	175	18.49	27688	49	0.00	11.8 ± 4.6	36.0	2.2 ± 0.3
VH-10	2.58 ± 0.1	49.56793	8.57542	-220	6	3.826	8	33.48	70	16.75	25346	19	0.15	30.8 ± 11.7	26.1	1.5 ± 0.1
P34-8	3.2 ± 0.2	49.46815	8.45852	-250	7	7.941	7	48.40	256	18.38	27688	4	0.46	44.9 ± 11.6	33.7	2.8 ± 0.7
P34-8-2	3.2 ± 0.2	49.46815	8.45852	-250	3	36.762	104	154.47	437	25.00	37817	23	0.10	95.6 ± 12.5	62.8	2.0 ± 0.2
P34-9	3.6 ± 0.2	49.46815	8.45852	-298	2	3.252	2	48.78	30	18.27	27688	79	0.00	19.4 ± 14.2	21.1	1.8 ± 0.5

Table 6.1: Results of AFT analyses including measured mean Dpar values of counted grains, geographic position data (WGS 84), and elevation of sampling locations. Note that for some samples two mounts were analysed. Depth for borehole samples is given in meter below surface. N, number of counted grains; Ns, number of spontaneous tracks; Ni, number of induced tracks on mica; Nd, number of counted tracks induced from monitor glasses; ρ(s, i, d), track density given in 10^5 tracks cm^{-2} (with s, spontaneous tracks; i, induced tracks; d, mean amount of induced tracks on mica); P(χ^2), probability of receiving Chi-square value for n degree of freedom (n is equal to the number of crystals minus 1); a value smaller than 5 % indicates that there could be more than one age population). $\zeta = 319 \pm 9$ (Durango & Fish Canyon standards, CN-5).

Sample	Stratigraphic age ± error (Ma)	n	Age range (Ma)	P1 peak age ±1σ Cl (Ma)	Frac (%)	P2 peak age ±1σ Cl (Ma)	Frac (%)	P3 peak age ±1σ Cl (Ma)	Frac (%)	P4 peak age ±1σ Cl (Ma)	Frac (%)
Aare	recent	77	3.7-63.2	-	-	10.9 ± 0.8	100	-	-	-	-
Reuss	recent	77	3.7-166.5	4.5 ± 2.4	5	11.4 ± 1.0	95	-	-	-	-
VH-15	0.40 ± 0.05	10	5.7-111.3	8.1 ± 4.3	70	-	-	-	-	57.1 ± 50	30
P34-2	0.93 ± 0.15	30	3.2-147.8	-	-	14.8 ± 2.6	68	-	-	68.4 ± 7	32
VH-14	1.0 ± 0.1	66	2.1-103.0	-	-	10.0 ± 1.1	98	-	-	83.8 ± 24	2
VH-13	1.19 ± 0.1	19	2.2-77.2	5.5 ± 3.3	75	-	-	-	-	73.5 ± 9	25
P34-4	2.2 ± 0.2	74	3.1-147.5	-	-	11.5 ± 1.5	88	-	-	76.2 ± 13	12
VH-11/12	2.29 ± 0.15	35	3.4-112.7	8.1 ± 2.8	67	-	-	27.8 ± 9.6	33	-	-
P34-5	2.58 ± 0.1	38	4.3-72.5	-	-	12.5 ± 1.8	100	-	-	-	-
P34-6	2.58 ± 0.1	3	4.8-16.9	-	-	11.8 ± 4.6	100	-	-	-	-
VH-10	2.58 ± 0.1	5	15.1-88.4	-	-	-	-	27.0 ± 11.1	100		
P34-8	3.2 ± 0.2	10	15.4-121.8	-	-	17.5 ± 9.2	31	-	-	83.9 ± 8	69
P34-9	3.6 ± 0.2	2	24.6-96.4	-	-	19.4 ± 16.0	100	-	-	-	-

Table 6.2: Results of peak fitting. N, number of grains analysed for binomial peak fitting. Frac, fraction of the specific age population.

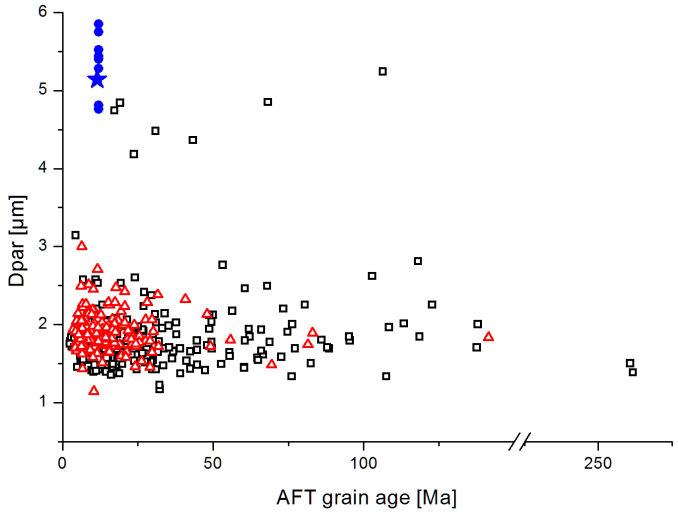

Fig. 6.5: Mean Dpar values plotted against AFT single grain ages. For reason of clarity no error bars are shown. Red dots show measured mean Dpar values presumably associated with Hegau volcanism. Their age is inferred from AHe dating (see text for further details). The red star shows an AFT dated single grain age (sample VH-14) of assumed Hegau origin. The black square symbols refer to samples of VH/P34 boreholes; the blue triangles to the Aare/Reuss river samples.

Sample	Stratigraphic age ± error (Ma)	n	Raw age (Ma)	Error raw age (Ma)	Corrected age (Ma)	Error (Ma)	FT factor	^{4}He (ncc)	Mass (mg)	Th/U ratio	^{149}Sm (ng)	^{232}Th (ng)	^{238}U (ng)
Aare # 1	recent	1	4.68	0.29	6.90	0.81	0.68	0.034	0.0019	0.1003	0.4196	0.0059	0.0584
Aare # 4	recent	1	4.53	0.28	6.18	0.73	0.73	0.041	0.0036	0.3138	0.6134	0.0217	0.0691
Aare # 5	recent	1	6.15	0.38	7.89	0.93	0.78	0.298	0.0050	0.1368	1.5752	0.0530	0.3873
Aare # 7	recent	1	5.35	0.33	7.64	0.90	0.70	0.025	0.0018	0.7073	0.1283	0.0233	0.0329
Reuss # 1	recent	1	4.83	0.30	6.09	0.72	0.79	0.109	0.0046	0.6472	1.1404	0.1040	0.1608
Reuss # 2	recent	1	4.08	0.25	4.99	0.59	0.82	0.139	0.0120	0.1342	2.5886	0.0364	0.2710
Reuss # 3	recent	1	5.05	0.31	6.48	0.76	0.78	0.078	0.0032	2.0000	0.5190	0.1728	0.0864
Reuss # 4	recent	1	3.98	0.25	5.54	0.65	0.72	0.097	0.0032	0.7689	0.2319	0.1311	0.1706
Reuss # 5	recent	1	3.95	0.24	4.83	0.57	0.82	0.081	0.0067	0.4806	0.9020	0.0730	0.1519
P34-2 # 1	0.93 ± 0.15	1	12.27	0.76	16.24	1.91	0.76	0.106	0.0050	0.3337	0.4597	0.0219	0.0657
VH-15 # 1	0.40 ± 0.05	1	6.80	0.42	10.62	1.25	0.64	0.063	0.0016	5.8749	0.2149	0.1878	0.0320
VH-15 # 2	0.40 ± 0.05	1	4.55	0.28	6.59	0.78	0.69	0.107	0.0024	1.3949	0.2264	0.2043	0.1465
VH-14 # 1	1.0 ± 0.10	1	10.07	0.62	12.39	1.46	0.81	0.276	0.0134	11.6053	1.2740	0.6963	0.0600
VH-14 # 2	1.0 ± 0.10	1	8.35	0.52	10.58	1.24	0.79	0.227	0.0135	15.7010	1.1847	0.7434	0.0473
VH-14 # 3abr	1.0 ± 0.10	1	13.95	0.86	13.95	0.86	1	0.054	0.0018	15.2833	0.3138	0.1045	0.0068
VH-14 # 4abr	1.0 ± 0.10	1	75.4	4.7	75.4	4.7	1	0.813	0.0010	0.4217	0.4067	0.0339	0.0803
VH-13 # 3abr	1.19 ± 0.09	1	12.60	0.78	12.60	0.78	1	0.062	0.0007	6.2765	0.1553	0.1021	0.0163
VH-13 # 4abr	1.19 ± 0.09	1	11.85	0.73	11.85	0.73	1	0.038	0.0015	6.0041	0.1336	0.0654	0.0109
VH-11 # 1abr	2.29 ± 0.15	1	69.7	4.3	69.7	4.3	1	0.550	0.0009	0.3491	0.1440	0.0209	0.0599
VH-10 # 1	2.58 ± 0.10	1	14.48	0.90	20.91	2.46	0.69	0.275	0.0020	0.2012	0.2797	0.0301	0.1498
VH-10 # 2	2.58 ± 0.10	1	86.9	5.4	102.6	12.1	0.85	3.239	0.0195	0.4225	2.7589	0.1164	0.2754
VH-03 # 1	3.0 ± 0.2	1	52.4	3.3	71.7	8.4	0.73	0.447	0.0021	3.4810	1.3694	0.1312	0.0377

Table 6.3: Results of the apatite (U-Th-Sm)/He analyses. 'abr' refers to air abrasion of apatite grains. No α-correction is necessary for these grains. N, number of analysed grains per aliquot. Routinely analysed Durango standards (15 aliquots) yielded a mean value of 31.5 Ma (standard deviation: 1.2 Ma).

6.6 Interpretation and discussion

6.6.1 Sources of the Upper Rhine Graben sedimentary rocks since the Pliocene

Generally, we assume that apatites with Cretaceous to early Paleogene AFT and AHe ages were derived from Variscan graben shoulders and their sedimentary cover, in agreement with published age patterns (Timar-Geng *et al.*, 2006; Danišik *et al.*, 2010; Link, 2010). The provenance of apatites with younger ages (≤30 Ma) is discussed below.

Deposition between 3.6 and 2.59 Ma

With a lag time of ~15 Myr, AFT ages of Pliocene strata are too young to be derived from Variscan graben shoulders and too old to be derived from basement of the Aar-Gotthard massif. Based on grain morphology and small Dpar values, the Kaiserstuhl volcanic complex can be largely ruled out as a source area. However, along the northern margin of the Alps, i.e., in the Subalpine Molasse and/or western Rhenodanubian Flysch units (Figs. 6.1 & 6.6; Trautwein *et al.*, 2001; Cederbom *et al.*, 2004; Vernon *et al.*, 2008), similar AFT ages occur. Thus, unlike previous assumptions (e.g., Ziegler & Fraefel, 2009), the Pliocene Rhine river received detritus from the Alps, although this seems to be derived from the north-Alpine margin, not from the Alpine core.

Deposition between 2.59 and 1.2 Ma

After the Plio-Pleistocene boundary, AFT age groups with 6-9 Myr lag times occur in the Rhine Graben, coeval with a change in the heavy mineral composition from stable minerals to garnet-epidote dominance (Fig. 6.2). The young AFT ages are most likely derived from the Central Alpine core region (i.e., Aar-Gotthard massif and Lepontine Dome). Thus, after ~2.6 Ma, the north-Alpine drainage system experienced a significant change, with the catchment of the paleo-Rhine river now reaching the Alpine core region. Temporally, this change approximately coincides with a change of the Alpine stress field (Sue *et al.*, 2007), and possibly with the change from an orogen-perpendicular to an orogen-parallel drainage network (Reinecker & Kuhlemann, 2008). A causal relationship to the observed change of the paleo-Rhine catchment, however, remains speculative.

Statistically, we can distinguish between a young age group with ~5 Myr lag time (~2.3-1.2 Ma depositional age) and a slightly older age group with ~9 Myr lag time (~2.6-2.2 Ma deposition; Fig. 6.4a). We tentatively assign younger AFT ages to the Aar-Gotthard massif and older AFT ages to the Lepontine Dome, in agreement with slightly older ages observed in present exposures of the Lepontine Dome. If true, this would mean that parts of the Lepontine Dome were drained northward until at least 2.2 Ma, in agreement with the suggestion of Schlunegger *et al.* (2007). The oldest Pleistocene deposits also contain AFT age groups of ~30 Ma. Similar AFT ages were reported from the Swiss Molasse Basin (Cederbom *et al.*, 2011). This indicates that, after changing its course, the paleo-Rhine incised into the Swiss Molasse Basin.

Deposition after 1.2 Ma

At 1.2 Ma, only one age group with a lag time of ~5 Ma is still present in the samples. If the assumption that the ~9 Ma lag times were derived from the Lepontine Dome is correct, then disappearance of detritus from the Lepontine Dome would indicate a shift of the main drainage divide to the north, in a similar position as today. This would agree with the drainage pattern described by Schlunegger *et al.* (2007). The increasing AFT ages upsection are contrary to what is expected for incision into crystalline basement but typical for sediment recycling. Below we discuss this topic in relation with hinterland exhumation. As described above, the Rhine Graben/VH samples contain euhedral, elongated apatites dated at ~12 Ma by AHe thermochronology (Table 6.3,

Fig. 6.4b). Grain morphology points to a volcanic source, and the age, the large Dpar values, and high amount of lattice defects are similar to the Hegau volcanics (Rahn & Selbekk, 2007; Meinert Rahn, pers. comm.). Thus, after 1.2 Ma the paleo-Rhine drained the Hegau area (Fig. 6.1), which indicates that the Rhine River followed essentially the same course as it does today.

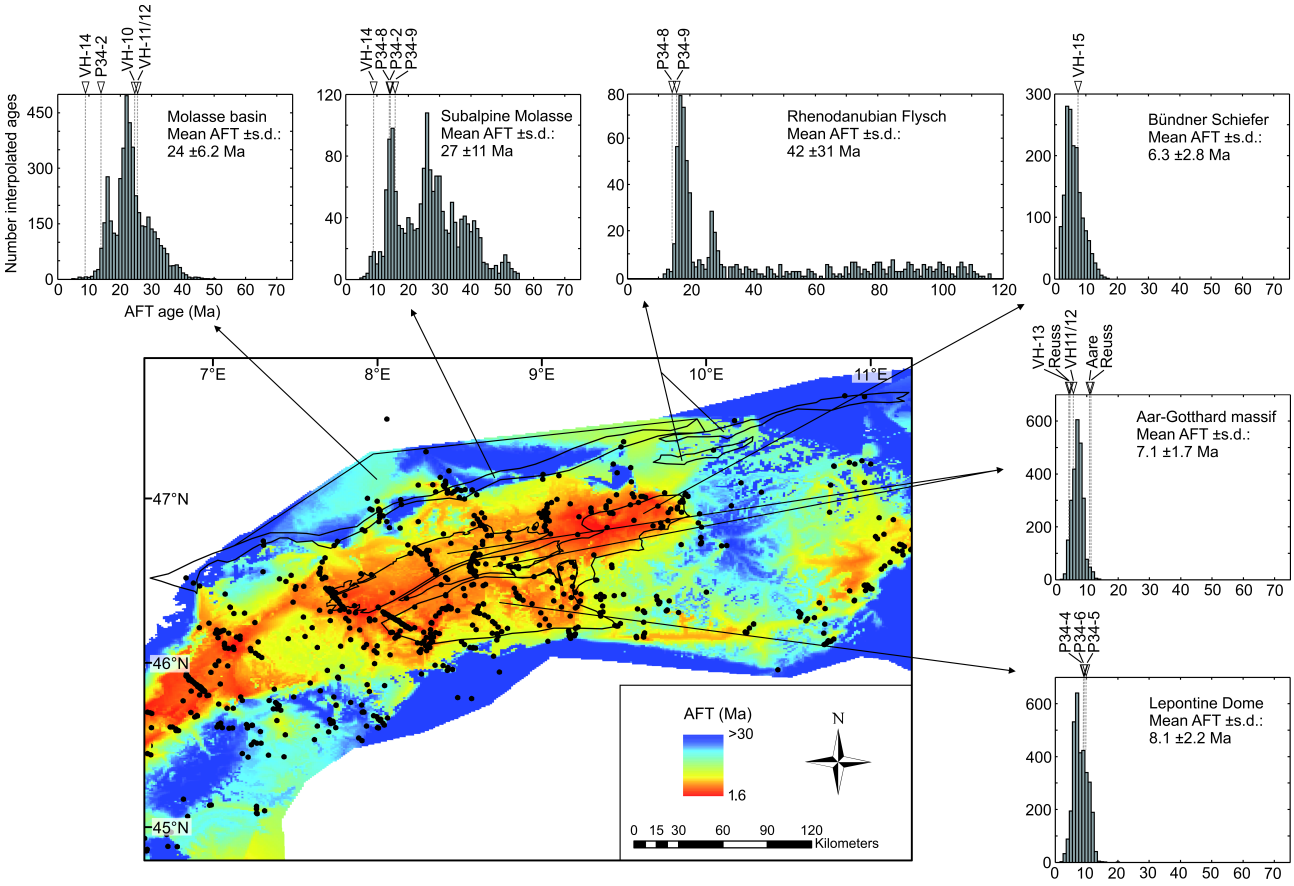

Fig. 6.6: Interpolated surface AFT age distribution of the Central Alps with age probability-density plots for each potential source area (outlined in black). AFT interpolation is based on a collection of Alpine hard-rock and detrital thermochronological data (see Glotzbach *et al.*, in revision). Black arrows show AFT lag times of peak ages from the Rhine Graben samples and the two modern Rhine tributaries. S.d. means standard deviation of the interpolated mean AFT age. Source area AFT data are compiled from the following studies: [i] *Aar-Gotthard massif*: Wagner & Reimer (1972), Schaer *et al.* (1975), Wagner *et al.* (1977), Michalski & Soom (1990), Soom (1990), Glotzbach *et al.* (2008), Reinecker *et al.* (2008), Vernon *et al.* (2009), Glotzbach *et al.* (2010), and unpublished data from Meinert Rahn; [ii] *Subalpine Molasse*: Cederbom *et al.* (2004), Rahn *et al.* (1997), von Hagke *et al.* (2012), and unpublished data from Meinert Rahn; [iii] *Rhenodanubian Flysch*: Trautwein *et al.* (2001); [iv] *Bündner Schiefer*: Michalski & Soom (1990), Weh (1998), and unpublished data from Meinert Rahn; [v] *Lepontine Dome*: Wagner & Reimer (1972), Wagner *et al.* (1977), Steiner (1984), Hurford (1986), Soom (1990), Giger (1991), Ciancaleoni (2004), Timar-Geng *et al.* (2004), Keller *et al.* (2005), Pignalosa *et al.* (2011), Vernon *et al.* (2009), and unpublished data from Simon Elfert and Meinert Rahn; [vi] *Molasse basin*: Cederbom *et al.* (2004), von Hagke *et al.* (2012), and unpublished data from Meinert Rahn.

Present-day situation

The present-day sediments of the Aare and Reuss rivers contain predominantly AFT ages of ~11 Ma and AHe ages of ~5 Ma. The AFT ages are in apparent contrast to the age pattern of the source area (Aar-Gotthard massif), where similar old ages are only observed on the top of the mountains, while the valleys display younger AFT ages around 5 to 7 Ma (Reinecker *et al.*, 2008; Glotzbach *et al.*, 2010). This may indicate that the majority of detritus is derived from the mountain tops and thus transported to the rivers by mass wasting processes such as landsliding (Larsen & Montgomery, 2012). This interpretation is in agreement with the pronounced relief and the oversteepened valleys of the source areas.

6.6.2 Paleo-denudation history of the Central Alps and its relation to Plio-Pleistocene climate change

Here we extract the paleo-denudation history of the sediment source areas from detrital ages and link it to climatic information stored in the Rhine Graben basin fill (see Fig. 6.3). Generally, a trend of decreasing lag times of the AFT age groups thought to be derived from Variscan graben shoulders throughout the sedimentary section is observed. Although age uncertainties are rather high, such a trend is in agreement with continuous and increasing incision into basement rocks and may indicate relief rejuvenation of the Black Forest and Vosges during Plio-Pleistocene glaciations. The following discussion, however, focuses on the younger age group thought to be of Alpine origin. Fig. 6.7 shows the relation between the youngest AFT age groups and Plio-Pleistocene glacial-interglacial cycles.

Paleo-denudation history between 2.59 and 1.2 Ma

Sediments deposited between ~2.6 and 1.2 Ma contain two age groups, both showing a steady exhumation trend. This is in agreement with Glotzbach *et al.* (2010) who describe steady exhumation of the Central Alps since ~7 Ma. Also, the lag times observed in our study are in line with those reported by Glotzbach *et al.* (2010), indicating exhumation rates of ~0.9 km Ma^{-1} and 0.6 km Ma^{-1} for the Aar-Gotthard massif and presumably the Lepontine Dome between 2.6 and 1.2 Ma (assuming a geothermal gradient of 20°C km^{-1}). At the same time, the Alps experienced their first major glaciation cycles, the Biber (/Praetiglian) and Günz (/Eburonian) glaciations (Figs. 6.3 & 6.7). The constant AFT lag times, however, show that this shift to a glacial erosion regime was not sufficient to disturb the long-term exhumational equilibrium of the Central Alps, at least within the sensitivity of the AFT system.

Paleo-denudation history between 1.2 and 0.9 Ma

From ~1.2 to ~0.9 Ma, a trend of strongly increasing AFT peak ages and lag times is observed, temporally coeval with the main glaciation period of the Alps (~Haslach-Mindel/Menapian). This seems contradictory, because enhanced valley incision and relief formation, interpreted as the erosional response to main Alpine glaciation, is assumed around ~1 Ma. Accordingly, we expected a glacially induced increase of erosion rates, opposite to the trend observed. The upsection trend of increasing AFT ages is typical for recycling of (unreset) sediment (e.g., Spiegel *et al.*, 2000), and may be explained by three scenarios: *(i)* the previous glacial cycles may have deposited glacial till that shields underlying bedrock from incision. The age trend would then reflect removal of this glacial sediment (see Koppes & Montgomery, 2009); *(ii)* glaciers covering the Central Alps were frozen to their beds thus impeding significant subglacial erosion (see Miller *et al.*, 2006). As a result, the locus of headwater erosion would shift to the north causing

erosion and recycling of (subalpine) Molasse sediment; *(iii)* following the reconstruction of Preusser *et al.* (2011) for the maximum ice extent, Alpine glaciers may have reached the southern border of the Black Forest. Again assuming that main erosion took place in front of the glaciers, the age trend may reflect reworking of sediment deposited in the southern Upper Rhine Graben. For the first and third scenario, reworked sediment would be recently deposited and the original source areas were presumably also situated in the Central Alps. Thus, we would expect younger AFT ages than observed (Fig. 6.6). Accordingly, we consider scenario two as the most likely, but do not exclude a combined effect of all three scenarios.

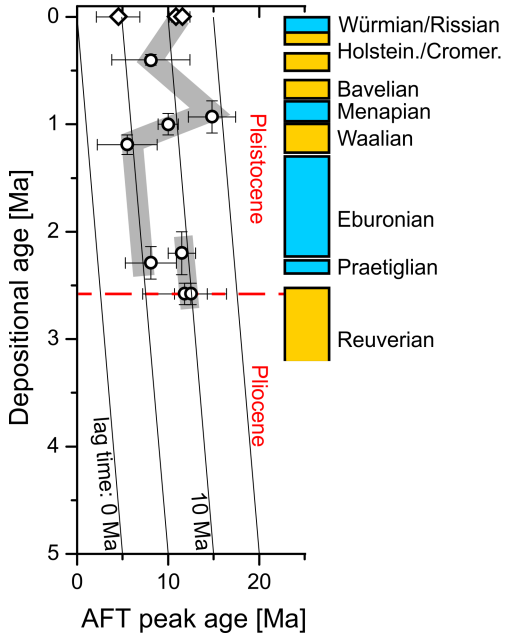

Fig. 6.7: AFT lag times for assumed Alpine source areas correlated with glacial cycles. Major trends of AFT peak ages from samples VH/P34 and Aare/Reuss are highlighted in grey.

Paleo-denudation history between 0.9 and 0.4 Ma

Between ~0.9 and ~0.4 Ma, both, AFT peak ages and lag times decrease once again, indicating an increase in denudation of the Central Alps. Within error limits, the long-term exhumational equilibrium of the Central Alps is thus resumed (Fig. 6.7). The increase occurs after the most extensive Alpine glaciation (Muttoni *et al.*, 2003; Ehlers & Gibbard, 2007; Preusser *et al.*, 2011). We interpret enhanced hinterland denudation as a delayed response to intense glaciation, resulting from warmer basal temperatures and thus enhanced erosive force of the retreating glaciers, similar to what is described for Patagonia and Greenland (Rignot *et al.*, 2003; Howat *et al.*, 2005; Koppes & Montgomery, 2009). Furthermore, exhumation likely accelerates due to isostatic adjustments of the Alps after glacial retreat. Apart from the changed denudation rates, the AFT age signature also shows that the main source area of the Rhine Graben sediments shifts toward the core region of the Central Alps (Fig. 6.6), thus indicating a change of the north-Alpine drainage network. Potential source units from the core region may be located again in the Aar-Gotthard massif, the northeastern Lepontine Dome, or the Bündner Schiefer. A more precise distinction is beyond the resolution of the AFT system. A change of the drainage system at that time was also proposed by Villinger (1998, 2003), Litt *et al.* (2005), and Ziegler & Fraefel (2009), although our data require

some changes to the previously published drainage reconstructions (Reiter *et al.*, in prep).

Present-day situation

Present-day sediments of the Aar-Gotthard massif predominantly contain AFT ages around ~11 Ma. As described above, such ages mainly occur on mountain tops of the source area, whereas in the valleys, rocks with AFT ages around ~5 Ma are exposed. Similar young 5 Ma ages also occur in Reuss sediments, but their contribution is minor compared to the older 11 Ma AFT age group. Thus, while glacial erosion obviously causes valley incision, the present interglacial period is related to erosion of more elevated areas. The most effective process for removing material from mountain tops and transporting it to the valleys/rivers is landsliding. Landsliding is known to become more frequent at the transition between glacial and interglacial periods (e.g., Ivy-Ochs *et al.*, 2009), and also during recent warming of the last decades, and may thus explain the AFT signal observed in recent sediments.

6.7 Conclusions

Plio-Pleistocene sedimentary rocks from the Upper Rhine Graben and two recent rivers were analysed by apatite fission-track and (U-Th-Sm)/He thermochronology. Our goal was to identify sediment provenance and to derive the denudation history of source areas in relation to the latest Neogene to Quaternary climate evolution. The following conclusions can be drawn from our data:

(i) Unlike previously thought, the paleo-Rhine received Alpine detritus already during the late Pliocene, although this was not derived from the Alpine core region, but presumably from the northern rim of the Alpine realm.

(ii) At the Plio-Pleistocene boundary, the (circum-)Alpine drainage system changed. The analysed sedimentary rocks indicate a fluvial connection between the Upper Rhine Graben and the Alpine core regions, i.e., the Aar-Gotthard massif and probably also the Lepontine Dome.

(iii) Despite first Alpine glaciations in the early Pleistocene, the Alps remained in a long-term exhumational steady-state.

(iv) Prior to the onset of main Alpine glaciations at about 1.2 Ma, the main drainage divide seems to have shifted toward the north to its present-day position.

(v) After ~1.2 Ma, denudation rates apparently decreased indicating that glaciation cut off the Central Alpine source regions and presumably caused a northward shift of main erosion toward the (subalpine) Molasse basin.

(vi) Onset of erosion of Hegau volcanics indicates that the Rhine river system essentially follows its present course since ~1 Ma.

(vii) As a delayed response to the most extensive glaciation, Alpine denudation rates again increased around ~0.4 Ma.

(viii) During the present-day interglacial period, Alpine erosion seems to be dominated by mass-wasting processes such as landsliding.

(ix) Generally, Pleistocene glacial erosion rates do not exceed pre-glacial erosion rates prevailing in the Alps since the late Miocene. Glaciation is responsible for strong changes in topography, but despite some disturbances of the erosion regime, it did not really alter the long-term exhumational steady state of the Central Alps.

6.8 Acknowledgements

This study is part of the EUROCORE project TopoEurope/ThermoEurope funded by the European Science Foundation and the German Science Foundation (project SP673/5-1). We like to thank Gerald Gabriel (Leibniz-Institut für Angewandte Geophysik at Hannover), Christian Hoselmann (Hessisches Landesamt für Umwelt und Geologie at Wiesbaden), Dietrich Ellwanger and Ulrike Wielandt-Schuster (both at Landesamt für Geologie, Rohstoffe und Bergbau at Freiburg) for providing the borehole samples and valuable information on the drilled section. Also special thanks to Meinert Rahn and Joachim Kuhlemann (both Eidgenössische Nuklearsicherheitsinspektorat at Brugg) for ongoing scientific exchange regarding Alpine geology and for providing unpublished data for the Central Alpine age compilation, Christian Schlüchter (University of Bern) for scientific exchange regarding Alpine glaciation, and to Barry Kohn (University of Melbourne) for his support regarding the AHe analyses. We also would like to thank Anke Toltz, Vera Kolb, Angelika Freesemann (all at University of Bremen), and Dorothea Mühlbayer-Renner and Dagmar Kost (both at University of Tübingen) for sample processing. Finally, we would like to thank Brian Horton for the editorial work, and Maria Laura Balestrieri, Frédéric Herman, and Matthias Hinderer for their helpful comments which greatly improved this paper.

6.9 References

Attal, M. & Lavé, J. (2009) Pebble abrasion during fluvial transport: Experimental results and implications for the evolution of the sediment load along rivers. *J. Geophys. Res., 114*, F04023, doi:10.1029/2009JF001328.

Barker, C.E. & Pawlewicz, M.J. (1986) The correlation of vitrinite reflectance with maximum temperature in humic organic matter. *Paleogeothermics*, *5*, 79–93.

Berger, J.-P., Reichenbacher, B., Becker, D., Grimm, M., Grimm, K., Picot, L., Storni, A., Pirkenseer, C., Derer, C. & Schaefer, A. (2005) Paleogeography of the Upper Rhine Graben (URG) and the Swiss Molasse Basin (SMB) from Eocene to Pliocene. *Int J Earth Sci*, *94*, 697–710.

Berger, A.L. & Spotila, J.A. (2008) Denudation and deformation in a glaciated orogenic wedge: The St. Elias orogen, Alaska. *Geology*, *36*, 523–526.

Boenigk, W. (1987) Petrographische Untersuchungen jungtertiärer und quartärer Sedimente am linken Oberrhein. *Jber. Mitt. oberrhein. geol. Ver.*, *69*, 357–394.

Brocklehurst, S.H., Whipple, K.L. & Foster, D. (2008) Ice thickness and topographic relief in glaciated landscapes of the western USA. *Geomorphology*, *97*, 35–51.

Campani, M., Herman, F. & Mancktelow, N. (2010) Two- and three- dimensional thermal modeling of a low-angle detachment: Exhumation history of the Simplon Fault Zone, central Alps. *Journal of Geophysical Research*, *115*, B10420, doi:10.1029/2009JB007036.

Cederbom, C.E., Sinclair, H.D., Schlunegger, F. & Rahn, M.K. (2004) Climate-induced rebound and exhumation of the European Alps. *Geology*, *32*, 709–712.

Cederbom, C.E., van der Beek, P., Schlunegger, F., Sinclair, H.D. & Oncken, O. (2011) Rapid extensive erosion of the North Alpine foreland basin at 5-4 Ma. *Basin Research*, *23*, 528–550.

Ciancaleoni, L. (2005) *Deformation processes during the last stages of the continental collision: the brittle–ductile fault systems in the Bergell and Insubric areas (Eastern Central Alps, Switzerland–Italy)*. Ph.D. thesis, University Neuchâtel, Switzerland.

Danišik, M., Pfaff, K., Evans, N.J., Manoloukos, C., Staude, S., McDonald, M.J. & Markl, G. (2010) Tectonothermal history of the Schwarzwald Ore District (Germany): An apatite triple dating approach. *Chemical Geology*, *278*, 58–69.

Donelick, R.A., Ketcham, R.A. & Carlson, W.D. (1999) Variability of apatite fission-track annealing kinetics: II. Crystallographic orientation effects. *American Mineralogist*, *84*, 1224–1234.

Dunkl, I. (2002) Trackkey: A windows program for calculation and graphical presentation of fission track data. *Comput. Geosci.*, *28*, 3–12.

Ehlers, J. & Gibbard, P.L. (2007) The extent and chronology of Cenozoic Global Glaciation. *Quaternary International*, *164–165*, 6–20.

Elfert, S., Reiter, W. & Spiegel, C. (2011) Doming and unroofing of the Lepontine Dome (Central European Alps). New insights from Low-Temperature thermochronology. *Geophysical Research Abstracts*, *13*, EGU2011-11983.

Ellwanger, D., Wielandt-Schuster, U., Franz, M. & Simon, T. (2011). The Quaternary of the southwest German Alpine Foreland (Bodensee, Oberschwaben, Baden-Württemberg, Southwest Germany). *Quaternary Science Journal*, *60*, 306–328.

Farley, K. (2002) (U-Th)/He Dating: Techniques, Calibrations, and Applications. *Reviews in Mineralogy and Geochemistry*, *47*, 819–844.

Farley, K., Wolf, R.A. & Silver, L.T. (1996) The effects of long alpha-stopping distances on (U-Th)/He ages. *Geochimica et Cosmochimica Acta*, *60*, 4223–4229.

Frisch, W., Dunkl, I. & Kuhlemann, J. (2000) Post-collisional orogen-parallel large-scale extension in the Eastern Alps. *Tectonophysics*, *327*, 239–265.

Gabriel, G., Ellwanger, D., Hoselmann, C. & Weidenfeller, M. (2010) The Heidelberg Basin Drilling Project – Characteristics of an outstanding archive of Quaternary sediments. *Geophysical Research Abstracts EGU General Assembly*, *12*, EGU2010-7791.

Garver, J.I., Brandon, M.T., Roden-Tice, M. & Kamp, P.J.J. (1999) Exhumation history of orogenic highlands determined by detrital fission-track thermochronology. *Geological Society Special Publications*, *154*, 283–304.

Garzanti, E., Vezzoli, G. & Andò, S. (2011) Paleogeographic and paleodrainage changes during Pleistocene glaciations (Po Plain, Northern Italy). *Earth-Science Reviews*, *105*, 25–48.

Giger, M. (1991) *Geochronologische und petrographische Studien an Geröllen und Sedimenten der Gonfolite Lombarda Gruppe (Südschweiz und Norditalien) und ihr Vergleich mit dem alpinen Hinterland*. Ph.D. thesis, University Bern, Switzerland.

Gleadow, A.J.W. (1981) Fission track dating methods: what are the real alternatives? *Nuclear Tracks and Radiation Measurements*, *5*, 3–14.

Gleadow, A.J.W. & Duddy, I.R. (1981) A natural long-term annealing experiment for apatite. *Nuclear Tracks and Radiation Measurements*, *5*, 169–174.

Glotzbach, C., Reinecker, J., Danišik, M., Rahn, M., Frisch, W. & Spiegel, C. (2008) Neogene exhumation history of the Mont Blanc massif, western Alps. *Tectonics*, *27*, TC4011, doi:10.1029/2008TC002257.

Glotzbach, C., Reinecker, J., Danišik, M., Rahn, M., Frisch, W. & Spiegel, C. (2010) Thermal history of the central Gotthard and Aar massifs, European Alps: Evidence for steady state, long-term exhumation. *J Geophys Res*, *115*, F03017, doi:10.1029/2009JF001304.

Glotzbach, C., van der Beek, P., Carcaillet, J. & Delunel, R. (in revision): Deciphering the driving forces of erosion rates on millennial to million year timescales in glacially impacted landscapes, an example from the Western Alps. *J. Geophys. Res.,* in revision.

Glotzbach, C., van der Beek, P. & Spiegel, C. (2011) Episodic exhumation and relief growth in the Mont Blanc massif, Western Alps from numerical modelling of thermochronology data.

Earth and Planetary Science Letters, *304*, 417–430.
Graf, H.R. (2009) Stratigraphie und Morphogenese von frühpleistozänen Ablagerungen zwischen Bodensee und Klettgau. *Quaternary Science Journal*, *58*, 12–53.
Habbe, K.A., Ellwanger, D. & Becker-Haumann, R. (2007) Stratigraphische Begriffe für das Quartär des süddeutschen Alpenvorlandes. *Quaternary Science Journal*, *56*, 66–83.
Haeuselmann, P., Granger, D.E., Jeannin, P.-Y. & Lauritzen, S.-E. (2007) Abrupt glacial valley incision at 0.8 Ma dated from cave deposits in Switzerland. *Geology*, *35*, 143–146.
Hagedorn, E.-M. & Boenigk, W. (2008) The Pliocene and Quaternary sedimentary and fluvial history in the Upper Rhine Graben based on heavy mineral analyses. *Netherlands Journal of Geosciences*, *87*, 21–32.
Hoselmann, C. (2008) The Pliocene and Pleistocene fluvial evolution in the northern Upper Rhine Graben based on results of the research borehole at Viernheim (Hessen, Germany). *Quaternary Science Journal*, *57*, 286–315.
Howat, I.M., Joughin, I., Tulaczyk, S. & Gogineni, S. (2005) Rapid retreat and acceleration of Helheim Glacier, east Greenland. *Geophysical Research Letters*, *32*, L22502, doi:10.1029/2005GL024737.
Hunze, S. & Wonik, T. (2008) Sediment Input into the Heidelberg Basin as determined from Downhole Logs. *Quaternary Science Journal*, *57*, 367–381.
Hurford, A.J. & Green, P.F. (1983) The zeta age calibration of fission-track dating. *Chem. Geol.*, *41*, 285–317.
Hurford, A.J. (1986) Cooling and uplift patterns in the Lepontine Alps South Central Switzerland and an age of vertical movement on the Insubric fault line. *Contrib Mineral Petrol*, *92*, 413–427.
Ivy-Ochs, S., Poschinger, A.V., Synal, H.-A. & Maisch, M. (2009) Surface exposure dating of the Flims landslide, Graubünden, Switzerland. *Geomorphology*, *103*, 104–112.
Keller, L.M., Hess, M., Fügenschuh, B. & Schmid, S. (2005) Structural and metamorphic evolution of the Camughera–Moncucco, Antrona and Monte Rosa units southwest of the Simplon line, Western Alps. *Eclogae geol. Helv.*, *98*, 19–49.
Keller, J., Kraml, M. & Henjes-Kunst, F. (2002) $^{40}Ar/^{39}Ar$ single crystal dating of early volcanism in the Upper Rhine Graben and tectonic implications. *Schweiz. Mineral. Petrogr. Mitt.*, *82*, 121–130.
Knipping, M. (2008) Early and Middle Pleistocene pollen assemblages of deep core drillings in the northern Upper Rhine Graben, Germany. *Netherlands Journal of Geosciences*, *87*, 51–65.
Koppes, M.N. & Montgomery, D.R. (2009) The relative efficacy of fluvial and glacial erosion over modern to orogenic timescales. *Nature Geosciences*, *2*, doi:10.1038/NGEO616.
Kuhlemann, J., Frisch, W., Székely, B., Dunkl, I. & Kázmer, M. (2002) Post-collisional sediment budget history of the Alps: tectonic versus climatic control. *Int J Earth Sci*, *91*, 818–837.
Kuhlemann, A. & Kempf, O. (2002) Post-Eocene evolution of the North Alpine Foreland Basin and its response to Alpine tectonics. *Sedimentary Geology*, *152*, 45–78.
Larsen, I.J. & Montgomery, D.R. (2012) Landslide erosion coupled to tectonics and river incision. *Nature Geoscience*, *5*, doi:10.1038/NGEO1479.
Lauer, T., Frechen, M., Hoselmann, C. & Tsukatomo, S. (2010) Fluvial aggradation phases in the Upper Rhine Graben - new insights by quartz OSL dating. *Proceedings of the Geologists' Association*, *121*, 154–161.
Link, K. (2010) *Die thermo-tektonische Entwicklung des Oberrheingraben-Gebietes seit der Kreid*e. Ph.D. thesis, Albert-Ludwigs Universität Freiburg, Germany, URL: http://www.freidok.uni-freiburg.de/volltexte/7847/.
Lippolt, HJ., Gentner, W. & Wimmenauer, W. (1963) Altersbestimmungen nach der Kalium-Argon-

Methode an tertiären Eruptivgesteinen Südwestdeutschlands. *Jh. geol. Landesamt Baden-Württemberg*, *6*, 507–538.

Litt, T. (2007) Das Quartär als chronostratigraphische Einheit. *Quaternary Science Journal*, *57*, 3–6.

Litt, T., Ellwanger, D., Villinger, E. & Wansa, S. (2005) Das Quartär in der Stratigraphischen Tabelle von Deutschland 2002. *Newsletters on Stratigraphy*, *41*, 385–399.

Litt, T., Schmincke, H.-U., Frechen, M. & Schlüchter, C. (2008) *Quaternary*. In: The Geology of Central Europe – Vol. 2: Mesozoic and Cenozoic (Ed. by T. McCann), pp. 1287–1340, The Geological Society, London.

Michalski, I. & Soom, M. (1990) The Alpine thermo-tectonic evolution of the Aar and Gotthard massifs, Central Switzerland: Fission Track ages on zircon and apatite and K-Ar mica ages. *Schweiz. Mineral. Petrogr. Mitt.*, *70*, 373–387.

Miller, G.H., Briner, J.P., Lifton, N.A. & Finkel, R.C. (2006) Limited ice-sheet erosion and complex exposure histories derived from in situ cosmogenic ^{10}Be, ^{26}Al, and ^{14}C on Baffin Island, Arctic Canada. *Quaternary Geochronology*, *1*, 74–85.

Muttoni, G., Carcano, C., Garzanti, E., Ghielmi, E.M., Piccin, A., Pini, R., Rogledi, S. & Sciunnach, D. (2003) Onset of major Pleistocene glaciations in the Alps. *Geology*, *31*, 989–992.

Nie, J., Horton, B.K., Saylor, J.E., Mora, A., Mange, M., Garzione, C.N., Basu, A., Moreno, C.J., Caballero, V. & Parra, M. (2012) Integrated provenance analysis of a convergent retroarc foreland system: U–Pb ages, heavy minerals, Nd isotopes, and sandstone compositions of the Middle Magdalena Valley basin, northern Andes, Colombia. *Earth Science Reviews*, *110*, 111–126.

Pignalosa, A., Zattin, M., Massironi, M. & Cavazza, W. (2011) Thermochronological evidence of a late Pliocene climate-induced erosion rate increase in the Alps. *Int J Earth Sci*, *100*, 847–859.

Preusser, F., Graf, H.R., Keller, O., Krayss, E. & Schlüchter, C. (2011) Quaternary glaciation history of northern Switzerland. *Quaternary Science Journal*, *60*, 282–305.

Rahn, M.K., Hurford, A.J. & Frey, M. (1997) Rotation and exhumation of a thrust plane: Apatite fission-track data from the Glarus thrust, Switzerland. *Geology*, *25*, 599–602.

Rahn, M.K. & Selbekk, R. (2007) Absolute dating of the youngest sediments of the Swiss Molasse basin by apatite fission track analysis. *Swiss J Geosci*, *100*, 371–381.

Reinecker, J., Danišik, M., Schmid, C., Glotzbach, C., Rahn, M., Frisch, W. & SPIEGEL, C. (2008) Tectonic control on the late stage exhumation of the Aar Massif (Switzerland): Constraints from apatite fission track and (U-Th)/He data. *Tectonics*, *27*, TC6009, doi:10.1029/2007TC002247.

Reinecker, J. & Kuhlemann, J (2008) Timing of orogen-parallel Rhône valley incision, Switzerland. *Geophysical Research Abstracts*, *10*, EGU2008-A-00000.

Reiter, W., Elfert, S., Glotzbach, C. & Spiegel, C. (in preparation) Plio-Pleistocene evolution of the north-Alpine drainage system – implications from Neogene foreland deposits.

Rignot, E., Rivera, A. & Casassa, G. (2003) Contribution of the Patagonia Icefields of South America to Sea Level Rise. *Science*, *302*, 434–437.

Rolf, C., Hambach, U. & Weidenfeller, M. (2008) Rock and palaeomagnetic evidence for the Plio-Pleistocene palaeoclimatic change recorded in Upper Rhine Graben sediments (Core Ludwigshafen-Parkinsel). *Netherlands Journal of Geosciences*, *87*, 41–50.

Rotstein, Y. & Schaming, M. (2011) The Upper Rhine Graben (URG) revisited: Miocene transtension and transpression account for the observed first-order structures. *Tectonics*, *30*, TC3007, doi:10.1029/2010TC002767.

Schaer, J.P., Reimer, G.M. & Wagner, G.A. (1975) Actual and ancient uplift rate in the Gotthard region, Swiss Alps: A comparison between precise levelling and fission-track apatite age. *Tectonophysics*, *29*, 293–300.

Schlunegger, F. & Mosar, J. (2011) The last erosional stage of the Molasse Basin and the Alps. *Int J Earth Sci*, *100*, 1147–1162.

Schlunegger, F., Rieke-Zapp, D. & Ramseyer, K. (2007) Possible environmental effects on the evolution of the Alps-Molasse Basin system. *Swiss J. Geosci.*, *100*, 383–405.

Schmid, S.M., Fügenschuh, B., Kissling, E. & Schuster, R. (2004) Tectonic map and overall architecture of the Alpine orogen. *Eclogae geol Helv*, *97*, 93–117.

Schreiner, A. (1992) *Erläuterungen zu Blatt Hegau und westlicher Bodensee*. Geologisches Landesamt Baden-Württemberg, Freiburg, Stuttgart.

Shuster, D.L., Ehlers, T.A., Rusmore, M.E. & Farley, K.A. (2005) Rapid Glacial Erosion at 1.8 Ma Revealed by $^{4}He/^{3}He$ thermochronometry. *Science*, *310*, 1668–1670.

Sissing, W. (1998) Comparative Tertiary stratigraphy of the Rhine Graben, Bresse Graben and Molasse Basin: correlation of Alpine foreland events. *Tectonophysics*, *300*, 249–284.

Soom, M. (1990) *Abkühlungs- und Hebungsgeschichte der Externmassive und der penninischen Decken beidseits der Simplon-Rhône-Linie seit dem Oligozän: Spaltspurendatierung an Apatit/Zirkon und K-Ar-Datierungen an Biotit/Muskovit (Westliche Zentralalpen)*. Ph.D. thesis, University of Bern, Switzerland.

Spiegel, C., Kohn, B., Belton, D., Berner, Z. & Gleadow, A. (2009) Apatite (U–Th–Sm)/He thermochronology of rapidly cooled samples: The effect of He implantation. *Earth and Planetary Science Letters*, *285*, 105–114.

Spiegel, C., Kohn, B., Raza, A., Rainer, T. & Gleadow, A. (2007) The effect of long-term low-temperature exposure on apatite fission track stability: A natural annealing experiment in the deep ocean. *Geochimica et Cosmochimica Acta*, *71*, 4512–4537.

Spiegel, C., Kuhlemann, J., Dunkl, I. & Frisch, W. (2001) Paleogeography and catchment evolution in a mobile orogenic belt: the Central Alps in Oligo–Miocene times. *Tectonophysics*, *341*, 33–47.

Spiegel, C., Kuhlemann, J., Dunkl, I., Frisch, W., von Eynatten, H. & Balogh, K. (2000) The erosion history of the Central Alps: evidence from zircon fission track data of the foreland basins. *Terra Nova*, *12*, 163–170.

Spiegel, C., Siebel, W., Kuhlemann, J. & Frisch, W. (2004) *Toward a comprehensive provenance analysis: A multi-method approach and its implications for the evolution of the Central Alps*. In: "Detrital thermochronology – Provenance Analysis, Exhumation, and Landscape Evolution in Mountain Belts" (Ed. by M. Bernet and C. Spiegel). pp. 37–50, GSA Special Paper 378.

Steck, A. & Hunziker, J. (1994) The Tertiary structural and thermal evolution of the Central Alps - compressional and extensional structures in an orogenic belt. *Tectonophysics*, *238*, 229–254.

Steiner, H. (1984) Mineralogisch-petrographische, geochemische und isotopengeologische Untersuchungen an einem Meta-Lamprophyr und seinem granodioritischen Nebengestein (Matorello-Gneis) aus der Maggia-Decke. *Schweiz. Mineral. Petrogr. Mitt.*, *64*, 227–259.

Stewart, R.J. & Brandon, M.T. (2004) Detrital-zircon fission-track ages for the "Hoh Formation": Implications for late Cenozoic evolution of the Cascadia subduction wedge. *Geological Society of America Bulletin*, *116*, 60–75.

Sue, C., Delacou, B., Champagnac, J.-D., Allanic, C., Tricart, P. & Burkhard, M. (2007) Extensional neotectonics around the bend of the Western/Central Alps: an overview. *Int J Earth Sci*, *96*, 1101–1129.

Teichmüller, R. & Teichmüller, M. (1986) Relations between coalification and palaeogeothermics in

Variscan and Alpidic foredeeps of western Europe. *Paleogeothermics, Lecture Notes in Earth Sciences*, *5*, 53–78.

Thomson, S.N., Brandon, M.T., Tomkin, J.H., Reiners, P.W., Vásquez, C. & Wilson, N.J. (2010) Glaciation as a destructive and constructive control on mountain building. *Nature*, *467*, doi:10.1038/nature09365.

Timar-Geng, Z., Fügenschuh, B., Wetzel, A. & Dresmann, H. (2006) Low-temperature thermochronology of the flanks of the southern Upper Rhine Graben. *Int J Earth Sci*, *95*, 685–702.

Timar-Geng, Z., Grujic, D. & Rahn, M. (2004) Deformation at the Leventina–Simano nappe boundary, Central Alps, Switzerland. *Eclogae geol. Helv.*, *97*, 265–278.

Trautwein, B., Dunkl, I. & Frisch, W. (2001) Accretionary history of the Rhenodanubian Flysch zone in the Eastern Alps – evidence from apatite fission-track geochronology. *Int J Earth Sci*, *90*, 703–713.

Valla, P.G., Shuster, D.L. & van der Beek, P. (2011) Significant increase in relief of the European Alps during mid-Pleistocene glaciations. *Nature Geoscience*, *4*, 688–692.

Valla, P.G., van der Beek, P., Shuster, D., Braun, J., Herman, F., Tassan-Got, L. & Gautheron, C. (2012) Late-Neogene exhumation and relief development of the Aar and Aiguilles Rouges massifs (Swiss Alps) from low-temperature thermochronology modeling and $^{4}He/^{3}He$ thermochronometry. *J. Geophys. Res.*, *117*, F01004.

Vermeesch, P. (2004) How many grains are needed for a provenance study? *Earth and Planetary Science Letters*, *224*, 441–451.

Vernon, A., van der Beek, P.A., Sinclair, H.D., Persano, C., Foeken, J. & Stuart, F.M. (2009) Variable late Neogene exhumation of the central European Alps: Low-temperature thermochronology from the Aar Massif, Switzerland, and the Lepontine Dome, Italy. *Tectonics*, *28*, TC5004, doi:10.1029/2008TC002387.

Vernon, A.J., van der Beek, P.A., Sinclair, H.D. & Rahn, M.K. (2008) Increase in late Neogene denudation of the European Alps confirmed by analysis of a fission-track thermochronology database. *Earth and Planetary Science Letters*, *270*, 316–329.

Villinger, E. (1998) Zur Flussgeschichte von Rhein und Donau in Südwestdeutschland. *Jahresberichte und Mitteilungen des Oberrheinischen Geologischen Vereins, 80*, 361–398.

Villinger, E. (2003) Zur Paläogeographie von Alpenrhein und oberer Donau. *Zeitschrift der deutschen geologischen Gesellschaft*, *154*, 193–253.

Von Hagke, C., Cederbom, C.E., Oncken, O., Stöckli, D.F., Rahn, M.K. & Schlunegger, F. (2012) Linking the northern Alps with their foreland: The latest exhumation history resolved by low-temperature thermochronology. *Tectonics*, *31*, TC5010, doi:10.1029/2011TC003078.

Wagner, G.A. & Reimer, G.M. (1972) Fission track tectonics: The tectonic interpretation of fission track apatite ages. *Earth and Planetary Science Letters*, *14*, 263–268.

Wagner, G.A., Reimer, G.M. & Jager, E. (1977) Cooling ages derived by apatite fission-track, mica Rb-Sr and K-Ar dating: The uplift and cooling history of the Central Alps. *Mem Ist Geo Min Univ Padova*, Vol. XXX.

Wedel, J. (2008) Pleistocene molluscs from research boreholes in the Heidelberg Basin. *Quaternary Science Journal*, *57*, 382–402.

Weh, M. (1998) *Tektonische Entwicklung der penninischen Sediment-Decken in Graubünden (Prättigau bis Oberhalbstein)*. Ph.D. thesis, University Basel, Switzerland.

Weidenfeller, M. & Kärcher, T. (2008) Tectonic influence on fluvial preservation: aspects of the architecture of Middle and Late Pleistocene sediments in the northern Upper Rhine Graben, Germany. *Netherlands Journal of Geosciences*, *87*, 33–40.

Weidenfeller, M. & Knipping, M. (2008) Correlation of Pleistocene sediments from boreholes in the

Ludwigshafen area, western Heidelberg Basin. *Quaternary Science Journal*, *57*, 270–285.
Willenbring Staiger, J., Gosse, J., Little, E.C., Utting, D.J., Finkel, R., Johnson, J.V. & Fastook, J. (2006) Glacial erosion and sediment dispersion from detrital cosmogenic nuclide analyses of till. *Quaternary Geochronology*, *1*, 29–42.
Willett, S.D., Schlunegger, F. & Picotti, V. (2006) Messinian climate change and erosional destruction of the central European Alps. *Geology*, *34*, 613–616.
Wolf, R.A., Farley, K.A. & Kass, D.M. (1998) Modeling of the temperature sensitivity of apatite (U-Th)/He thermochronometer. *Chemical Geology*, *148*, 105–114.
Ziegler, P.A. & Dèzes, P. (2007) Cenozoic uplift of Variscan Massifs in the Alpine foreland: Timing and controlling mechanisms. *Global and Planetary Change*, *58*, 237–269.
Ziegler, P.A. & Fraefel, M. (2009) Response of drainage systems to Neogene evolution of the Jura fold-thrust belt and Upper Rhine Graben. *Swiss J. Geosci.*, *102*, 57–75.

6.10 Supplement

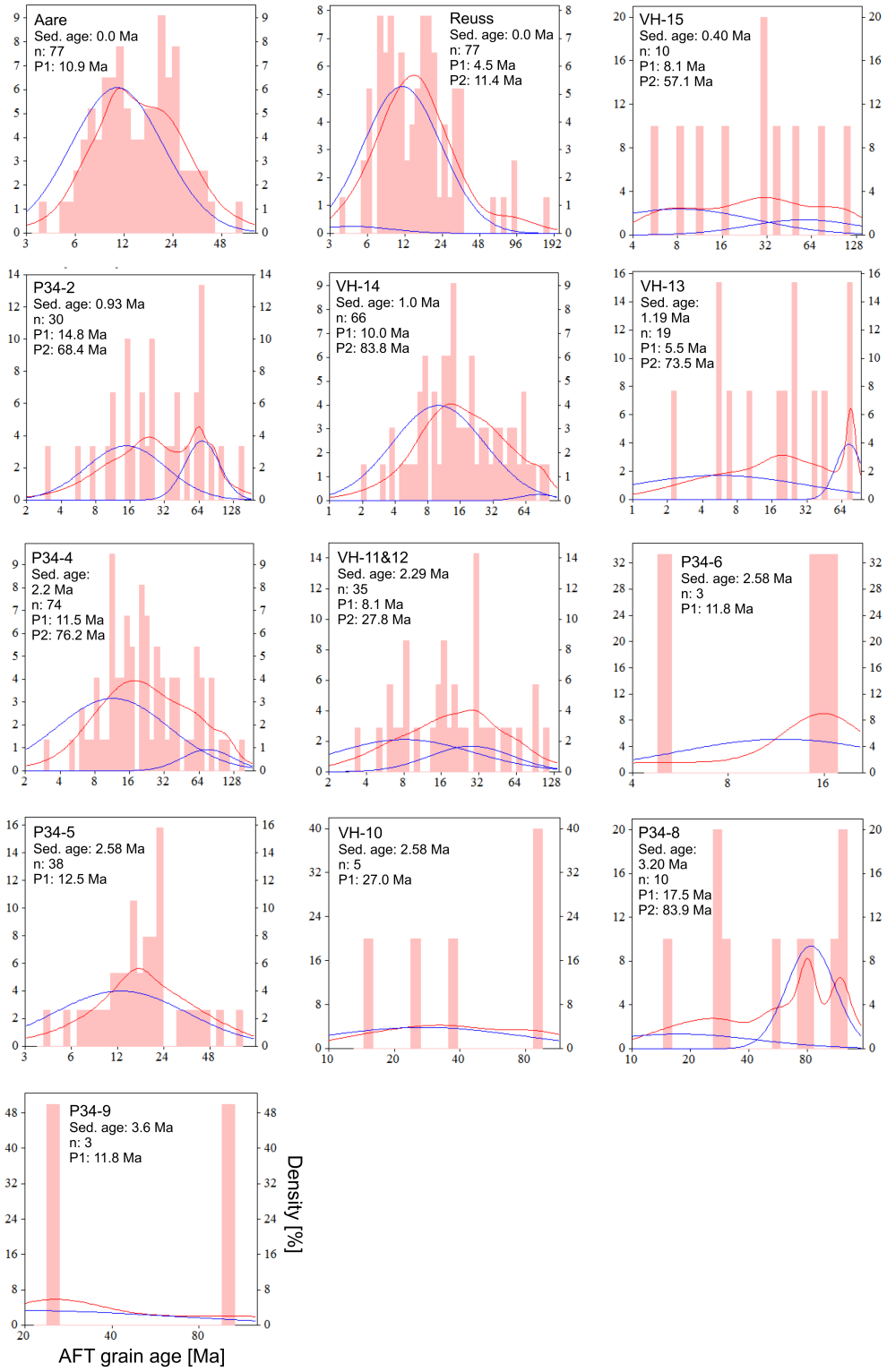

Fig. DR-6.1: Probability-density plots of AFT grain ages (AFT ages vs. density). Sample name, depositional age (Sed. age), number of counted grains (n) and modelled peak ages (P1/P2) are given.

7 Second paper:

Plio-Pleistocene evolution of the north-Alpine drainage system – implications from Neogene foreland deposits

Wolfgang Reiter[1*], Simon Elfert[1], Christoph Glotzbach[2] and Cornelia Spiegel[1]

[1]*Department of Geosciences, University of Bremen, Germany*
[2]*Institute of Geosciences, University of Hannover, Germany*

[*]Corresponding author: Wolfgang Reiter, Department of Geosciences, University of Bremen, Klagenfurter Strasse, 28359 Bremen, Germany. E-mail address: wreiter@uni-bremen.de

7.1 Abstract

The evolution of drainage systems in and around active orogens may be strongly affected by climatic or tectonic processes. Information on the drainage evolution is stored in the sediments of the foreland depocenters. We investigated the provenance of two key deposits adjacent to the Central Alps, the Pliocene Sundgau gravel and the Pleistocene Höhere Deckenschotter by detrital thermochronology. Based on these data, and on provenance information from Rhine Graben deposits, we propose a reconstruction of the north-Alpine drainage system since the middle Pliocene, and discuss potential controlling mechanisms. Our data show that the Rhine Graben received detritus from the Alpine realm already during the Pliocene, incidating two different river systems – the proto-Rhine and the Aare-Doubs – draining the Alpine realm towards the North Sea and Mediterranean Sea. The investigated sediments contained detritus from two central-Alpine sources, one showing a regional exhumational equilibrium, and the other characterized by increasing exhumation rates. Discharge of the latter source ceased after ~2 Ma, reflecting a northward shift of the main Alpine drainage divide. Between ~2.0 and 1.2 Ma, the drainage system was affected by a major change, which we explain as resulting from a change of the Alpine stress field leading to tectonic exhumation and topography reduction in the area of the southern Aar massif. Generally, it seems that between ~4 and 1.2 Ma, the drainage system was mainly controlled by tectonic processes, despite first glaciations that already affected the north-Alpine foreland by ~2 Ma. The drainage system only seems to have reacted to the late Cenozoic climate changes after ~1.2 Ma, i.e., at the time of the most intense Alpine glaciation. At that time, the course of the Rhine river shifted towards the area of the Hegau volcanics, and the size of the Rhine river catchment became strongly reduced.

7.2 Introduction

The drainage system of an active orogenic environment controls the deposition patterns of the adjacent sedimentary basins. It is strongly influenced by topographic changes, which in turn are the results of tectonic and climatic processes. The exact relations between climate, tectonic and

topographic changes on the one hand, and drainage and sediment deposition patterns on the other hand are still not fully understood. Here, we study the Plio-Pleistocene drainage evolution of the north-Alpine realm and relate it to climatic and tectonic processes. As a basis, we use the previously published drainage reconstructions by Liniger (1966), Giamboni *et al.* (2004), Berger *et al.* (2005), and Ziegler & Fraefel (2009) and refine them by applying thermochronological dating methods to key sedimentary deposits adjacent to the Central Alps. Previous sediment provenance analyses were mainly based on petrographic studies, i.e., clast compositions of conglomerates and heavy mineral compositions of sandstones. These, however, may yield ambiguous results (e.g., Spiegel *et al.*, 2002). Using detrital thermochronology, i.e., comparing cooling age patterns of detrital sediments with those of potential source areas, allows a more precise provenance analysis. Furthermore, detrital thermochronology yields information on paleo-exhumation rates of the catchment and thus allows to directly relating the geodynamic evolution of the hinterland to the drainage evolution of the foreland.

For this study, we combine recently published apatite fission track (AFT) and apatite (U-Th-Sm)/He analysis (AHe) from the Upper Rhine Graben (Reiter *et al.*, in press) with new data from the Sundgau gravel and the Höhere Deckenschotter. The Upper Rhine Graben is one of the major circum-Alpine depocenters during the Late Neogene. The deposition of the Sundgau gravel marks one of the main changes of the north-Alpine drainage network, while the Höhere Deckenschotter is the oldest deposit of Alpine lowland glaciation and represents the major glacial drainage network of the Swiss foreland (Graf, 1993). Our main goals are: Firstly, identifying the source areas of the analysed sediment deposits, secondly, using these provenance information for reconstructing the evolution of the drainage system since the Pliocene, and thirdly, obtaining a more general understanding of drainage network evolution, and its relation to climatic and tectonic changes.

7.3 Geological setting

7.3.1 Geological setting and age patterns of potential source areas

The major entities of the study area are the Central (and Eastern) Alps in the south(west), bordered towards the northwest by the Swiss Molasse basin, the Jura mountains, the Bresse Graben, the Rhine Graben, and the Black Forest and Vosges (Fig. 7.1). The Central Alps comprise the Aar-Gotthard massif, which belongs to the Alpine external massifs (Helvetic realm, European crust), and the Lepontine Dome (Penninic realm, European continental crust and oceanic crust). The Aar-Gotthard massif is mostly composed of magmatic and metamorphic rocks predominantly of Variscan age, which experienced a low-grade metamorphic overprint during Alpine orogeny. Most of the Aar-Gotthard massif is constantly exhumed at steady rates since the Late Miocene (Glotzbach *et al.*, 2010). Only the southwesternmost part of the Aar-Gotthard massif shows a different cooling pattern, with accelerated exhumation since ~3.5 Ma, presumably due to normal faulting activity along the adjacent Rhône line (Reinecker *et al.*, 2008). AFT cooling ages of the Aar-Gotthard massif range between 3 and 15 Ma, but are mostly between 6 and 10 Ma (Reinecker *et al.*, 2008, Glotzbach *et al.*, 2010, and references therein; Fig. 7.2). AHe ages vary between 2 and 9 Ma (Reinecker *et al.*, 2008, Vernon *et al.*, 2009, Glotzbach *et al.*, 2010). AFT cooling ages of the Lepontine area range between 2 and 19 Ma (Vernon *et al.*, 2008, and references therein, Pignalosa *et al.*, 2010; Elfert *et al.*, 2011; Fig. 7.2), with a trend to older ages at the northern and southern periphery. Thus, AFT age patterns of Aar-Gotthard massif and Lepontine Dome overlap, but the exposures of the Lepontine area also contain old AFT ages >14 Ma, which are not observed in the Aar-Gotthard massif. The Central Alps are bordered by the Silvretta nappe of the Eastern Alps

(Austroalpine realm, Adriatic crust). Its AFT ages are between 11 and 31 Ma, but are mostly older than 20 Ma (Hurford, 1989; Fig. 7.2). To the north, the Eastern Alps are bordered by the Rhenodanubian Flysch, whose western part also extends into the area west of Lake Constance. Its AFT ages range between 17 and 136 Ma (Trautwein *et al.*, 2001; Fig. 7.2).

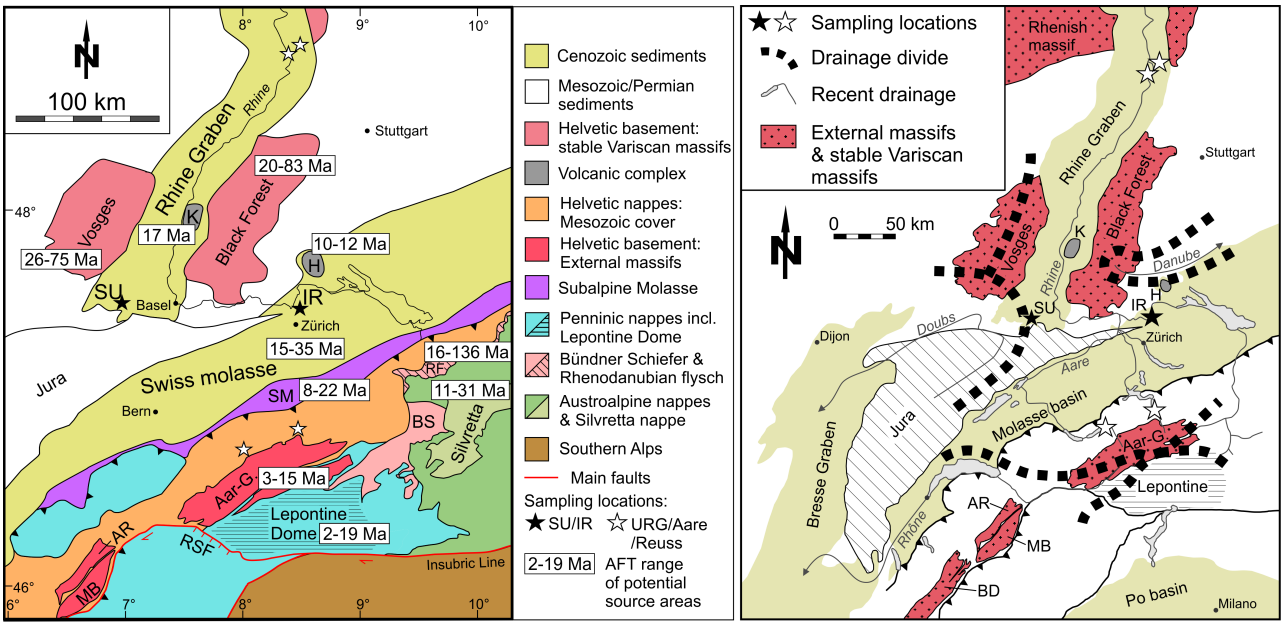

Fig. 7.1: (left) Simplified geological map (modified after Schmid *et al.*, 2004) of the potential source areas with their AFT ranges (Hurford *et al.*, 1989; Trautwein *et al.*, 2001; Timar-Geng *et al.*, 2006; Rahn & Selbekk, 2007; Reinecker *et al.*, 2008; Vernon *et al.*, 2008 and references therein; Danišik *et al.*, 2010; Glotzbach *et al.*, 2010; Link, 2010; Elfert *et al.*, 2011). Black-filled stars, sampling locations of the Sundgau gravel and Höhere Deckenschotter; white-filled stars, sampled borehole sites of the Upper Rhine Graben (for details see Reiter *et al.*, in press). (right) Overview of present-day north-Alpine drainage system (modified after Berger *et al.*, 2005, Giamboni *et al.*, 2004, and Ziegler & Fraefel, 2009). AR, Aiguilles Rouges; Aar-G., Aar-Gotthard massif; BD, Belledonne; BS, Bündner Schiefer; H, Hegau; IR, Höhere Deckenschotter (Irchel); K, Kaiserstuhl; MB, Mont Blanc; RF, Rhenodanubian flysch; RSF, Rhône-Simplon fault; SM, Subalpine Molasse; SU, Sundgau gravel (Seppois).

Adjacent to the Central Alps is the Swiss Molasse basin, containing syntectonic sediments deposited during the Oligocene to Miocene. The Swiss Molasse basin is subdivided into the proximal Subalpine Molasse deformed by the Alpine orogeny, and the more distal and largely undeformed Plateau Molasse. AFT ages from surface exposures of the Subalpine Molasse range between 8 and 22 Ma, and from the Plateau Molasse between 15 and 35 Ma (Vernon *et al.*, 2008, and references therein; Cederbom *et al.*, 2011), with the majority of ages around 30 Ma. The Jura mountains were also folded in the course of the Alpine orogeny. Thin-skinned tectonics started at ~9 Ma, changing to probably still ongoing thick-skinned tectonics in the Late Pliocene (Becker, 2000; Ustaszewski & Schmid, 2007). Since the Jura mountains are predominantly composed of limestone, they do not contain apatite, so that no AFT or AHe data are available. The Rhine and Bresse Graben opened simultaneously during the Paleogene (e.g., Dèzes *et al.*, 2004). They are linked by a sinistral transtensive fault zone called the Rhine-Bresse Transfer Zone. The flanks of the Upper Rhine Graben are formed by the Variscan basement and sedimentary cover of the Black Forest and the Vosges. These two areas are characterized by AFT ages ranging between 20 and 83 Ma, but are

mostly older than 30 Ma. AHe ages vary between ~8 and 190 Ma but are mostly between 20 and 50 Ma (Timar-Geng *et al.*, 2006; Danišik *et al.*, 2010; Link, 2010). Graben formation was accompanied by volcanic activity, most notably of the Kaiserstuhl (between ~18 and 15 Ma; Lippolt *et al.*, 1963; Keller *et al.*, 2002) and the Hegau area (between ~14 and 9 Ma; Schreiner, 1992; Rahn & Selbekk, 2007).

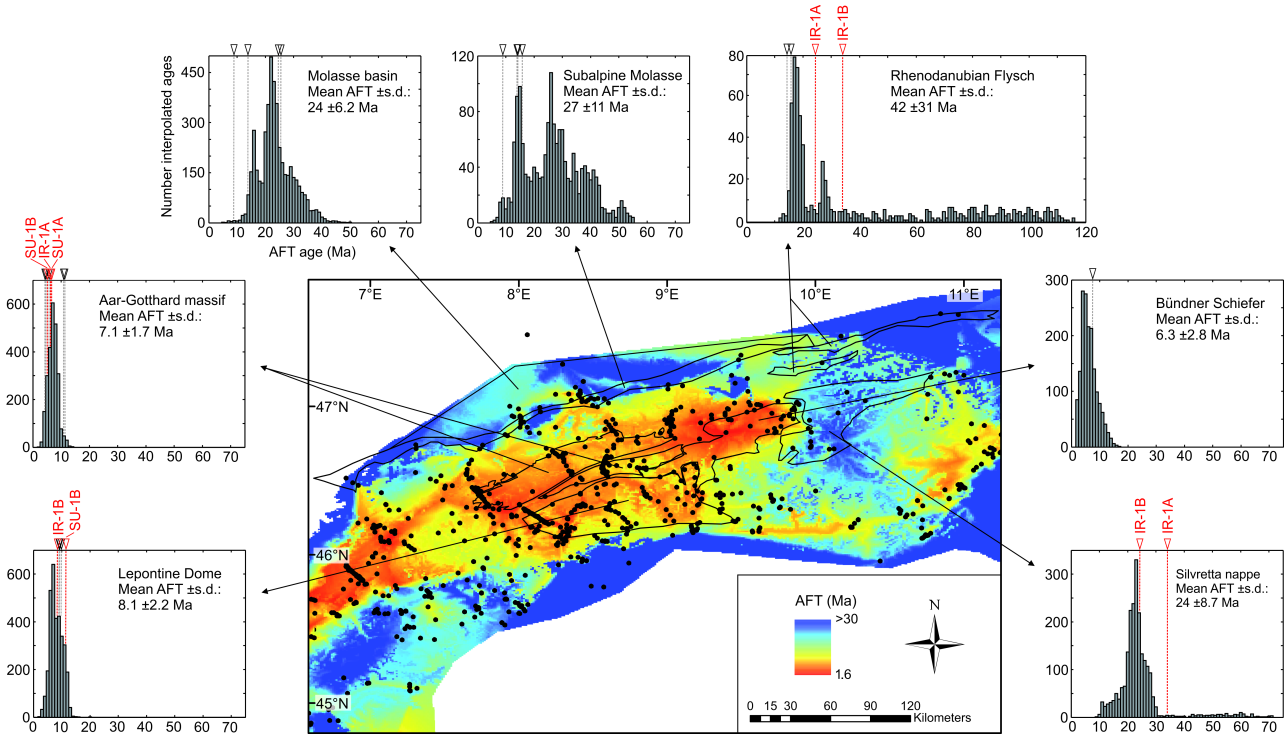

Fig. 7.2: Interpolated surface AFT age distribution of the Central Alps with age probability-density plots for the individual potential source area which are outlined in black. The interpolation is based on a collection of thermochronological data from hard rock and detrital studies of the Western and Central Alps (for further details see Glotzbach *et al.*, in revision). Red arrows show the lag times of AFT peak ages from the Sundgau gravel and the Höhere Deckenschotter, and black arrows show the lag times of Rhine Graben samples and two modern Rhine tributaries from Reiter *et al.* (in press). S.d. means standard deviation of the interpolated mean AFT age. Source area AFT data are compiled from the following studies: [i] *Aar-Gotthard massif*: Wagner & Reimer (1972), Schaer *et al.* (1975), Wagner *et al.* (1977), Michalski & Soom (1990), Soom (1990), Glotzbach *et al.* (2008), Reinecker *et al.* (2008), Vernon *et al.* (2008, 2009), Glotzbach *et al.* (2010), and unpublished data from Meinert Rahn; [ii] *Subalpine Molasse*: Cederbom *et al.* (2004), Rahn *et al.* (1997), von Hagke *et al.* (2012), and unpublished data from Meinert Rahn; [iii] *Rhenodanubian Flysch*: Trautwein *et al.* (2001); [iv] *Bündner Schiefer*: Michalski & Soom (1990), Weh (1998), and unpublished data from Meinert Rahn; [v] *Lepontine Dome*: Wagner & Reimer (1972), Wagner *et al.* (1977), Steiner (1984), Hurford (1986), Soom (1990), Giger (1991), Ciancaleoni (2004), Timar-Geng *et al.* (2004), Keller *et al.* (2005), Pignalosa *et al.* (2011), Vernon *et al.* (2009), and unpublished data from Simon Elfert and Meinert Rahn; [vi] *Molasse basin*: Cederbom *et al.* (2004), von Hagke *et al.* (2012), and unpublished data from Meinert Rahn; [vii] *Silvretta nappe*: Wagner *et al.* (1977), Flisch (1986).

7.3.2 Drainage evolution of the central-Alpine realm since the Late Miocene

Fig. 7.1 shows the recent drainage pattern of the north-Alpine realm with the three principal drainage systems, i.e., the Danube river system draining towards the Black Sea, the Rhône river

system draining towards the Mediterranean Sea, and the Rhine river system draining towards the North Sea. In the following, the north-Alpine drainage evolution since the late Miocene is briefly outlined:

In the Late Miocene, the sedimentation of the northern Alpine molasse ceased (Berger, 1985; Kuhlemann & Kempf, 2002). The molasse sediments contain primarily detritus derived from the Alps, but also detritus from the Vosges-Black Forest arch in the north (Füchtbauer 1959; Sissingh, 2006). Between the late Miocene and the early Pliocene, the folding of the Jura mountains (e.g., Laubscher, 1986; Madritsch *et al.* 2008), caused the division of the former southwestern sediment pathway into two drainage systems with different directions: *(i)* the proto-Doubs river, which drained the northern Jura mountains and most of the Vosges-Black Forest arch towards the Mediterranean, and *(ii)* the Aare-Danube river system, which drained the southern Jura mountains, the eastern Black Forest, and the Alps towards the east (e.g., Liniger, 1966; Ziegler & Fraefel, 2009).

Progressive subsidence of the Bresse Graben caused the separation of the paleo-Aare from the Danube drainage system and the deflection of the paleo-Aare towards the west at ~4.2 Ma (e.g., Ziegler & Dézes, 2007; Ziegler & Fraefel, 2009). This led to the amalgamation of the paleo-Aare with the proto-Doubs resulting in the Aare-Doubs river system, which transported central-Alpine detritus towards the Mediterranean Sea via the Bresse Graben. According to Giamboni *et al.* (2004) and to Ziegler & Fraefel (2009), the main drainage divide between the North Sea and the Mediterranean Sea was situated in the central part of the southern Rhine Graben, approximately in the Kaiserstuhl area. The Aare-Doubs river deposited the Sundgau gravel at the junction between the northern Jura mountains and the southern Rhine Graben between ~4.2 and 2.9 Ma (Fig. 7.1; e.g., Liniger, 1966, 1967; Petit *et al.*, 1996). Based on their clast composition, the Sundgau gravel may either represent recycled sediments from the Swiss Molasse basin as suggested, e.g., by Schlunegger & Mosar (2011) or they may predominantly be derived from a central-Alpine source, as assumed by Liniger (1966, 1967). Regarding the Alpine hinterland, Schlunegger *et al.* (2007) suggested that during the Pliocene, the main Alpine drainage divide shifted from the core region of the Central Alps, i.e., the Lepontine Dome, towards the north into the Aar-Gotthard massif.

Around the Plio-Pleistocene boundary (~2.59 Ma), uplift of the Bresse Graben and coeval subsidence of the southern Rhine Graben led to the deflection of the paleo-Aare to the north into the Rhine Graben and finally to the amalgamation with the proto-Rhine. The drainage divide between the North Sea and the Mediterranean Sea shifted towards the south, now being situated at the southern end of the Rhine Graben and the northern Jura mountains. The Central Alps were drained by the Aare-Rhine river towards the North Sea and by the Rhône river towards the Mediterranean Sea. At about the same time, the drainage system of the Central Alpine hinterland may have changed from orogen-perpendicular to orogen-parallel (Berger *et al.*, 2005, their Fig. 20). The northward deflection of the Aare and the establishment of the Aare-Rhine river system also led to a change in the composition of the Rhine Graben sediments: at the Plio-Pleistocene boundary, the heavy mineral composition changes from a stable, zircon-rutile-turmaline-dominated suite assumed to be derived from the Variscan graben shoulders and their sedimentary cover towards an instable, garnet-epidote-dominated suite assumed to be derived from the Alps (Hagedorn & Boenigk, 2008; Hoselmann, 2008).

In the Early Pleistocene, first glacial cycles affected the Alpine realm leaving fluvio-glacial deposits behind. One of the earliest preserved fluvio-glacial deposits are the Höhere Deckenschotter of the Swiss Molasse basin, which were delivered by the glacier system of the Central Alps (Bolliger *et al*., 1996; Graf, 2009). At ~1.7 Ma, ongoing subsidence of the Upper Rhine Graben caused eastwards directed incision of the Aare-Rhine tributaries towards the Danube system (Ziegler & Fraefel, 2009). The separation process of the Alpine Rhine from the Danube system and

its deflection towards the Upper Rhine Graben is assumed to has been largely finished with the Günz glacial at ~0.8 Ma (Villinger, 1998, 2003; Litt *et al.*, 2005; Habbe *et al.*, 2007), or probably has not been finished until the end of the Rissian glacial at ~0.2 Ma (Ellwanger *et al.*, 2011). Maximum glaciation of the Alpine realm was reached during the Pleistocene, presumably around ~1 Ma, with enhanced valley incision in the Alps (e.g., Haeuselmann *et al.*, 2007; Valla *et al.*, 2012), and glaciers reaching far into the southern and northern Alpine forelands (Muttoni *et al.*, 2003; Preusser *et al.*, 2010, 2011).

7.4 Material and methods

7.4.1 Sampling strategy

The Sundgau gravel were deposited at the junction between the Jura fold belt and the Upper Rhine Graben between ~4.2 and 2.9 Ma by a braided-river system (Petit *et al.*, 1996). Their deposition marks the westward deflection of the paleo-Aare and the new establishment of the westwards-draining Aare-Doubs river system. Two gravel pits close to the villages of Seppois le Haute (also described by Ustaszewski & Schmid, 2007) and Seppois le Bas were sampled. The Sundgau gravel at these particular sites are grain-supported conglomerates with intercalated sand lenses and layers. The clasts are poorly sorted and range in size from ~2 to 40 cm. They comprise dark schists, cherts, rhyolites, flysch, limestones, quartzites, and granitic rocks. Most of the granitic rocks are light-coloured, and some of them are slighty deformed with a weak foliation. The sand layers are mostly coarse-grained, poorly sorted, and frequently contain iron-oxide coatings. We took one sample from a sandy lense in the gravel pit of Seppois le Haute, and sampled both the sandy layers and the granitic pebbles in the gravel pit of Seppois le Bas.

In addition, we sampled sediments of the Höhere Deckenschotter. These unconformably cover the Miocene molasse sediments (hence the name, meaning “cover gravel”). The glacio-fluvial Höhere Deckenschotter are the earliest glacial remnants of the Swiss midlands. They consist of channel fillings, representing the north-Alpine glacial network during the early Pleistocene (Graf, 1993). We sampled the well-studied outcrop of Irchel, about 25 km north of Zurich. This outcrop is of particular interest because of two reasons: Firstly, it contains mammal fossils and thus its deposition age was relatively precisely dated by bio- and magnetostratigraphy as 2.1 to 1.8 Ma (Bolliger *et al.*, 1996). And secondly, it is located close to the easternmost extension of the Jura fold belt. Since all major rivers draining the Central Alps were flowing around the Jura mountains, they all crossed the Irchel area on their way to the north or the west. Three samples of the Höhere Deckenschotter were taken at a gravel pit at the foot of the Irchel mountain near Irchel-Ebni. The sampled outcrop comprises clast-supported conglomerates with limestone, silt-/claystone, quartzite, granite and gneiss clasts, interlayered by coarse-grained sandstone. As for the Sundgau gravel, the sand layers as well as the crystalline pebble fraction have been sampled. Since the sandstone sample was very coarse and contained a lot of small pebbles and lithic fragments, we separated it into a coarser (>355 μm) and finer-grained (<355 μm) fraction.

Out of the six samples taken from the Sundgau gravel and the Höhere Deckenschotter, four samples yielded sufficient apatite for further analyses, namely the sandstone and pebble samples from Seppois le Bas and the coarse- and fine-grained sandstone samples from Irchel. Sample coordinates are given in Table 7.1, for further details on sample processing and analysis we refer to the appendix.

7.4.2 Methods and concept of detrital thermochronology

For characterizing the provenance of the sampled sediments, we applied apatite fission track and (U-Th-Sm)/He thermochronology. AFT analysis is based on the accumulation of lattice damages (=fission tracks) in the apatite crystal during exhumation/cooling of the source rock through and below the temperature range of ~110 to 60°C. Fission tracks result from the spontaneous decay of ^{238}U within the apatite crystal through time. At elevated temperatures >~110°C, fission tracks are produced at the same rate as they anneal by diffusion. In the temperature range between ~110 and 60°C (partial annealing zone) fission tracks are partially preserved, and at temperatures below ~60°C, they are nearly stable (e.g., Gleadow & Duddy, 1981). Thus, the track density can be used as a measure for the time elapsed since the source rock cooled below ~110 to 60°C, i.e., since the source rock has reached shallow crustal levels between ~5 and 2 km. Exact temperature sensitivity of apatite depends on its chemical composition (Donelick *et al.*, 1999). The chemical composition also influences the etching velocity, thus the size of the fission track etch pit parallel to the crystallographic c-axis (=Dpar value) is used as a measure for the annealing properties of apatite (Burtner *et al.*, 1994; Donelick *et al.*, 1999). The chemical composition of apatite may also be indicative for its source rock. For instance, apatites derived from strongly alkaline volcanic rocks often show very large Dpar values of 5 µm and more (e.g., Rahn & Selbekk, 2007; Spiegel *et al.*, 2007). We therefore used Dpar-values as an additional provenance indicator for the circum-Alpine foreland sediments.

AHe thermochronology is sensitive to even lower temperatures between ~85 and 40°C (Wolf *et al.*, 1998). It is based on the production of ^{4}He due to decay of U, Th, and Sm in apatite. At temperatures >~85°C, ^{4}He diffuses out of the apatite grain, whereas at temperatures between 85 and 40°C, it is partially retained. At temperatures <40°C, corresponding to a crustal depth of ~1 to 2 km, ^{4}He is nearly completely retained. Thus, the accumulated ^{4}He gives a measure for the time elapsed since the sample has reached shallow crustal levels.

For using detrital thermochronology in provenance analysis, the following requirements have to be met: *(i)* no reheating to temperatures higher than the thermal sensitivity of the thermochronological system post-deposition, and *(ii)* the cooling age signatures between the potential source areas should differ. Regarding the first requirement, the general geological setting, the young deposition age of the sediments as well as their weak lithifications make a deeper burial and thus reheating of the samples highly unlikely. Regarding the second aspect, the different potential source areas as described in the geological setting show distinct age groups, although with some overlap.

For a direct comparison between age patterns of detrital sediments and those of present-day exposures in the foreland, the time elapsed since sediment deposition has to be taken into account. Thus, we are rather using lag times than absolute ages for comparison. Lag time is defined as the difference between the cooling age and the deposition age (Garver *et al.*, 1999). The lag time thus restores the cooling age of the surface exposure in the source region at the time of erosion and sediment deposition (assuming that the time of transport from source to sink is negligible). Furthermore, lag time trends along a stratigraphic section give information on the cooling history of the hinterland, presuming that the source region did not change during deposition. For example, constant lag times upsection (i.e., to stratigraphically younger deposits) indicate exhumational equilibrium of the source area, whereas decreasing lag times reflect accelerated hinterland exhumation. Increasing lag times indicate a slow-down of exhumation rates. However, an increase not only of lag times but also of absolute cooling ages upsection cannot be explained by slower incision into crystalline basement but requires recycling of (thermally unreset) clastic sediments. In summary, detrital thermochronology not only provides provenance information, but it also allows to

connect the provenance information with the geodynamic evolution of the source area. It should, however, be kept in mind that detrital AFT & AHe thermochronology only records erosion and exhumation of lithologies containing apatite. Thus, the contribution of source areas dominated by lithologies such as limestone, mudstone, or fine-grained volcanic rocks is not monitored.

7.5 AFT and AHe thermochronology on Plio-Pleistocene deposits of the Upper Rhine Graben and modern tributaries

In this paragraph, we summarize the main results of AFT and AHe analysis on Plio-Pleistocene fluvial sediments from the Upper Rhine Graben and present-day sediments of the Aare and Reuss rivers (Reiter *et al.,* in press). Originally, these data were used for constraining the paleo-denudation history of the source areas in relation to climate changes and glaciation. Here, we will interpret the data in terms of their provenance information and incorporate these information into the north-Alpine river network reconstructions.

The Plio-Pleistocene sediments are derived from two drill cores taken close to the city of Heidelberg in the northern Upper Rhine Graben. All studied sediments contain AFT age groups >50 Ma, which we interpret as being derived from the Variscan graben shoulders (i.e., Black Forest and Vosges). In the following, we only discuss the provenance of the younger age groups. Apatite yield of Pliocene deposits was extremely poor. However, although poorly defined, the Pliocene sediments contain an age group of ~18 Ma, with lag times of ~15 Ma. These ages are too young to be derived from the European Variscan massifs, but too old to be derived directly from the core regions of the Central Alps. Similar ages occur at the northern rim of the Central Alps (Vernon *et al.*, 2008), in the Subalpine Molasse (Cederbom *et al.*, 2011), and in the Kaiserstuhl volcanics. Volcanic apatites, however, show a characteristic habitus, and the Kaiserstuhl volcanics contain such high-quality apatites that they were even recommended as age standard (Kraml *et al.*, 2007). Similar apatites were (unfortunately) not contained in the Rhine Graben samples, so we exclude a provenance of the 18 Ma age group from the Kaiserstuhl, but instead suggest that apatites of this age were derived from the southern Molasse basin or northern Central Alps.

A major change of the sediment cooling age signature is observed after the Plio-Pleistocene boundary, coeval with the change in the heavy mineral composition. Sediments with deposition ages between 2.6 and 2.2 Ma contain age groups with AFT ages of ~8 Ma and ~12 Ma. Both age groups are interpreted as being derived from the Central Alps. With a lag time of ~6 Ma, the younger age group fits well to the recent age pattern of the Aar-Gotthard massif. Because of the slightly older AFT ages of the present-day exposures, we tentatively assign the older age group to the Lepontine Dome. After 2.2 Ma, discharge from this older source ceased.

Between ~1.2 and 0.9 Ma, during the most intense Alpine glaciation, a strong trend toward older ages upsection is observed. Such a trend excludes further incision into crystalline basement, but reflects recycling of clastic sediments. Thus, after 1.2 Ma, the Upper Rhine Graben has not received detritus from the Central Alps anymore, but instead erosion shifted to the foreland, either recycling sediments of the Swiss Molasse basin, or reworking glacial till deposited beneath or in front of the north draining glaciers.

At around 1 Ma, apatites with unusual high amounts of crystal defects and high Dpar values occur in the Rhine Graben sediments. AHe thermochronology yields ages of 12 to 10 Ma for these apatites. Age and habitus are in very good agreement with descriptions of apatites from the Hegau volcanics (Rahn & Selbekk, 2007). After ~0.4 Ma, the Rhine Graben again received detritus from Central Alpine sources.

7.6 Results and discussion

7.6.1 Thermochronological ages and provenance of the Sundgau gravel and Höhere Deckenschotter

Results of AFT and AHe analyses and statistical deconvolution are shown in Tables 7.1, 7.2, and 7.3, and in Figs. 7.3 & 7.4. Fig. 7.2 contains the recent AFT age distribution of the Central Alps as well as age probability-density plots of the potential source areas. From the Sundgau gravel, we analysed one sand sample (SU-1B) and one sample containing a mixture of whitish granitic pebbles, some of them were slightly deformed (SU-1A). The latter yielded a single AFT age group of ~10 Ma and an AHe age also around 10 Ma, suggesting that the granitic pebbles were all derived from the same source. With a lag time of 7 to 6 Ma, the most likely source is the Aar-Gotthard massif, where similar AFT and AHe ages and lithologies frequently occur in the present-day exposures. The sand sample from the Sundgau gravel (SU-1B) also contains a ~10 Ma age group, but additionally an older age group of ~15 Ma (11-12 Ma lag time). The single apatite grain dated by AHe analysis from this sample yielded an age of ~13 Ma and thus seems to belong to this older age group. Schlunegger *& Mosar* (2011) suggested that the Sundgau gravel contain reworked material from the Swiss Molasse basin. However, the AFT signature, even of the older age group, is slightly too young to be derived from the Molasse basin. Furthermore, the heavy mineral composition of the Sundgau deposits also argues against a major contribution from the Swiss Molasse basin (Liniger, 1966, 1967). Instead, because of the slightly older AFT ages of the present-day exposures (compared to the Aar-Gotthard massif), and in accordance with the interpretation of AFT ages from the Rhine Graben sediments (Reiter *et al.*, in press), we assign the older age group to the erosion of the Lepontine Dome, although this assumption may be speculative.

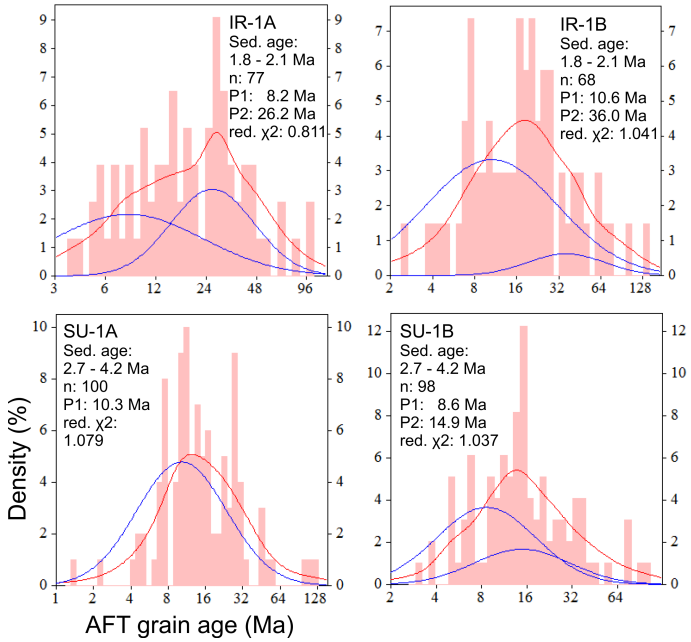

Fig. 7.3: Probability-density plots of AFT grain ages (AFT ages vs. density). Red curves represent the probability density plots for the whole sample, whereas the blue curves represents the probability density plots of the best-fit peaks. Sample name, sedimentation age (Sed. age), number of counted grains (n) and modeled peak ages (P1/P2) are given. Red. χ^2, reduced Chi-square test (see also Table 7.2).

Sample	Stratigraphic age [Ma]	Latitude	Longitude	Elevation [m]	n	ρs	Ns	ρi	Ni	ρd	Nd	P(χ^2) [%]	Dispersion	Central age ±1σ [Ma]	U [ppm]	Mean Dpar ±s.d. [µm]
IR-1A [1]	1.8 – 2.1	47.55718	8.60504	463	42	3.32	118	38.26	1360	18.81	27688	39	0.04	26.0 ±2.6	23.2	1.7 ±0.2
IR-1A-2 [1]	1.8 – 2.1	47.55718	8.60504	463	36	2.17	92	76.35	3240	25.00	37817	3	0.57	9.8 ±1.6	33.3	1.6 ±0.1
IR-1B [2]	1.8 – 2.1	47.55718	8.60504	463	21	1.58	25	21.24	337	18.86	27688	23	0.33	23.1 ±5.1	14.3	1.8 ±0.1
IR-1B-2 [2]	1.8 – 2.1	47.55718	8.60504	463	47	1.32	74	46.29	2602	25.00	37817	23	0.46	11.2 ±1.6	22.2	1.6 ±0.1
SU-1A [3]	2.9 – 4.2	47.54097	7.17827	391	26	1.32	76	49.40	2856	22.93	34284	5	0.04	9.7 ±1.2	26.8	1.4 ±0.1
SU-1A-3 [3]	2.9 – 4.2	47.54097	7.17827	391	47	1.87	79	70.12	2967	25.00	37817	73	0.00	10.6 ±1.2	32.9	1.5 ±0.2
SU-1A-4 [3]	2.9 – 4.2	47.54097	7.17827	391	27	1.08	46	39.92	1694	25.00	37817	34	0.17	11.0 ±1.7	20.8	1.5 ±0.2
SU-1B [4]	2.9 – 4.2	47.54097	7.17827	391	53	1.01	142	39.45	5575	22.87	34284	1	0.29	10.2 ±1.0	24.6	1.5 ±0.2
SU-1B-4 [4]	2.9 – 4.2	47.54097	7.17827	391	15	1.27	41	51.11	1647	25.00	37817	74	0.01	9.9 ±1.6	24.6	1.6 ±0.2
SU-1B-5 [4]	2.9 – 4.2	47.54097	7.17827	391	30	1.47	61	48.11	2000	25.00	37817	57	0.02	12.2 ±1.6	23.0	1.6 ±0.1

Table 7.1: Results of AFT analyses including mean Dpar values of counted grains, geographic positions (WGS 84), and elevation of sampling locations. Note that up to three mounts were analysed per sample. N, number of counted grains; Ns, number of spontaneous tracks; Ni, number of induced tracks on mica; Nd, number of counted tracks induced from dosimeter glasses; ρ(s, i, d), track density given in 10^5 tracks cm^{-2} (with s, spontaneous tracks; i, induced tracks; d, induced tracks from dosimeter glass); P(χ^2), probability of receiving Chi-square value for n degree of freedom (n is equal to the number of crystals minus 1); a value of <5 % indicates that there may be more than one age population. ζ = 319 ±9 (Durango & Fish Canyon standards, CN-5). [1] sample of sand fraction <355 µm; [2] sample of sand fraction >355 µm; [3] sample of granitic pebbles; [4] sample of whole sand fraction.

Sample	Stratigraphic age [Ma]	n	Raw age [Ma]	Error raw age [Ma]	Corrected age [Ma]	Error corr age [Ma]	FT factor	Sphere radius [µm]	^{4}He [ncc]	Mass [mg]	Th/U ratio	^{149}Sm [ng]	^{232}Th [ng]	^{238}U [ng]
SU-1A #1	2.9 – 4.2	1	7.2	0.5	10.5	1.2	0.69	48.5	0.106	0.0023	0.6341	1.1015	0.0665	0.1048
SU-1B #2	2.9 – 4.2	1	9.5	0.6	13.3	1.6	0.72	56.0	0.144	0.0017	0.5122	0.7684	0.0570	0.1113

Table 7.3: Results of apatite (U-Th-Sm)/He analyses. n, number of analysed grains per aliquot.

Sample	Stratigraphic age [Ma]	n	Age range [Ma]	P1 peak age ±1σ Cl [Ma]	Frac [%]	P2 peak age ±1σ Cl [Ma]	Frac [%]	P3 peak age ±1σ Cl [Ma]	Frac [%]	red. $\chi 2$
IR-1A	1.8 – 2.1	77	3.7-99.2	8.2 ±1.4	56	-	-	26.2 ±3.0	44	0.811
IR-1B	1.8 – 2.1	68	2.4-135.3	10.6 ±1.5	90	-	-	36.0 ±12	10	1.041
SU-1A	2.9 – 4.2	100	1.4-120.8	10.3 ±0.8	100	-	-	-	-	1.079
SU-1B	2.9 – 4.2	98	3.1-98.7	8.6 ±2.1	70	14.9 ±6.5	30	-	-	1.037

Table 7.2: Results of binomial peak fitting. N, number of grains analysed for binomial peak fitting. Frac, fraction of the analysed grains belonging to an age population in percent. red. χ^2, reduced Chi-square test describing the probability of the fitting curve where a value of 1 coincides with a good fit.

Both sand samples from the Höhere Deckenschotter contain one young AFT age group (~8 and 11 Ma) and one old AFT age group (~26 and 36 Ma). The samples did not contain apatites with sufficient quality for AHe analysis. The two young AFT age groups overlap within error limits and may or may not be derived from the same source. Lag times are ~6 and 9 Ma, similar to those derived from the Sundgau gravel. When compared with present-day exposures, again similar AFT ages are observed in the Central Alps, i.e., the Aar-Gotthard massif and the Lepontine Dome. The two older AFT age groups are too old to be derived from the Central Alps. Similar AFT ages also occur in the early Pleistocene sediments of the Rhine Graben (PG3 in Fig. 7.4a). These old ages may either represent erosion of the Rhenodanubian Flysch and/or the Silvretta nappe of the Eastern Alps, or they reflect reworking of molasse sediments. We prefer the first interpretation, because particularly the ~36 Ma age group is a bit too old to be derived from the Swiss Molasse basin, and because the PG3 age group does not display a "recycling trend" (i.e., increasing AFT ages upsection, assuming that the PG3 ages from the Rhine Graben and from the Höhere Deckenschotter were derived from the same source).

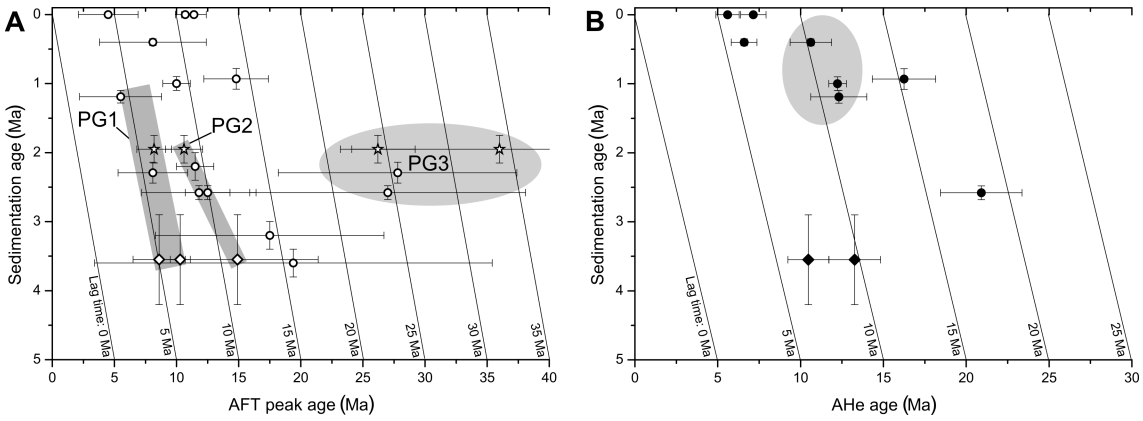

Fig. 7.4: (a) AFT age groups plotted against deposition ages with contours of equal lag times. Circles represent data from the Rhine Graben and modern Rhine tributaries (without data of Variscan sources), diamonds represent ages derived from the Sundgau samples, and stars represent ages of the Höhere Deckenschotter samples. Grey highlighted areas: PG1 most likely reflect erosion of the Aar-Gotthard massif, PG2 reflects erosion of a source area south of PG1 (presumably Lepontine Dome or southernmost external massifs), and PG3 is either derived from an east-Alpine source or from erosion of the Swiss Molasse basin. (b) AHe ages plotted against deposition ages. The black-filled circles represent AHe ages of Rhine Graben samples and from modern Rhine tributaries, and black-filled diamonds represent AHe ages yielded by Sundgau samples. The grey highlighted area contains AHe ages associated with erosion of Hegau volcanics.

7.6.2 Paleo-exhumation trends and source area evolution

If the data from the Upper Rhine Graben (Reiter *et al.*, in press), from the Sundgau gravel, and from the Höhere Deckenschotter are plotted together (Fig. 7.4), we can observe two trends: *(i)* one source (PG1) shows a steady exhumation with a constant lag time of ~6 Ma between ~4 and 1 Ma depositional age. Assuming a geothermal gradient of 25 ±5°C km^{-1} , this lag time can be transferred to an exhumation rate of ~0.8 ±0.2 mm year^{-1}. Both, exhumation rate and exhumational equilibrium are in agreement with the observations of Reinecker *et al.* (2008) and Glotzbach *et al.* (2010) for the northern Aar and Gotthard massif, thus supporting our interpretation that the PG1 age group was derived from the central-Alpine external massifs. *(ii)* Provided that the PG2 age groups of the Rhine Graben, the Sundgau gravel and the Höhere Deckenschotter are indeed from the same tectonic unit, then the PG2 trend reflects a source area with decreasing lag time and thus steadily increasing exhumation rates between ~4 and 2 Ma deposition age. Again assuming a geothermal gradient of 25 ±5°C km^{-1}, the lag times can be transferred into exhumation rates between 0.35 ±0.08 mm year^{-1} at ~3.6 Ma and ~0.64 ±0.14 mm year^{-1} at ~2 Ma. Similar rates combined with increasing exhumation for that time were reported for the southwestern Aar massif (Reinecker *et al.*, 2008) and for the eastern and central part of the northern Lepontine Dome (Elfert *et al.*, 2011). In either case, the source for the PG2 ages would be located south of the PG1 source.

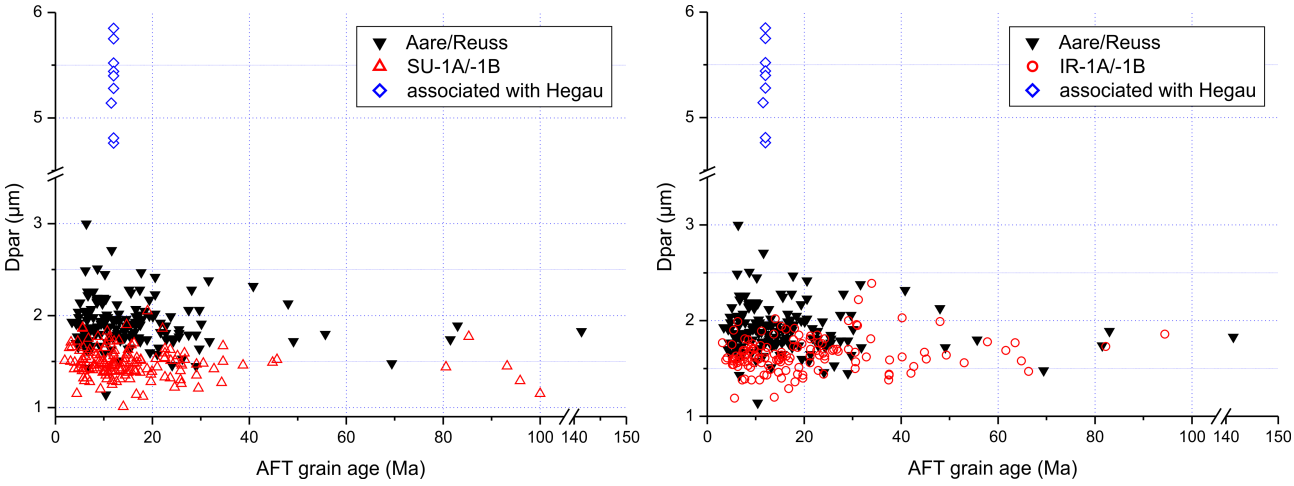

Fig. 7.5: Dpar values plotted against AFT grain ages. For reasons of clarity, uncertainties related to AFT ages and Dpar values are not shown. For the Sundgau samples (SU-1A/-1B), the majority of Dpar values is below ~1.5 µm, whereas for the Höhere Deckenschotter samples (IR-1A/-1B), most Dpar values are above 1.5 µm. Both samples are compared to Dpar values of apatites from the modern Aare/Reuss rivers sourced in the Aar-Gotthard massif and to Dpar values associated with Hegau volcanics. For samples presumably derived from the external massifs of the Central Alps, a general trend towards higher Dpar values through time is observed.

An additional trend observed in our data is a change of the apatite Dpar values through time. Fig. 7.5 shows the Dpar values of apatites from the Sundgau gravel (deposition 4.2 – 2.9 Ma), from the Höhere Deckenschotter (deposition 2.1 – 1.8 Ma), and from the modern Aare and Reuss river sediments. For all three areas, the Aar-Gotthard massif is assumed as the main sediment source. While a large part of the apatites from the Sundgau gravel shows Dpar values <1.5 µm, the majority of apatites from the Höhere Deckenschotter has Dpar values between 1.5 and 2 µm. Apatites with Dpar values >2 µm mainly occur in the modern river sands. Thus, erosion of the Aar-Gotthard massif seems to have gradually exposed rocks containing apatite with increasingly higher Dpar

values. Dpar is a proxy for the chemical composition of apatite. Systematic relations between Dpar value and source rock geochemistry have not been studied so far, and to the knowledge of the authors, no similar Dpar-trend was described in provenance analysis before. We suggest that the shift in Dpar values reflects the geochemical evolution and/or differentiation of the (meta-)magmatic source rocks exposed in the Aar-Gotthard massif, although of course further investigations are required here.

7.6.3 Reconstruction of the north-Alpine drainage system

Based on the provenance analysis and the implications by the lag time plot, we propose the following evolution of the north-Alpine drainage system since the middle Pliocene:

Drainage system between 4.2 and 2.9 Ma

The drainage pattern of this period was more complex than previously thought. The Sundgau gravel were part of the Aare-Doubs system, transporting Alpine debris to the west into the Bresse Graben (in agreement with previous studies, e.g., Liniger, 1966, 1967; Giamboni *et al.*, 2004). The Aare-Doubs system originated in the Aar-Gotthard massif and probably the northern Lepontine Dome, thus the main Alpine drainage divide was presumably located south of the external massif. This is in good agreement with Schlunegger *et al.* (2007), who suggested that the drainage divide was situated in the Lepontine Dome area during or prior to the Pliocene. The age signature of the Rhine Graben sediments differs from the age signature of the contemporaneously deposited Sundgau gravel. This implies that the proto-Rhine and the Aare-Doubs rivers were not connected with each other. The proto-Rhine most likely received detritus from the southern Molasse basin or northern Central Alps, and thus the proto-Rhine headwaters reached further south than previously assumed (e.g., Ziegler & Fraefel, 2009). Accordingly, the drainage divide between the North Sea and the Mediterranean Sea was not situated in the Kaiserstuhl area, as previously suggested, and the Alpine realm was at least partly drained towards the North Sea. The two river systems, the Aare-Doubs and the proto-Rhine were flowing more or less parallel to each other while passing the northern Jura mountains. After leaving behind the passage between the northern Jura and the Black Forest, the proto-Rhine headed northwards into the Rhine Graben (Fig. 7.6a).

Drainage system between ~2.6 and 2.0 Ma

After the Plio-Pleistocene boundary, the AFT age signature of the Rhine Graben deposits has changed significantly, indicating that the Aare-Rhine river now received debris from the external massifs of the Central Alps and presumably from an Eastern Alpine source (Fig. 7.6b). This corroborates previous reconstructions describing a deflection of the Aare river towards the north into the Rhine Graben (e.g., Petit *et al.*, 1996). The Höhere Deckenschotter and the – slightly older – Rhine Graben sediments show similar age signatures, implying that *(i)* they belonged to the same river system, and *(ii)* that the drainage network was unchanged by first glaciation of the Alpine foreland, that resulted in the deposition of the Höhere Deckenschotter. The main Alpine drainage divide was still situated either in the southernmost Aar massif or in the Lepontine Dome (source area of the PG2 age group, Fig. 7.4a). This southern rim of the Aare-Rhine catchment shows constantly increasing exhumation. In accordance with previous studies, we explain the drainage change between 2.9 and 2.6 Ma with tectonic reasons, namely the uplift of the Bresse Graben and the subsidence of the southern Rhine Graben (e.g., Dèzes *et al.*, 2004), probably related to the change from thin-skinned to thick-skinned deformation in the Jura fold belt (Ustaszewski & Schmid, 2007; Ziegler & Fraefel, 2009).

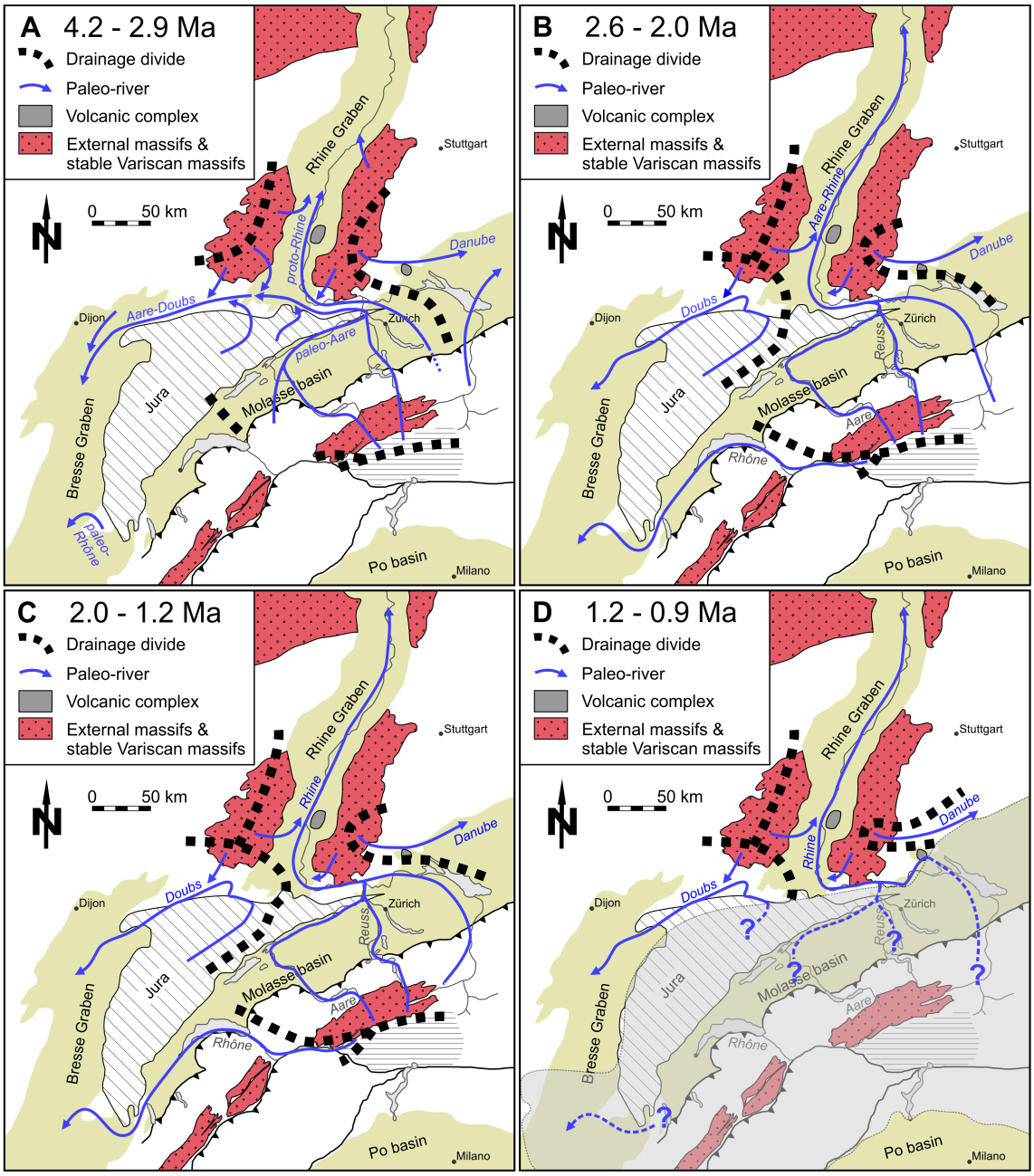

Fig. 7.6: Evolution of the northwestern Alpine drainage system (modified from Giamboni *et al*., 2004; Berger *et al*., 2005; Ziegler & Fraefel, 2009). (a) During deposition of the Sundgau gravel, the Aare-Doubs and the proto-Rhine were flowing parallel to each other towards the northwest. After passing the passage between the Jura mountains and the Black Forest, the Aare-Doubs headed southwestwards to the Mediterranean Sea and the proto-Rhine northwards in the Upper Rhine Graben. The central-Alpine main water divide was most likely located in the northern Lepontine Dome. (b) The Aare-Rhine river drained the Central Alps and a more easterly located source area. (c) The Rhine river drained the Central Alps with a northward moving main Alpine water divide. (d) During the most intense glaciation of the Alps, the connection between the Rhine Graben and the Central Alps was cut off, and the headwaters of the Rhine river shifted towards the north. The grey-highlighted area reflects the assumed maximum glacial extent (adapted from Preusser *et al.,* 2010, 2011). In addition, the Rhine catchment now includes the Hegau volcanic complex.

Drainage system between ~2.0 and 1.2 Ma

After 2.0 Ma, the age signature of the Rhine Graben sediments changes again, with the PG2 and PG3 age groups disappearing and only the PG1 age group still present. This implies another change of the drainage system, associated with a northward shift of the main Alpine drainage divide (Fig. 7.6c). Different tectonic changes, which may explain the changes of the drainage system, were suggested to have taken place during or since the Pliocene. The detailed timing of the latest stage Alpine evolution, however, is poorly constrained, thus making a temporal correlation with the drainage evolution difficult. Based on the literature data and our own thermochronological data, we propose the following scenario: Since ~3.5 Ma (Reinecker *et al.*, 2008), the central-Alpine core region was affected by orogen-perpendicular extension caused by a decrease or cessation of convergence (Sue *et al.*, 2007). Extension led to normal faulting along the Rhône valley, resulting in accelerated exhumation of the southwestern Aar massif (as reflected in the lag time trend of the PG2 age group), and finally southward migration of the Rhône river down the normal fault and the change towards an orogen-parallel drainage system (Reinecker *et al.*, 2008; Reinecker & Kuhlemann, 2008). Extension normally causes decreasing topography, thus a reduced topography in the area of the southwestern Aar massif may have triggered the shift of the main Alpine drainage divide towards the north (cf. Schlunegger *et al.*, 2007). After this shift, the southwestern Aar massif and the Lepontine Dome were drained towards the west and south, reflected by the disappearence of the PG2 age group in the basin deposits. If this scenario is true, then the establishment of an orogen-parallel river network and the associated northward shift of the main drainage divide can be dated as having occurred between 2.0 and 1.2 Ma, and was the result of a change in the Alpine stress field, as described by Sue *et al.* (2007).

Drainage system between ~1.2 and 0.9 Ma

According to Muttoni *et al.* (2003), Litt *et al.* (2005), Haeuselmann *et al.* (2007), Valla *et al.* (2011, 2012), most intense Alpine glaciation was reached at ~1.0 Ma. We therefore adopted the maximum ice extent as reconstructed by Preusser *et al.* (2010, 2011) for that time slice (Fig. 7.6d). The age signature of the Rhine Graben sediments again strongly changed, now indicating sediment recycling instead of crustal incision. Glaciation seems to have effectively sealed the Alpine landscape, thus causing strong reduction of the catchment size of the Rhine river, a shift of the sediment source area towards the north into the north-Alpine foreland, and a cut-off of the connection between the Alps and the Rhine Graben/North Sea. Also at that time, debris from the Hegau volcanics started to occur in the Rhine Graben deposits, indicating that the course of the Rhine river across the north-Alpine foreland was now essentially the same as it is today, i.e., crossing the area of the Hegau volcanics.

Drainage system between 0.4 Ma to recent

After the end of main glaciation, the connection of the Rhine river with the Alpine source areas was re-established. Erosion of the Hegau volcanics went on. During this period the modern drainage system has been fully established.

7.7 Conclusions

Based on the thermochronological analysis, we reconstructed the provenance of the Sundgau gravel and the Höhere Deckenschotter, and, combined with previous data from the Upper Rhine Graben and the Aare/Reuss rivers, we proposed a refined model for the evolution of the Alpine drainage system from the Middle Pliocene until the present.

Provenance analysis revealed that the Sundgau gravel predominantly consist of debris from the Central Alps (Aar-Gotthard massif and Lepontine Dome) with a possible minor quantity of uppermost molasse sediments. The Höhere Deckenschotter also consist of detritus derived from central-Alpine sources, but additionally from a more (north)easterly located source area (Silvretta nappe, Rhenodanubian Flysch, and/or Swiss Molasse basin).

Between the Middle Pliocene and the middle Pleistocene (between ~4.2 and 2 Ma), one central-Alpine source (most likely the central external massifs) showed constant exhumation, whereas the other central-Alpine source (most likely the southwestern Aar massif and/or the northern Lepontine Dome) experienced an increase in exhumation rates of about 25%.

Regarding the evolution of the drainage system, we assume two separated drainage systems between 4.2 and 2.9 Ma; the Aare-Doubs which deposited the Sundgau gravel and drained the core region of the Central Alps, and the proto-Rhine which drained the southern Molasse basin or the northern rim of the Central Alps via the Upper Rhine Graben. From 4.2 until ~2 Ma, the main water divide of the Central Alps shifted northwards from the Lepontine Dome or southernmost Aar massif to the central Aar-Gotthard massif, and most likely reached its present-day position after deposition of the Höhere Deckenschotter. Simultaneously with the deposition of the Höhere Deckenschotter, the catchment area was temporarily extended towards (north)easterly source areas. The reduction of the catchment area due to the major Alpine glaciation led to sediment reworking in front of the glaciers and to a shift of the Rhine river towards the Hegau volcanic complex. At ~0.4 Ma, the present-day drainage system was largely established.

7.8 Acknowledgements

This study is part of the EUROCORE project TopoEurope/ThermoEurope funded by the European Science Foundation and the German Science Foundation (project SP673/5-1). We thank Meinert Rahn and Joachim Kuhlemann (both Eidgenössische Nuklearsicherheitsinspektorat at Brugg, Switzerland) for ongoing scientific exchange regarding Alpine geology. Especially Joachim Kuhlemann for collecting and providing the Irchel samples, and Meinert Rahn for providing the unpublished data for the AFT compilation. Thanks to Peter A. Ziegler (University of Basel, Switzerland) for scientific exchange regarding the Alpine drainage system and general advice (bon courage!), and to Barry Kohn (University of Melbourne) for his support regarding the AHe analyses. We also like to thank Anke Toltz, Vera Kolb and Angelika Freesemann (University of Bremen), and Dorothea Mühlbayer-Renner and Dagmar Kost (University of Tübingen) for sample preparation and laboratory support.

7.9 References

Becker, A. (2000) The Jura Mountains – and active foreland fold-and-thrust belt? *Tectonophysics*, *321*, 381–406.

Berger, J.P. (1985) La transgression de la Molasse marine supérieure (OMM) en Suisse occidentale. *Münchn geowiss Abh*, *5*, 1–207.

Berger, J.-P., Reichenbacher, B., Becker, D., Grimm, M., Grimm, K., Picot, L., Storni, A., Pirkenseer, C., Derer, C. & Schaefer, A. (2005) Paleogeography of the Upper Rhine Graben (URG) and the Swiss Molasse Basin (SMB) from Eocene to Pliocene. *Int J Earth Sci*, *94*, 697–710.

Bolliger, T., Fejfar, O., Graf, H. & Kälin, D. (1996) Vorläufige Mitteilung über Funde von pliozänen

Kleinsäugern aus den höheren Deckenschottern des Irchels (Kt. Zürich). *Eclogae geol. Helv.*, *89*, 1043–1048.

Burtner, R.L., Nirgini, A. & Donelick, R.A. (1994) Thermochronology of Lower Cretaceous Source Rocks in the Idaho-Wyoming Thrust Belt. *AAPG Bulletin*, *78*, 1613–1636.

Cederbom, C.E., Sinclair, H.D., Schlunegger, F. & Rahn, M.K. (2004) Climate-induced rebound and exhumation of the European Alps. *Geology*, *32*, 709–712.

Cederbom, C.E., van der Beek, P., Schlunegger, F., Sinclair, H.D. & Oncken, O. (2011) Rapid extensive erosion of the North Alpine foreland basin at 5-4 Ma. *Basin Research, 23*, 528–550.

Ciancaleoni, L. (2005) *Deformation processes during the last stages of the continental collision: the brittle–ductile fault systems in the Bergell and Insubric areas (Eastern Central Alps, Switzerland–Italy)*. Ph.D. thesis, University Neuchâtel, Switzerland.

Danišik, M., Pfaff, K., Evans, N.J., Manoloukos, C., Staude, S., McDonald, M.J. & Markl, G. (2010) Tectonothermal history of the Schwarzwald Ore District (Germany): An apatite triple dating approach. *Chemical Geology*, *278*, 58–69.

Dézes, P., Schmid, S.M. & Ziegler, P.A. (2004) Evolution of the European Cenozoic Rift System: interaction of the Alpine and Pyrenean orogens with their foreland lithosphere. *Tectonophysics*, *389*, 1–33.

Donelick, R.A., Ketcham, R.A. & Carlson, W.D. (1999) Variability of apatite fission-track annealing kinetics: II. Crystallographic orientation effects. *American Mineralogist*, *84*, 1224–1234.

Elfert, S., Reiter, W. & Spiegel, C. (2011) Doming and unroofing of the Lepontine Dome (Central European Alps). New insights from Low-Temperature thermochronology. *Geophysical Research Abstracts*, *13*, EGU2011-11983.

Ellwanger, D., Wielandt-Schuster, U., Franz, M. & Simon, T. (2011) The Quaternary of the southwest German Alpine Foreland (Bodensee, Oberschwaben, Baden-Württemberg, Southwest Germany). *Quaternary Science Journal*, *60*, 306–328.

Flisch, M. (1986) Die Hebungsgeschichte der oberostalpinen Silvretta-Decke seit der mittleren Kreide. *Bulletin der Vereinigung schweizerische Petroleum-Geologen und Ingenieure*, *53*, 23–49.

Füchtbauer, H. (1959) Zur Nomenklatur der Sedimentgesteine. *Erdöl Kohle*, *12*, 605–613.

Garver, J.I., Brandon, M.T., Roden-Tice, M. & Kamp, P.J.J. (1999) Exhumation history of orogenic highlands determined by detrital fission-track thermochronology. *Geological Society Special Publications*, *154*, 283–304.

Giamboni, M., Ustaszewski, K., Schmid, S.M., Schumacher, M.E. & Wetzel, A. (2004) Plio-Pleistocene transpressional reactivation of Paleozoic and Paleogene structures in the Rhine-Bresse transform zone (northern Switzerland and eastern France). *Int J Earth Sci*, *93*, 207–223.

Giger, M. (1991) *Geochronologische und petrographische Studien an Geröllen und Sedimenten der Gonfolite Lombarda Gruppe (Südschweiz und Norditalien) und ihr Vergleich mit dem alpinen Hinterland*. Ph.D. thesis, University Bern, Switzerland.

Gleadow, A.J.W. (1981) Fission track dating methods: what are the real alternatives? *Nuclear Tracks and Radiation Measurements*, *5*, 3–14.

Gleadow, A.J.W. & Duddy, I.R. (1981) A natural long-term annealing experiment for apatite. *Nuclear Tracks and Radiation Measurements*, *5*, 169–174.

Glotzbach, C., Reinecker, J., Danišik, M., Rahn, M., Frisch, W. & Spiegel, C. (2008) Neogene exhumation history of the Mont Blanc massif, western Alps. *Tectonics*, *27*, TC4011, doi:10.1029/2008TC002257.

Glotzbach, C., Reinecker, J., Danišik, M., Rahn, M., Frisch, W. & Spiegel, C. (2010) Thermal history of the central Gotthard and Aar massifs, European Alps: Evidence for steady state, long-term exhumation. *J Geophys Res*, *115*, F03017, doi:10.1029/2009JF001304.

Glotzbach, C., van der Beek, P., Carcaillet, J. & Delunel, R. (in revision): Deciphering the driving forces of erosion rates on millennial to million year timescales in glacially impacted landscapes, an example from the Western Alps. *J. Geophys. Res.,* in revision.

Glotzbach, C., van der Beek, P. & Spiegel, C. (2011) Episodic exhumation and relief growth in the Mont Blanc massif, Western Alps from numerical modelling of thermochronology data. *Earth and Planetary Science Letters*, *304*, 417–430.

Graf, H.R. (1993) *Die Deckenschotter der zentralen Nordschweiz*. Ph.D thesis, ETH Zürich, URL: http://e-collection.library.ethz.ch/view/eth:39047.

Graf, H.R. (2009) Stratigraphie und Morphogenese von frühpleistozänen Ablagerungen zwischen Bodensee und Klettgau. *Quaternary Science Journal*, *58*, 12–53.

Habbe, K.A., Ellwanger, D. & Becker-Haumann, R. (2007) Stratigraphische Begriffe für das Quartär des süddeutschen Alpenlandes. *Quaternary Science Journal*, *56*, 66–83.

Haeuselmann, P., Granger, D.E., Jeannin, P.-Y. & Lauritzen, S.-E. (2007) Abrupt glacial valley incision at 0.8 Ma dated from cave deposits in Switzerland. *Geology*, *35*, 143–146.

Hagedorn, E.-M. & Boenigk, W. (2008) The Pliocene and Quaternary sedimentary and fluvial history in the Upper Rhine Graben based on heavy mineral analyses. *Netherlands Journal of Geosciences*, *87*, 21–32.

Hoselmann, C. (2008) The Pliocene and Pleistocene fluvial evolution in the northern Upper Rhine Graben based on results of the research borehole at Viernheim (Hessen, Germany). *Quaternary Science Journal*, *57*, 286–315.

Hurford, A.J. (1986) Cooling and uplift patterns in the Lepontine Alps South Central Switzerland and an age of vertical movement on the Insubric fault line. *Contrib Mineral Petrol*, *92*, 413–427.

Hurford, A.J., Flisch, M. & Jäger, E. (1989) *Unravelling the thermo-tectonic evolution of the Alps: a contribution from fission track analysis and mica dating*. In: Alpine Tectonics, (Ed. by M. P. Coward, D. Dietrich and R. G. Park), *Geological Society Special Publication*, *45*, 369–398.

Keller, L.M., Hess, M., Fügenschuh, B. & Schmid, S. (2005) Structural and metamorphic evolution of the Camughera–Moncucco, Antrona and Monte Rosa units southwest of the Simplon line, Western Alps. *Eclogae geol. Helv.*, *98*, 19–49.

Keller, J., Kraml, M. & Henjes-Kunst, F. (2002) $^{40}Ar/^{39}Ar$ single crystal dating of early volcanism in the Upper Rhine Graben and tectonic implications. S*chweiz. Mineral. Petrogr. Mitt.*, *82*, 121–130.

Kraml, M., Pik, R., Rahn, M., Selbekk, R., Carignan, J. & Keller, J. (2007) A New Multi-mineral Age Reference Material for 40Ar/39Ar, (U-Th)/He and Fission Track Dating Methods: The Limberg t3 Tuff. *Geostandards and Geoanalytical Research*, *30*, 73–86.

Kuhlemann, A. & Kempf, O. (2002) Post-Eocene evolution of the North Alpine Foreland Basin and its response to Alpine tectonics. *Sedimentary Geology*, *152*, 45–78.

Laubscher, H.P. (1986) The eastern Jura: relations between thin-skinned and basement tectonics, local and regional. *Geol Rundsch*, *75*, 535–553.

Liniger, H. (1966) Das plio-altpleistozäne Flussnetz der Nordschweiz. *Regio Bas*, *7*, 158–177.

Liniger, H. (1967) Pliozän und Tektonik des Juragebirges. *Eclogae geol Helv*, *60*, 407–490.

Link, K. (2010) *Die thermo-tektonische Entwicklung des Oberrheingraben-Gebietes seit der Kreide*. Ph.D. thesis, Albert-Ludwigs Universität Freiburg, URL: http://www.freidok.uni-freiburg.de/volltexte/7847/.

Lippolt, H.J., Gentner, W. & Wimmenauer, W. (1963) Altersbestimmungen nach der Kalium-Argon-Methode an tertiären Eruptivgesteinen Südwestdeutschlands. *Jh. geol. Landesamt Baden-Württemberg*, *6*, 507–538.

Litt, T., Ellwanger, D., Villinger, E. & Wansa, S. (2005) Das Quartär in der Stratigraphischen Tabelle von Deutschland 2002. *Newsletters on Stratigraphy*, *41*, 385–399.

Madritsch, H., Schmid, S.M. & Fabbri, O. (2008) Interactions between thin- and thick-skinned tectonics at the northwestern front of the Jura fold-and-thrust belt (eastern France). *Tectonics*, *27*, TC5005, doi:10.1029/2008TC002282.

Michalski, I. & Soom, M. (1990) The Alpine thermo-tectonic evolution of the Aar and Gotthard massifs, Central Switzerland: Fission Track ages on zircon and apatite and K-Ar mica ages. *Schweiz. Mineral. Petrogr. Mitt.*, *70*, 373–387.

Muttoni, G., Carcano, C., Garzanti, E., Ghielmi, E.M., Piccin, A., Pini, R., Rogledi, S. & Sciunnach, D. (2003) Onset of major Pleistocene glaciations in the Alps. *Geology*, *31*, 989–992.

Petit, C., Campy, M., Chaline, J. & Bonvalot, J. (1996) Major palaeohydrographic changes in Alpine foreland during the Pliocene-Pleistocene. *Boreas*, *25*, 131–143.

Pignalosa, A., Zattin, M., Massironi, M. & Cavazza, W. (2011) Thermochronological evidence of a late Pliocene climate-induced erosion rate increase in the Alps. *Int J Earth Sci*, *100*, 847–859.

Preusser, F., Graf, H.R., Keller, O., Krayss, E. & Schlüchter, C. (2011) Quaternary glaciation history of northern Switzerland. *Quaternary Science Journal*, *60*, 282–305.

Preusser, F., Reitner, J.M. & Schlüchter, C. (2010) Distribution, geometry, age and origin of overdeepened valleys and basins in the Alps and their foreland. *Swiss J Geosci, 103*, 407–426.

Rahn, M.K., Hurford, A.J. & Frey, M. (1997) Rotation and exhumation of a thrust plane: Apatite fission-track data from the Glarus thrust, Switzerland. *Geology*, *25*, 599–602.

Rahn, M. & Selbekk, R. (2007) Absolute dating of the youngest sediments of the Swiss Molasse basin by apatite fission track analysis. *Swiss J Geosc*, *100*, 371–381.

Reinecker, J., Danišik, M., Schmid, C., Glotzbach, C., Rahn, M., Frisch, W. & Spiegel, C. (2008) Tectonic control on the late stage exhumation of the Aar Massif (Switzerland): Constraints from apatite fission track and (U-Th)/He data. *Tectonics*, TC6009, doi:10.1029/2007TC002247.

Reinecker, J. & Kuhlemann, J. (2008) Timing of orogen-parallel Rhône valley incision, Switzerland. *Geophysical Research Abstracts*, *10*, EGU2008-A-00000.

Reiter, W., Elfert, S., Bernet, M., Glotzbach, C. & Spiegel, M. (in press) Relations between denudation, glaciation, and sediment deposition: implications from the Plio-Pleistocene Central Alps. *Basin Research*, doi: 10.1111/bre.12023.

Schaer, J.P., Reimer, G.M. & Wagner, G.A. (1975) Actual and ancient uplift rate in the Gotthard region, Swiss Alps: A comparison between precise levelling and fission-track apatite age. *Tectonophysics*, *29*, 293–300.

Schlunegger, F. & Mosar, J. (2011) The last erosional stage of the Molasse Basin and the Alps. *Int J Earth Sci*, *100*, 1147–1162.

Schlunegger, F., Rieke-Zapp, D. & Ramseyer, K. (2007) Possible environmental effects on the evolution of the Alps-Molasse Basin system. *Swiss J. Geosci.*, *100*, 383–405.

Schmid, S.M., Fügenschuh, B., Kissling, E. & Schuster, R. (2004) Tectonic map and overall architecture of the Alpine orogen. *Eclogae geol Helv*, *97*, 93–117.

Schreiner, A. (1992) *Erläuterungen zu Blatt Hegau und westlicher Bodensee*. Geologisches Landesamt Baden-Württemberg, Freiburg, Stuttgart.

Sissingh, W. (2006) Syn-kinematic palaeogeographic evolution of the West European Platform:

correlation with Alpine plate collision and foreland deformation. *Netherlands J Geosc*, *85*, 131–180.

Soom, M. (1990) *Abkühlungs- und Hebungsgeschichte der Externmassive und der penninischen Decken beidseits der Simplon-Rhône-Linie seit dem Oligozän: Spaltspurendatierung an Apatit/Zirkon und K-Ar-Datierungen an Biotit/Muskovit (Westliche Zentralalpen)*. Ph.D. thesis, University of Bern, Switzerland.

Spiegel, C., Kohn, B., Raza, A., Rainer, T. & Gleadow, A. (2007) The effect of long-term low-temperature exposure on apatite fission track stability: A natural annealing experiment in the deep ocean. *Geochimica et Cosmochimica Acta*, *71*, 4512–4537.

Spiegel, C., Siebel, W. & Berner, Z. (2002) Sr and Nd isotope ratios and trace element geochemistry of detrital epidote as provenance indicators: implications for the reconstruction of the exhumation history of the Central Alps. *Chemical Geology*, *189*, 231–250.

Steiner, H. (1984) Mineralogisch-petrographische, geochemische und isotopengeologische Untersuchungen an einem Meta-Lamprophyr und seinem granodioritischen Nebengestein (Matorello-Gneis) aus der Maggia-Decke. *Schweiz. Mineral. Petrogr. Mitt.*, *64*, 227–259.

Sue, C., Delacou, B., Champagnac, J.-D., Allanic, C., Tricart, P. & Burkhard, M. (2007) Extensional neotectonics around the bend of the Western/Central Alps: an overview. *Int J Earth Sci*, *96*, 1101–1129.

Timar-Geng, Z., Fügenschuh, B., Wetzel, A. & Dresmann, H. (2006) Low-temperature thermochronology of the flanks of the southern Upper Rhine Graben. *Int J Earth Sci*, *95*, 685–702.

Timar-Geng, Z., Grujic, D. & Rahn, M. (2004) Deformation at the Leventina–Simano nappe boundary, Central Alps, Switzerland. *Eclogae geol. Helv.*, *97*, 265–278.

Trautwein, B., Dunkl, I. & Frisch, W. (2001) Accretionary history of the Rhenodanubian Flysch zone in the Eastern Alps – evidence from apatite fission-track geochronology. *Int J Earth Sci*, *90*, 703–713.

Ustaszewski, K. & Schmid, S.M. (2007) Latest Pliocene to recent thick-skinned tectonics at the Upper Rhine Graben – Jura Mountains junction. *Swiss J. Geosc.*, *100*, 293–312.

Valla, P.G., Shuster, D.L. & van der Beek, P. (2011) Significant increase in relief of the European Alps during mid-Pleistocene glaciations. *Nature Geoscience*, *4*, 688–692.

Valla, P.G., van der Beek, P., Shuster, D., Braun, J., Herman, F., Tassan-Got, L. & Gautheron, C. (2012) Late-Neogene exhumation and relief development of the Aar and Aiguilles Rouges massifs (Swiss Alps) from low-temperature thermochronology modeling and $^{4}He/^{3}He$ thermochronometry. *J. Geophys. Res.*, *117*, F01004.

Vernon, A.J., van der Beek, P.A., Sinclair, H.D., Persano, C., Foeken, J. & Stuart, F.M. (2009) Variable late Neogene exhumation of the central European Alps: Low-temperature thermochronology from the Aar Massif, Switzerland, and the Lepontine Dome, Italy. *Tectonics*, *28*, TC5004, doi:10.1029/2008TC002387.

Vernon, A.J., van der Beek, P.A., Sinclair, H.D. & Rahn, M.K. (2008) Increase in late Neogene denudation of the European Alps confirmed by analysis of a fission-track thermochronology database. *Earth and Planetary Science Letters*, *270*, 316–329.

Villinger, E. (1998) Zur Flussgeschichte von Rhein und Donau in Südwestdeutschland. *Jahresberichte und Mitteilungen des Oberrheinischen Geologischen Vereins, 80*, 361–398.

Villinger, E. (2003) Zur Paläogeographie von Alpenrhein und oberer Donau. *Zeitschrift der deutschen geologischen Gesellschaft*, *154*, 193–253.

Von Hagke, C., Cederbom, C.E., Oncken, O., Stöckli, D.F., Rahn, M.K. & Schlunegger, F. (2012) Linking the northern Alps with their foreland: The latest exhumation history resolved by low-temperature thermochronology. *Tectonics*, *31*, TC5010, doi:10.1029/2011TC003078.

Wagner, G.A. & Reimer, G.M. (1972) Fission track tectonics: The tectonic interpretation of fission track apatite ages. *Earth and Planetary Science Letters*, *14*, 263–268.

Wagner, G.A., Reimer, G.M. & Jäger, E. (1977) Cooling ages derived by apatite fission-track, mica Rb-Sr and K-Ar dating: The uplift and cooling history of the Central Alps. *Mem Ist Geo Min Univ Padova*, Vol. XXX.

Weh, M. (1998) *Tektonische Entwicklung der penninischen Sediment-Decken in Graubünden (Prättigau bis Oberhalbstein)*. Ph.D. thesis, University Basel, Switzerland.

Wolf, R.A., Farley, K.A. & Kass, D.M. (1998) Modeling of the temperature sensitivity of the apatite (U-Th)/He thermochronometer. *Chemical Geology*, *148*, 105–114.

Ziegler, P.A. & Dèzes, P. (2007) Cenozoic uplift of Variscan Massifs in the Alpine foreland: Timing and controlling mechanisms. *Global and Planetary Change*, *58*, 237–269.

Ziegler, P.A. & Fraefel, M. (2009) Response of drainage systems to Neogene evolution of the Jura fold-thrust belt and Upper Rhine Graben. *Swiss J. Geosci.*, *102*, 57–75.

7.10 Supplement

7.10.1 Analytical procedure for the AFT and AHe analyses

For AFT analysis, the external detector method (Gleadow & Duddy, 1981) and the zeta calibration approach (Hurford & Green, 1983) were applied. Standard heavy liquid and magnetic separation techniques were used for sample processing. Apatites were mounted in epoxy resin on a glass slide, ground, and polished to reveal the inner surfaces of the crystals. For revealing the spontaneous tracks, the mounts were etched in 5 M HNO_3 at 20°C for 20 seconds. The mounts were irradiated at the reactor facility FRM II in Garching, Germany. After irradiation, micas were etched using 40% HF at 22 ±1°C for 30 minutes for revealing the induced tracks. Single grain ages were calculated by the program Trackkey of Dunkl (2002). Cooling age errors are given at the 1σ confidence level. Due to the good sample quality, we were able to analyse between ~70 and 100 grains for each sample, which corresponds to a 95% confidence that no fraction ≥0.08 and ≥0.06, respectively, is missed (Vermeesch, 2004). The mixed grain age distributions obtained by the AFT analysis have been statistically decomposed into age populations (=age groups) by the program Binomfit, as described by Brandon (1992, 2002).

For AHe thermochronology apatite crystals were selected after the criteria described by Farley (2002). Appropiate apatite grains were put into cleaned Pt tubes. For cleaning, the Pt tubes were exposed to 37% HCl at a temperature between 35 and 40°C for 48 hours. AHe analysis was carried out at the University of Melbourne. ^{4}He was extracted by laser heating and then measured with a Balzers quadrupole mass spectometer by using the ^{3}He isotope dilution method. For analysing U, Th, and Sm contents, mass spectrometry using a second-generation Varian quadrupole ICP-MS was applied. All apatites were corrected for ^{4}He loss at the grain margins according to the alpha correction approach of Farley *et al.* (1996). A comparison between dating of alpha-corrected and mechanical abraded apatites from the Rhine Graben showed that at least for these samples sediment transport did not affect AHe ages (Reiter *et al.*, in press). However, a slight overcorrection for the samples of this study cannot be excluded.

7.10.2 References

Brandon, M.T. (1992) Decomposition of fission-track grain-age distributions. *American Journal*

of Science, *292*, 535–564.
Brandon, M.T. (2002) Decomposition of mixed grain age distributions using Binomfit. *On Track*, *24*, 13–18.
Dunkl, I. (2002) Trackkey: A windows program for calculation and graphical presentation of fission track data. *Comput. Geosci.*, *28*, 3–12.
Farley, K. (2002) (U-Th)/He Dating: Techniques, Calibrations, and Applications. *Reviews in Mineralogy and Geochemistry*, *47*, 819–844.
Farley, K., Wolf, R.A. & Silver, L.T. (1996) The effects of long alpha-stopping distances on (U-Th)/He ages. *Geochimica et Cosmochimica Acta*, *60*, 4223–4229.
Gleadow, A.J.W. & Duddy, I.R. (1981) A natural long-term annealing experiment for apatite. *Nuclear Tracks and Radiation Measurements*, *5*, 169–174.
Hurford, A.J. & Green, P.F. (1983) The zeta age calibration of fission-track dating. *Chem. Geol.*, *41*, 285–317.
Vermeesch, P. (2004) How many grains are needed for a provenance study? *Earth and Planetary Science Letters*, *224*, 441–451.

8 Third paper:

Reconstructing hinterland cooling history from foreland deposits – a detrital apatite (U-Th-Sm)/He case study from the Western Alps

Wolfgang Reiter[1*], Simon Elfert[1], Christoph Glotzbach[2] and Cornelia Spiegel[1]

[1]*Department of Geosciences, University of Bremen, Germany*
[2]*Institute of Geology, Leibnitz University of Hannover, Germany*

*Corresponding author: Wolfgang Reiter, Department of Geosciences, University of Bremen, Klagenfurter Strasse, 28359 Bremen, Germany. E-mail address: wreiter@uni-bremen.de

8.1 Abstract

Previous studies suggested that the Western European Alps are in a long-term exhumational equilibrium since ~10 Ma. We address this hypothesis of steady-state exhumation by analyzing Miocene to recent deposits of a west-Alpine foreland basin by apatite (U-Th-Sm)/He thermochronology. The new data is combined previously published apatite fission-track data from the same sediments, and used for provenance analysis and reconstructing cooling paths of major Alpine source areas by thermal history modeling. Our results show that the central-Alpine Lepontine area contributed detritus between ~13 and 10 Ma, and additionally revealed a formerly unknown input of volcanic material (Massif Central/Upper Rhine Graben) into the basin between ~15 and 13 Ma. Thermal histories modeled from a combination of apatite (U-Th-Sm)/He and fission track data do not corroborate exhumational equilibrium of the Western Alps, but show distinct cooling styles with changing cooling rates ranging between 3 and 40°C Ma^{-1}.

8.2 Introduction

Recent thermochronological studies suggest that the Central and Western Alps are in a long-term exhumational equilibrium, which is not significantly influenced by glacial relief development (e.g. Glotzbach *et al.*, 2011; Valla *et al.*, 2012). Most studies have been applying detrital thermochronology because as a source area erodes, its thermal information containing detritus is transported and deposited as foreland sediments. On the one hand, foreland deposits in turn provide information about a whole catchment and allows a correlation with synsedimentary climatic conditions. Therefore, detrital thermochronology performed on foreland sediments holds the key to a better understanding of the youngest Alpine cooling history (e.g., Stock *et al.*, 2006). On the other hand, thermal modeling of detrital thermochronological data sets include some special characteristics. Usually apatite fission-track (AFT) data sets are used for thermal reconstructions of present-day hard rock exposures. Inversion of AFT data requires analysing the fission track lengths distribution. However, measuring track lengths in detrital samples is somewhat a Sisyphean challenge as most samples contain more than one source, and length distributions are only useful if

they can be attributed to a certain AFT age group. Thermal history models can be significantly refined when AFT data are combined with apatite (U-Th-Sm)/He data (AHe), because temperature sensitivities of the AFT (~110-60°C, Gleadow and Duddy, 1981) and AHe system (~85-40°C, Wolf *et al.*, 1998) overlap. The most reliable way of doing so is AFT/AHe double dating, i.e., using the same apatite grain for AFT and AHe analyses. Since this approach requires large and pristine apatites, its application in detrital studies is strongly limited.

Aim of this study is to evaluate the following questions: (a) to what extent AHe data is usable to refine detrital AFT data regarding provenance analysis, even when not using the double dating approach and only a limited number of analyses, and (b) to test the hypothesis whether the Western Alps are indeed in an exhumational equilibrium since ~10 Ma (Glotzbach *et al.,* 2011). For addressing these two questions, we: *(i)* analysed sediments from the west-Alpine Chambaran basin by AHe thermochronology, *(ii)* deconvoluted the AHe data into age groups, identifying outliers by the program Outlier (by István Dunkl, for details see personal download section at URL: http://www.sediment.uni-goettingen.de) and calculating central ages for each group (Vermeesch, 2008), *(iii)* combined the central AHe ages with the next oldest AFT age group of the same sample, as reported by Glotzbach *et al.* (2011), assuming that both age groups were derived from the same source, and *(iv)* proposed thermal histories of the source area that are in agreement with combined AFT/AHe data using the forward modeling function of the HeFTy code (Ketcham, 2005).

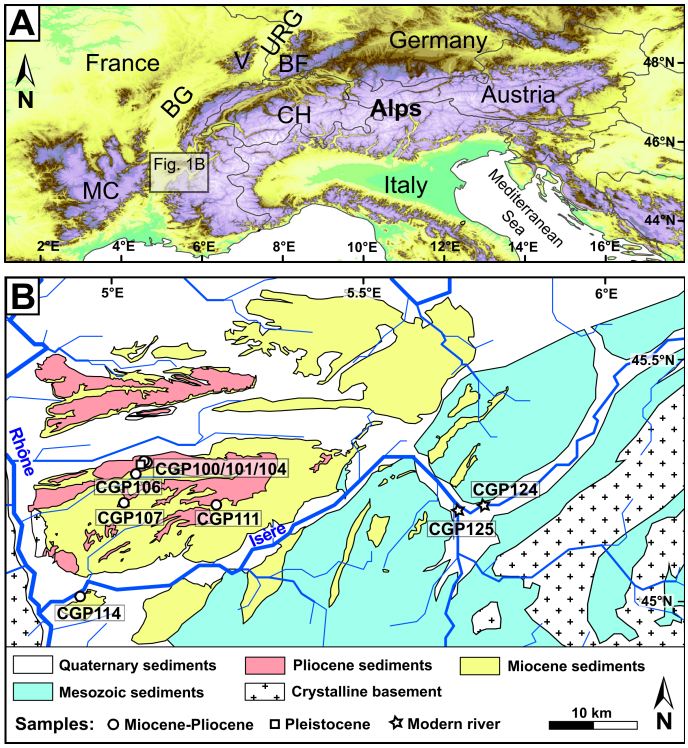

Fig. 8.1: (a) Topographic map of the European Alps and circum-Alpine foreland basins. BF, Black Forest; BG, Bresse Graben; CH, Switzerland; MC, Massif Central; URG, Upper Rhine Graben; V, Vosges. (b) Sampling locations of the Chambaran basin sediments and stratigraphic layers are shown (modified after Glotzbach *et al.*, 2011).

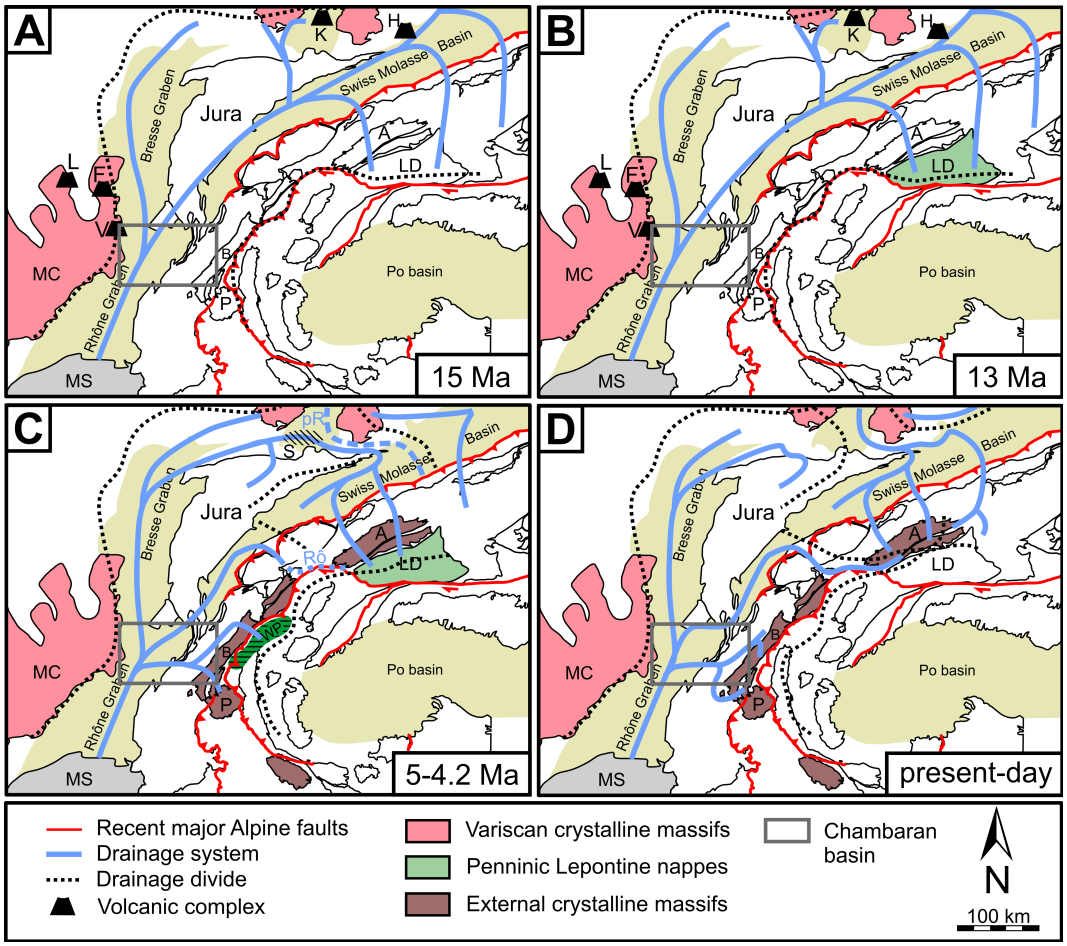

Fig. 8.2: Reconstruction of the Alpine drainage system with changing main water divides (adapted after Kuhlemann *et al.,* 2001; Schmid *et al.*, 2004; Reiter *et al.*, in prep). (a) Main drainage direction was towards the Mediterranean Sea (MS). Potential volcanic source areas for Chambaran basin fill from the Massif Central (MC) and Upper Rhine Graben are shown: F, Forez; H, Hegau; K, Kaiserstuhl; L, Limagne; V, Velay. (b) The crystalline Lepontine nappes (LD) are exhumed in the central-Alpine catchment area. Ongoing volcanic activity in the Massif Central and Hegau area. (c) During deposition of the Sundgau gravel (S, diagonal hachured area) the Isère river presumably drain the west-Alpine External Crystalline Massifs (Belledonne, B, and Pelvoux-Ecrins massif, P). It is speculated that the Rhône river system begins to drain the SW-Aar-Gotthard massif area (Rô, dotted blue line; Reinecker *et al.*, 2008). WP (horizontal hachured area) representing parts of the west-Alpine Penninic units which acted as major sediment supplier for the Chambaran basin as implied by Fügenschuh and Schmid (2003). pR, potential course of the proto-Rhine river as implied by AFT data from Upper Rhine sediments (dotted blue line in the Molasse and Upper Rhine area). (d) Present-day situation where most of the detritus is delivered by the Belledonne and Pelvoux-Ecrins massifs.

8.3 Basin evolution and potential source areas since the Miocene

The Chambaran basin is located between the Variscan Massif Central and Western Alps (Figs. 8.1a & 8.2d). Basin fill consists of a ~1 km thick sediment succession that contains deposits from mainly Alpine source areas (Clauzon, 1990). During the Miocene, marine conditions prevailed in north- and west-Alpine foreland basins, with southwestward sediment transport toward the Mediterranean Sea (Figs. 8.2a & b; Mortaz-Djalili and Perriaux, 1979; Kuhlemann *et al.*, 2001; Sissingh, 2001). Marine conditions retreated toward west-Alpine foreland basins around the Middle Miocene and were replaced by terrestrial sedimentation (Kuhlemann and Kempf, 2002; Ziegler and

Fraefel, 2009). In the latest Miocene, the Messinian salinity crisis led to a lowering of the erosional base level of the Alpine drainage system. During the Pliocene, a marine transgression partially flooded the west-Alpine foreland basins, but never reached the Miocene extent (Sissingh, 2001). The Quaternary was dominated by a fluvio-glacial environment due to glaciations affecting the Western Alps and Massif Central (Clauzon, 1990).

One potential source area of Middle Miocene Chambaran sediments is the central-Alpine Lepontine area as suggested by Glotzbach *et al.* (2011), where this area experienced accelerated exhumation at that time (e.g., Spiegel *et al.*, 2000). Present-day exposures of the Lepontine show AFT cooling ages ranging from 2-19 Ma (Vernon *et al.*, 2008, and references therein, Pignalosa *et al.*, 2011; Elfert *et al.*, 2011). Another potential source are the Variscan massifs representing European basement, i.e., the Massif Central, Vosges and Black Forest, mostly showing Paleogene AFT ages (Barbarand *et al.*, 2001; Timar-Geng *et al.*, 2006). Drainage reorganisations changed the sediment pathways as follows: *(i)* at ~10 Ma, a drainage divide located at the southern Black Forest and the NW-Jura mountains cut off the sediment transport from the Central Alps toward the Mediterranean (Kuhlemann *et al.*, 2001); *(ii)* at ~4.2 Ma, this divide was shifted eastward, partially re-establishing the northern sediment pathway toward the Mediterranean but also toward the North Sea (e.g., Ziegler and Fraefel, 2009; Reiter *et al.*, in press). At this time, the Sundgau gravel (southernmost Upper Rhine Graben, Fig. 8.2c) were deposited, mainly consisting of central-Alpine detritus, i.e., Aar-Gotthard massif and Lepontine area (Liniger, 1966; Reiter *et al.*, in prep); and *(iii)* after ~2.9 Ma, the west-Alpine drainage system mainly drained the Western Alps but also the Vosges and Massif Central. Further potential source areas are the volcanic complexes associated with the Cenozoic European Rift System, i.e., Forez, Limagne and Velay complexes (Massif Central) which have been active from ~15-1 Ma (Nehlig *et al.*, 2003), and Kaiserstuhl/Hegau complexes (Upper Rhine Graben) being active from ~18-9 Ma (e.g., Keller *et al.*, 2002; Rahn and Selbekk, 2007).

8.4 Material and methods

8.4.1 Sampling strategy

Sampled Chambaran deposits span the period between 15 Ma and the present. For this study, we used the same samples as Glotzbach *et al.* (2011) comprising of six samples from Miocene to Pliocene molasse sediments, one Pleistocene glacial deposit, and two modern fluvial sand deposits (Fig. 8.1b). Samples were taken from sandy layers and lenses within (glacio-)fluvial deposits, and showed no or only slight signs of sediment compaction. 36 single apatite grains were analysed by AHe thermochronometry.

8.4.2 Methods and concept of detrital thermochronology

Due to its sensitivity to low temperatures, AHe data reflect processes affecting shallow crustal levels between ~3 and ~1 km. For details on analytical procedures see supplement. Provenance analysis is usually performed by comparing cooling signatures from present-day outcrops of potential source areas with detrital cooling signatures of associated sediment deposits. A prerequisite is that age patterns of source areas differ from each other, as it is the case for Variscan units with Cretaceous-Paleogene AFT ages and Alpine units with Neogene AFT ages. Distinguishing between Alpine units is challenging as their ages patterns do not differ strongly.

However, in addition to just comparing the ages, we also took into account the modeled cooling histories of the detrital age groups and compared them to published thermal histories of potential source areas.

With the lag time approach, where lag time is defined as the difference between stratigraphic and cooling age (Garver *et al.*, 1999), it is possible to identify changes in long-term exhumation patterns of source areas. Under the assumption of largely constant isotherm positions, general interpretations are: *(i)* decreasing lag times upsection (towards stratigraphically younger deposits) represent enhanced hinterland exhumation, *(ii)* constant lag times reflect steady exhumation, and *(iii)* a post-orogenic and erosive phase of the source area is reflected by increasing lag times. It should be kept in mind, however, that detrital thermochronology only monitors apatite bearing lithologies. Fine-grained sedimentary rocks such as limestones or mudstones usually have a low apatite yield and are therefore difficult to trace. Furthermore, individual erodibility of the source rocks also influences data interpretation (e.g., Attal and Lave, 2009; Nie *et al.*, 2012).

8.5 Results and interpretation

Results of AHe analysis, central AHe calculation and forward modeling are shown in Tables 8.1, 8.2 and 8.3, and Figs. 8.3 & 8.4. Single AHe ages range from 2.7 to 37.2 Ma. One data outlier and five samples where AHe analysis yielded only single AHe ages were excluded from further interpretation (see Table 8.1). As a remark, for reasons of clarity associated AHe/AFT age pairs are abbreviated as follows, e.g., youngest AHe/AFT pair at 15 Ma depositional age is equal to 15-1, second youngest age pair at 15 Ma equal to 15-2, and so forth. Forward modeling the AFT and AHe data is based on the annealing model by Ketcham *et al.* (2007) and the diffusion model after Farley (2000).

The AHe and AFT lag times of ~0 Ma (within error) of Miocene sample pairs 15-1 and 13-1 are remarkable (Fig. 8.3), suggesting that cooling of the source was extremely fast. Between 13 and 0 Ma depositional age, AHe(/AFT) lag times of ~6 Ma could indicate a steady-state exhumation of the hinterland. Forward modeling of most sample pairs (13-2, 5-1, 4-1 & 0-2) yielded constant cooling paths at distinct rates (Table 8.3, Fig. 8.4). Higher cooling rates of sample pairs 13-2 and 4-1 are correlated with smaller lag times (~6 Ma), and lower cooling rates of 5-1 and 0-2 with higher lag times (~10-17 Ma). More interestingly, two sample pairs show a change in their cooling pattern, a decreasing cooling rate since ~7 Ma for 0-1 and an increasing rate since ~15 Ma for 4-2.

AHe/AFT pair	Depositional age (Ma)	Cooling rate (°C Ma^{-1})	Exhumation rate (km Ma^{-1})
0-1	recent	40 → 9	1.6 → 0.4
0-2	recent	9	0.4
4-1	4.2 ±0.5	12	0.5
4-2	4.2 ±0.5	3 → 7	0.1 → 0.3
5-1	5.0 ±0.3	7	0.3
13-2	13 ±2	12	0.5

Table 8.3: Calculated cooling and exhumation rates. Cooling rates are extracted from modeled cooling paths. For calculating exhumation rates, a geothermal gradient of 25 °C km^{-1} was assumed. Modeling of 0-1 and 4-2 yielded changing cooling rates through time (see also Fig. 8.4).

Sample	Strat. age ±error (Ma)	N	Raw age (Ma)	Error raw age (Ma)	Corrected age (Ma)	Error corr age (Ma)	FT factor	Sphere radius (µm)	^{4}He (ncc)	Mass (mg)	Th/U ratio	^{149}Sm (ng)	^{232}Th (ng)	^{238}U (ng)
*CGP-124 #1**	*recent*	*1*	*1.75*	*0.11*	*2.67*	*0.31*	*0.66*	*45.48*	*0.029*	*0.0019*	*3.8512*	*0.1143*	*0.2754*	*0.0715*
CGP-124 #2	recent	1	5.65	0.35	7.24	0.85	0.78	71.77	0.101	0.0061	1.9394	0.5056	0.1958	0.1010
CGP-125 #1	recent	1	4.68	0.29	6.08	0.72	0.77	68.28	0.093	0.0061	2.6270	0.7205	0.2657	0.1011
CGP-125 #2	recent	1	5.75	0.36	7.44	0.88	0.77	74.85	0.127	0.0049	0.5400	0.4998	0.0872	0.1614
CGP-125 #4	recent	1	4.70	0.29	6.21	0.73	0.76	69.73	0.045	0.0026	1.9957	0.5231	0.1067	0.0535
CGP-125 #6	recent	1	5.60	0.35	6.92	0.81	0.81	87.45	0.131	0.0091	2.9008	0.9291	0.3303	0.1139
CGP-125 #7	recent	1	7.20	0.45	8.79	1.03	0.82	89.03	0.351	0.0108	1.4283	1.3210	0.4294	0.3006
*CGP-104 #1**	*2.5 ±1*	*1*	*22.30*	*1.38*	*31.43*	*3.70*	*0.71*	*55.12*	*0.313*	*0.0019*	*0.3552*	*0.6111*	*0.0378*	*0.1063*
*CGP-100A**	*3.5 ±1*	*1*	*10.88*	*0.67*	*14.87*	*1.75*	*0.73*	*59.61*	*0.119*	*0.0021*	*0.7490*	*0.0814*	*0.0575*	*0.0786*
CGP-101 #1	4.2 ±0.5	1	6.74	0.42	8.37	0.99	0.81	75.30	0.201	0.0087	6.8400	1.0964	0.6407	0.0937
CGP-101 #2	4.2 ±0.5	1	9.14	0.57	13.41	1.58	0.68	47.02	0.077	0.0016	0.7162	0.4418	0.0423	0.0591
CGP-101 #3	4.2 ±0.5	1	7.46	0.46	9.92	1.17	0.75	60.94	0.106	0.0036	1.2346	0.9275	0.1112	0.0901
CGP-101 #4	4.2 ±0.5	1	10.33	0.64	13.61	1.60	0.76	67.01	0.296	0.0062	1.8047	0.9740	0.2982	0.1653
CGP-101 #6	4.2 ±0.5	1	9.70	0.60	13.07	1.54	0.74	61.48	0.263	0.0041	0.6187	0.4517	0.1209	0.1953
CGP-107 #1	5.0 ±0.3	1	11.20	0.69	15.88	1.87	0.71	55.37	0.207	0.0033	2.0551	0.8269	0.2100	0.1022
CGP-107 #2	5.0 ±0.3	1	9.54	0.59	11.85	1.39	0.81	88.89	0.552	0.0095	0.9952	0.6884	0.3847	0.3865
*CGP-107 #4**	*5.0 ±0.3*	*1*	*14.62*	*0.91*	*21.23*	*2.50*	*0.69*	*51.64*	*0.158*	*0.0014*	*1.6329*	*0.3117*	*0.1048*	*0.0642*
CGP-107 #5	5.0 ±0.3	1	11.45	0.71	17.59	2.07	0.65	50.82	0.037	0.0015	0.6095	0.5101	0.0139	0.0228
CGP-107 #6	5.0 ±0.3	1	13.33	0.83	17.82	2.10	0.75	63.29	0.121	0.0024	0.6160	0.5828	0.0400	0.0650
CGP-106 #1	13 ±2	1	11.20	0.69	13.87	1.63	0.81	82.43	0.151	0.0095	0.6051	1.9355	0.0578	0.0956
CGP-106 #2	13 ±2	1	9.80	0.61	13.01	1.53	0.75	61.15	0.158	0.0038	0.3906	1.8431	0.0469	0.1200
CGP-106 #3	13 ±2	1	7.68	0.48	10.28	1.21	0.75	55.69	0.032	0.0019	0.3186	0.5117	0.0100	0.0315
CGP-106 #4	13 ±2	1	10.50	0.65	15.35	1.81	0.68	45.04	0.057	0.0020	0.7337	0.4317	0.0277	0.0378
*CGP-106 #5**	*13 ±2*	*1*	*28.48*	*1.77*	*37.20*	*4.38*	*0.77*	*68.28*	*0.061*	*0.0057*	*0.7703*	*0.3555*	*0.0112*	*0.0146*
CGP-106 #6	13 ±2	1	15.26	0.95	19.53	2.30	0.78	72.23	0.201	0.0065	0.3050	0.2771	0.0309	0.1013

Table 8.1: Results of (U-Th-Sm)/He analyses. Strat. age, stratigraphical age. N, number of analyzed grains. Sample names marked with stars represent data outliers and single cooling ages which were not included for central AHe age determination.

Sample	Strat. age ±error (Ma)	N	Raw age (Ma)	Error raw age (Ma)	Corrected age (Ma)	Error corr age (Ma)	FT factor	Sphere radius (μm)	^{4}He (ncc)	Mass (mg)	Th/U ratio	^{149}Sm (ng)	^{232}Th (ng)	^{238}U (ng)
CGP-111 #1	13 ±2	1	15.29	0.95	19.07	2.24	0.80	79.74	0.856	0.0089	0.0274	1.7882	0.0125	0.4581
CGP-111 #2	13 ±2	1	12.68	0.79	15.69	1.85	0.81	77.70	0.588	0.0082	0.7949	1.7143	0.2552	0.3210
CGP-111 #3	13 ±2	1	12.29	0.76	15.91	1.87	0.77	64.92	0.276	0.0039	0.8397	1.0758	0.1292	0.1539
CGP-111 #5	13 ±2	1	14.53	0.90	18.67	2.20	0.78	72.00	0.594	0.0067	1.3732	1.0077	0.3491	0.2542
CGP-111 #6	13 ±2	1	13.58	0.84	16.86	1.98	0.81	81.78	0.401	0.0094	1.5632	1.0270	0.2772	0.1773
CGP-114 #1	15 ±1	1	10.69	0.66	12.52	1.47	0.85	113.13	1.929	0.0291	6.8622	5.4149	3.8822	0.5657
CGP-114 #2	15 ±1	1	12.35	0.77	15.21	1.79	0.81	84.60	0.537	0.0106	0.7444	2.5773	0.2256	0.3031
CGP-114 #3	15 ±1	1	11.92	0.74	15.17	1.79	0.79	74.45	0.688	0.0079	0.8174	2.6837	0.3249	0.3975
CGP-114 #4	15 ±1	1	11.73	0.73	13.80	1.62	0.85	106.25	1.199	0.0214	0.7457	6.3831	0.5312	0.7123
CGP-114 #5	15 ±1	1	10.58	0.66	13.50	1.59	0.78	72.60	0.123	0.0064	0.6187	0.0720	0.0589	0.0822
*CGP-114 #6**	*15 ±1*	*1*	*7.91*	*0.49*	*9.69*	*1.14*	*0.82*	*87.85*	*0.065*	*0.0114*	*2.2517*	*2.6548*	*0.0950*	*0.0422*

Table 8.1 (continued).

Sample	Stratigraphic age ±error (Ma)	Samples for central age calculation	Central AHe age (Ma)	Standard error (Ma)	N^{c}	Associated AFT age group (Ma)	2σ CI (Ma)	F (%)
CGP-124/-125 **P1**	recent	CGP-124#2, CGP-125#1-7	7.3	0.4	6	11.6	−1.4, +1.6	68
CGP-101 **P1**	4.2 ±0.5	CGP-101#1 / #3	10.2	0.4	2	11.2	−1.1, +1.2	20
CGP-101 **P2**	4.2 ±0.5	CGP-101#2 / #4 / #6	13.7	0.2	3	21.1	−2.0, +2.2	79
CGP-107 **P1**	5.0 ±0.3	CGP-107#1 / #2 / #5 / #6	16.0	1.4	4	19.6	−2.1, +2.4	66
CGP-106/-111 **P1**	13 ±2	CGP-106#2 / #3	11.9	1.4	2	13.7	−1.8, +2.1	82
CGP-106/-111 **P2**	13 ±2	CGP-106#1 / #4 / #6, CGP-111#1-6	17.7	1.0	8	20.1	−1.7, +1.9	97
CGP-114 **P1**	15 ±1	CGP-114#1-5	15.2	0.6	5	16.2	−1.7, +1.9	72

Table 8.2: Calculated central AHe ages. P1 and P2 represent the youngest and second youngest central AHe ages. N^{c}, number of single AHe ages used for central age calculation. Associated AFT age group represents the next older age group (Glotzbach *et al.,* 2011) assumed to belong to the younger centralAHe age. F, percentage of single AFT grain ages of the specified age group; the basis for each sample consists of 100 grain ages.

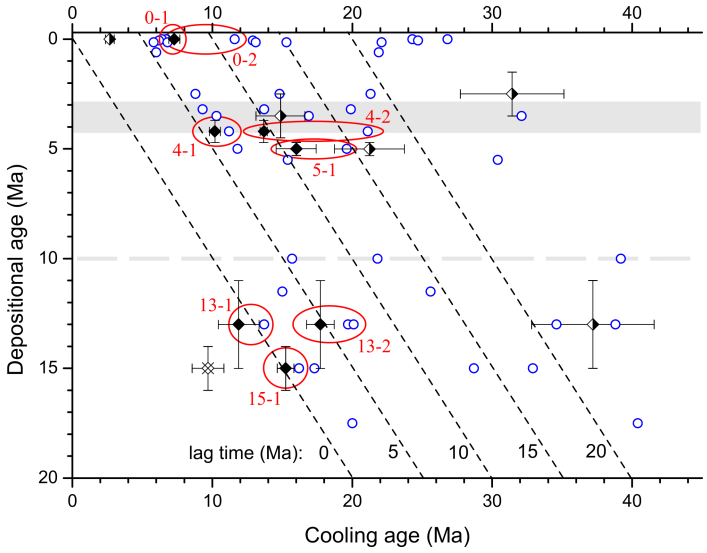

Fig. 8.3: AHe data and AFT peak ages plotted against depositional ages with lines of equal lag times (broken lines). Dotted, horizontal line represents timing of drainage reorganisation at ~10 Ma. Grey-highlighted area indicates deposition time of the Sundgau gravel (~4.2-2.9 Ma). White-filled (crossed) diamonds represents the statistical outlier. Half-white/half-black-filled diamonds represent single AHe ages. Black diamonds represent central AHe ages. Blue circles represent AFT age groups from Glotzbach *et al.* (2011); for reason of clarity AFT errors are not shown. Red ellipses represent AHe/AFT pairs used for modeling cooling histories of major source areas.

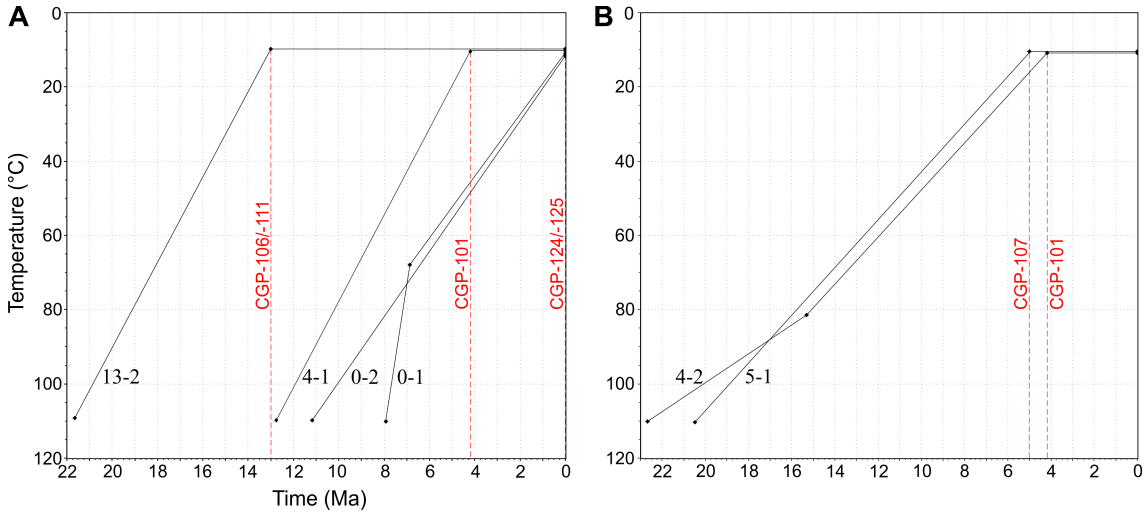

Fig. 8.4: (a) Modeled time-temperature paths of the AHe/AFT pairs 13-2, 4-1, 0-1, and 0-2 used for refinement of provenance analysis and testing the hypothesis of steady-state exhumation for the Western Alps. (b) Modeled thermal histories for AHe/AFT pairs 5-1 and 4-2.

8.6 Discussion

8.6.1 Refined provenance analysis of Chambaran sediments since the Miocene

Deposition during the Miocene

Glotzbach *et al.* (2011) suggested that a main sediment contributor was the Lepontine area associated with the youngest AFT lag times at 15 and 13 Ma depositional age, but Spiegel *et al.* (2000) showed that first large exposure of this area is not recorded in the Swiss Molasse sediments before ~14 Ma. Hence, zero AHe/AFT lag times at 15 and 13 Ma depositional ages cannot represent the Lepontine area but may be explained by *(i)* thermal resetting of the AHe(/AFT) system or *(ii)* substantial input of volcanic material into the basin.

Regarding *(i)*, thermal resetting seems unlikely as sampled Miocene sediments are lacking severe compaction, and maximum burial temperatures are estimated as ~25°C (vitrinite reflectance: 0.21, Moss, 1992; temperature calculation after Barker & Pawlewicz, 1986). Sampled sediments showed also no signs of hydrothermal activity as reported from the modern Rhône Graben (Garibaldi *et al.*, 2010). Regarding *(ii)*, the explanation of volcanic input is supported by the occurrence of plastic clay layers (benthonite?) in Burdigalian sediments of the Chambaran basin (BRGM borehole St. Lattier-2), and the morphology of analyzed apatite grains (length up to 300 µm, flat, angular to subangular) which may indicate volcanic origin and short sediment transport. Potential source areas are volcanic complexes located at the Massif Central and/or Upper Rhine Graben (Fig. 8.2a). Regarding 13-2, AFT lag times of ~7 Ma coincides with the thermal signature of modern Lepontine exposures (Vernon *et al.*, 2008, and references therein; Elfert *et al.*, 2011). In addition, the cooling rate of ~12°C Ma^{-1}, which may be equivalent to an exhumation rate of ~0.5 km Ma^{-1} (Table 8.3), agrees with thermal reconstructions of the Lepontine (Hurford *et al.*, 1986; Pignalosa *et al.*, 2011).

Deposition during the Pliocene

Until ~2.9 Ma, the west-Alpine foreland, and thus the Chambaran basin, was connected with the NW-Alpine drainage system (e.g., Ziegler & Fraefel, 2009). As this drainage system drained the Central Alps via the Sundgau gravel and the west-Alpine foreland toward the Mediterranean Sea, it can be speculated if the ~6 Ma lag time of sample pair 4-1 represents a thermal signature of the central-Alpine Aar-Gotthard massif. This would be in line with the interpretation of the youngest AFT age groups of the Sundgau samples (Liniger, 1966; Reiter *et al.*, in prep) and the thermal signature of modern rock exposures of the Aar-Gotthard massif (Vernon *et al.*, 2008). In addition, the modeled constant exhumation rate of ~0.5 km Ma^{-1} for sample pair 4-1 (Table 8.3) is in agreement with the reconstructed exhumation history of the Aar-Gotthard massif by Glotzbach *et al.* (2010). Based on these observation, we assume that the Aar-Gotthard massif is one of the major source areas for the Pliocene Chambaran deposits. The older AFT lag times between ~15 and 17 Ma of sample pairs 5-1 and 4-2 show comparable age signatures as reported from modern outcrops of the middle Penninic domain (Houillère zone) in the Western Alps (Fügenschuh & Schmid, 2003; Vernon *et al.*, 2008). Thermal modeling with sample pair 5-1 shows that the Houillère zone must have experienced constant cooling at a rate of ~7°C Ma^{-1} since the Early Miocene. This observation is in good agreement with the thermal reconstruction from the northern part of this area (Fügenschuh & Schmid, 2003). However, modeling of sample pair 4-2 compared to 5-1 displaying slower cooling in the beginning, but closely followed by an increased rate of 7°C Ma^{-1} since ~15 Ma (Fig. 8.4b). A similar cooling history is described for the southern Houillère area, where tilting of this area is assumed to have started at ~17 Ma (Fügenschuh & Schmid, 2003). Both cooling paths show constant cooling of the whole Houillère area from ~15 Ma until at least ~4 Ma.

Present-day situation

The sample pairs 0-1 and 0-2 of the present-day Chambaran samples show predominantly AHe ages of ~7 Ma and AFT ages of ~12 Ma (Glotzbach *et al.*, 2011), comparable to what is reported from the Pelvoux and Belledonne massifs (Vernon *et al.*, 2008; van der Beek *et al.*, 2010). Additionally, the modeled cooling histories of sample pairs 0-1 and 0-2 show constant exhumation rates since the Late Miocene (~7 Ma; Fig. 8.4) consistent with thermal reconstructions from modern rock exposures of the Belledonne and Pelvoux massifs (Lelarge, 1993; van der Beek *et al.,* 2010).

8.6.2 Testing the hypothesis of steady-state exhuming Western Alps

The hypothesis of a steady exhumation requires constant cooling styles at similar rates of the potential source rocks since ~10 Ma. The thermal reconstructions of the individual sample pairs do not meet those requirements, as the cooling(/exhumation) rates vary significantly between 3 and 40°C Ma^{-1} (/0.1 and 1.6 km Ma^{-1}; Fig. 8.4, Table 8.3). As the observed cooling styles are neither constant nor uniform, a generally suggested steady-state exhumation for the Western Alps is not reflected by our results.

8.7 Conclusions

The combination of statistical methods and forward modeling applied on detrital data, comprising of our own AHe data and AFT data of Glotzbach *et al.* (2011), showed its capability to refine the interpretation of existing detrital AFT studies regarding provenance analysis and reconstructing cooling histories of the hinterland. In case of the west-Alpine Chambaran foreland basin, we were able to:

(i) refine provenance analysis solely based on AFT data through detrital (U-Th-Sm)/He thermochronometry, i.e., to show that an influence of the Lepontine area on the Chambaran basin fill is not observed before ~13 Ma, and to identify a formerly unknown volcanic input of volcanic complexes from the Massif Central and/or Upper Rhine Graben on the Middle Miocene sediment record;

(ii) show that the new combination of statistical techniques, linked with the assumption that the mean value of AHe ages was derived from the same source as the next oldest AFT age group, allows to interpret smaller AHe data sets for detrital studies. Thermal modeling can be efficiently used to refine the allocation of the source area as well as to test hypotheses about potential exhumation equilibria of mountain ranges, e.g. the Western Alps where a generally suggested steady-state exhumation since 10 Ma seems unlikely.

8.8 Acknowledgements

This study is part of the EUROCORE project Thermo-Europe and was funded by the European Science Foundation (ESF) and the German Science Foundation (DFG – project SP673/5-1). Many thanks to Peter van der Beek and Matthias Bernet (both at Fourier University in Grenoble/France) for providing the detrital samples and scientific discussion about chronostratigraphy. We also would like to thank BRGM (France) for their support regarding borehole information in the study area. And special thanks to Barry Kohn (University of

Melbourne/Australia) for his support regarding the AHe analyses.

8.9 References

Attal, M. & Lavé, J. (2009) Pebble abrasion during fluvial transport: Experimental results and implications for the evolution of the sediment load along rivers. *J. Geophys. Res.*, *114*, F04023, doi:10.1029/2009JF001328.

Barbarand, J., Lucazeau, F., Pagel, M. & Séranne, M. (2001) Burial and exhumation history of the south-eastern Massif Central (France) constrained by apatite fission-track thermochronology. *Tectonophysics*, *335*, 275–290.

Barker, C.E. & Pawlewicz, M.J. (1986) The correlation of vitrinite reflectance with maximum temperature in humic organic matter. *Paleogeothermics*, *5*, 79–93.

Clauzon, G. (1990) *Genèse et évolution du piémont néogène subalpin du Bas-Dauphiné*. Livret-Guide du 3e Forum National de Géomorphologie, Université d'Aix-Marseille II, Aix-en-Provence, 71 pp.

Elfert, S., Reiter, W. & Spiegel, C. (2011) Doming and unroofing of the Lepontine Dome (Central European Alps). New insights from Low-Temperature thermochronology. *Geophysical Research Abstracts*, *13*, EGU2011-11983.

Farley, K. (2000) Helium diffusion from apatite: General behaviour as illustrated by Durango flourapatite. *Journal of Geophysical Research*, *105*, 2903–2914.

Fügenschuh, B. & Schmid, S.M. (2003) Late stages of deformation and exhumation of an orogen constrained by fission-track data: A case study in the Western Alps. *Geological Society of America Bulletin*, *115*, 1425–1440.

Garibaldi, C., Guillou-Frottier, L., Lardeaux, J.-M., Bonté, D., Lopez, S., Bouchot, V. & Ledru, P., (2010) Thermal anomalies and geological structures in the Provence basin: Implications for hydrothermal circulations at depth. *Bull. Soc. géol. Fr.*, *181*, 363–376.

Garver, J.I., Brandon, M.T., Roden-Tice, M. & Kamp, P.J.J. (1999) Exhumation history of orogenic highlands determined by detrital fission-track thermochronology. *Geological Society Special Publications*, *154*, 283–304.

Gleadow, A.J.W. & Duddy, I.R. (1981) A natural long-term annealing experiment for apatite. *Nuclear Tracks and Radiation Measurements*, *5*, 169–174.

Glotzbach, C., Bernet, M. & van der Beek, P. (2011) Detrital thermochronology records changing source areas and steady exhumation in the Western European Alps. *Geology*, *39*, 239–242.

Keller, J., Kramel, M. & Henjes-Kunst, F. (2002) $^{40}Ar/^{39}Ar$ single crystal dating of early volcanism in the Upper Rhine Graben and tectonic implications. *Schweiz. Mineral. Petrogr. Mitt.*, *82*, 121–130.

Ketcham, R.A. (2005) Forward and Inverse Modeling of Low-Temperature Thermochronometry Data. *Reviews in Mineralogy & Geochemistry*, *58*, 275–314.

Ketcham, R.A., Carter, A., Donelick, R.A., Barbarand, J. & Hurford, A.J. (2007) Improved modeling of fission-track annealing in apatite. *American Mineralogist*, *92*, 799–810.

Kuhlemann, A. & Kempf, O. (2002) Post-Eocene evolution of the North Alpine Foreland Basin and its response to Alpine tectonics. *Sedimentary Geology*, *152*, 45–78.

Kuhlemann, J., Frisch, W., Dunkl, I., Székely, B. & Spiegel, C. (2001) Miocene shifts of the drainage divide in the Alps and their foreland basin. *Z. Geomorph. N. F.*, *45*, 239–265.

Liniger, H. (1966) Das plio-altpleistozäne Flussnetz der Nordschweiz. *Regio Bas*, *7*, 158–177.

Mortaz-Djalili, D. & Perriaux, J. (1979) Le Néogène du Plateau de Chambaran (Bas-Dauphiné, France). *Géologie Alpine*, *55*, 133–152.

Moss, S. (1992) Organic maturation in the French Subalpine Chains: regional differences in the burial history and the size of tectonic loads. *Journal of the Geological Society*, *149*, 503–515.

Nehlig, P., Boivin, P., de Goër, A., Mergoil, J., Prouteau, G., Sustrac, G. & Thiéblemont, D. (2003) *Les volcans du Massif central*. Revue Géologues Numéro spécial Massif central, BRGM, Orleans, 41 pp.

Nie, J., Horton, B.K., Saylor, J.E., Mora, A., Mange, M., Garzione, C.N., Basu, A., Moreno, C.J., Caballero, V. & Parra, M. (2012) Integrated provenance analysis of a convergent retroarc foreland system: U–Pb ages, heavy minerals, Nd isotopes, and sandstone compositions of the Middle Magdalena Valley basin, northern Andes, Colombia. *Earth Science Reviews*, *110*, 111–126.

Pignalosa, A., Zattin, M., Massironi, M. & Cavazza, W. (2011) Thermochronological evidence of a late Pliocene climate-induced erosion rate increase in the Alps. *Int J Earth Sci*, *100*, 847–859.

Rahn, M.K. & Selbekk, R. (2007) Absolute dating of the youngest sediments of the Swiss Molasse basin by apatite fission track analysis. *Swiss J Geosci*, *100*, 371–381.

Reinecker, J., Danišik, M., Schmid, C., Glotzbach, C., Rahn, M., Frisch, W. & Spiegel, C. (2008) Tectonic control on the late stage exhumation of the Aar Massif (Switzerland): Constraints from apatite fission track and (U-Th)/He data. *Tectonics*, *27*, TC6009, doi:10.1029/2007TC002247.

Reiter, W., Elfert, S., Glotzbach, C., Bernet, M. & Spiegel, C. (in press). Relations between denudation, glaciation, and sediment deposition: implications from the Plio-Pleistocene Central Alps. *Basin Research*, doi:10.1111/bre.12023.

Reiter, W., Elfert, S., Glotzbach, C. & Spiegel, C. (in preparation) Plio-Pleistocene evolution of the north-Alpine drainage system – implications from Neogene foreland deposits.

Schmid, S.M., Fügenschuh, B., Kissling, E. & Schuster, R. (2004) Tectonic map and overall architecture of the Alpine orogen. *Eclogae geol Helv*, *97*, 93–117.

Sissingh, W. (2001) Tectonostratigraphy of the West Alpine Foreland: correlation of Tertiary sedimentary sequences, changes in eustatic sea-level and stress regimes. *Tectonophysics*, *333*, 361-400.

Spiegel, C., Kuhlemann, J., Dunkl, I., Frisch, W., von Eynatten, H. & Balogh, K. (2000) The erosion history of the Central Alps: evidence from zircon fission track data of the foreland basin sediments. *Terra Nova*, *12*, 163–170.

Stock, G.M., Ehlers, T.A. & Farley, K.A. (2006) Where does sediment come from? Quantifying catchment erosion with detrital apatite (U-Th)/He thermochronometry. *Geology*, *34*, 725–728.

Timar-Geng, Z., Fügenschuh, B., Wetzel, A. & Dresmann, H. (2006) Low-temperature thermochronology of the flanks of the southern Upper Rhine Graben. *Int J Earth Sci*, *95*, 685–702.

Valla, P.G., van der Beek, P.A., Shuster, D.L., Braun, J., Herman, F., Tassan-Got, L. & Gautheron, C. (2012) Late Neogene exhumation and relief development of the Aar and Aiguilles Rouges massifs (Swiss Alps) from low-temperature thermochronology modeling and $^{4}He/^{3}He$ thermochronometry. *Journal of Geophysical Research*, *117*, F01004.

Van der Beek, P., Valla, P.G., Herman, F., Braun, J, Persano, C., Dobson, K.J. & Labrin, E. (2010) Inversion of thermochronological age-elevation profiles to extract independent estimates of denudation and relief history – II: Application to the French Western Alps. *Earth and Planetary Science Letters*, *296*, 9–22.

Vermeesch, P. (2008) Three new ways to calculate average (U-Th)/He ages. *Chemical Geology*, *249*,

339–347.
Vernon, A.J., van der Beek, P.A., Sinclair, H.D. & Rahn, M.K. (2008) Increase in late Neogene denudation of the European Alps confirmed by analysis of a fission-track thermochronology database. *Earth and Planetary Science Letters*, *270*, 316–329.
Wolf, R.A., Farley, K.A. & Kass, D.M. (1998) Modeling of the temperature sensitivity of the apatite (U-Th)/He thermochronometer. *Chemical Geology*, *148*, 105–114.
Ziegler, A. & Fraefel, M. (2009) Response of drainage systems to Neogene evolution of the Jura fold-thrust belt and Upper Rhine Graben. *Swiss J. Geosci.*, *102*, 57–75.

8.10 Supplement

8.10.1 Analytical procedure for AHe analysis

For AHe thermochronology apatite crystals were selected after the criteria described by Farley (2002). Appropiate apatite grains were put into cleaned Pt tubes. For cleaning, the Pt tubes were exposed to 37% HCl at a temperature between 35 and 40°C for 48 hours. AHe analysis was carried out at the University of Melbourne. ^{4}He was extracted by laser heating and then measured with a Balzers quadrupole mass spectometer by using the ^{3}He isotope dilution method. For analysing U, Th, and Sm contents, mass spectrometry using a second-generation Varian quadrupole ICP-MS was applied. All apatites were corrected for ^{4}He loss at the grain margins according to the alpha correction approach of Farley *et al.* (1996). A comparison between dating of alpha-corrected and mechanical abraded apatites from the Rhine Graben showed that at least for these samples sediment transport did not affect AHe ages (Reiter *et al.*, in press). However, a slight overcorrection for the samples of this study cannot be excluded.

8.10.2 References

Farley, K. (2002) (U-Th)/He Dating: Techniques, Calibrations, and Applications. *Reviews in Mineralogy and Geochemistry*, *47*, 819–844.
Farley, K., Wolf, R.A. & Silver, L.T. (1996) The effects of long alpha-stopping distances on (U-Th)/He ages. *Geochimica et Cosmochimica Acta*, *60*, 4223–4229.
Reiter, W., Elfert, S., Glotzbach, C., Bernet, M. & Spiegel, C. in press. Relations between. denudation, glaciation, and sediment deposition: implications from the Plio-Pleistocene Alps. *Basin Research*, doi:10.1111/bre.12023.

9 Complete bibliography

Attal, M. & Lavé, J. (2009) Pebble abrasion during fluvial transport: Experimental results and implications for the evolution of the sediment load along rivers. *J. Geophys. Res.*, *114*, F04023, doi:10.1029/2009JF001328.

Avdeev, B., Niemi, N.A. & Clark, M.K. (2011) Doing more with less: Bayesian estimation of erosion models with detrital thermochronometric data. *Earth and Planetary Science Letters*, *305*, 385–395.

Barbarand, J., Lucazeau, F., Pagel, M. & Séranne, M. (2001) Burial and exhumation history of the south-eastern Massif Central (France) constrained by apatite fission-track thermochronology. *Tectonophysics*, *335*, 275–290.

Barker, C.E. & Pawlewicz, M.J. (1986) The correlation of vitrinite reflectance with maximum temperature in humic organic matter. *Paleogeothermics*, *5*, 79–93.

Becker, A. (2000) The Jura Mountains – and active foreland fold-and-thrust belt? *Tectonophysics*, *321*, 381–406.

Berger, J.P. (1985) La transgression de la Molasse marine supèrieure (OMM) en Suisse occidentale. *Münchn geowiss Abh*, *5*, 1–207.

Berger, J.-P., Reichenbacher, B., Becker, D., Grimm, M., Grimm, K., Picot, L., Storni, A., Pirkenseer, C., Derer, C. & Schaefer, A. (2005) Paleogeography of the Upper Rhine Graben (URG) and the Swiss Molasse Basin (SMB) from Eocene to Pliocene. *Int J Earth Sci*, *94*, 697–710.

Berger, A.L. & Spotila, J.A. (2008) Denudation and deformation in a glaciated orogenic wedge: The St. Elias orogen, Alaska. *Geology*, *36*, 523–526.

Boenigk, W. (1987) Petrographische Untersuchungen jungtertiärer und quartärer Sedimente am linken Oberrhein. *Jber. Mitt. oberrhein. geol. Ver.*, *69*, 357–394.

Bolliger, T., Fejfar, O., Graf, H. & Kälin, D. (1996) Vorläufige Mitteilung über Funde von pliozänen Kleinsäugern aus den höheren Deckenschottern des Irchels (Kt. Zürich). *Eclogae geol. Helv.*, *89*, 1043–1048.

Brocklehurst, S.H., Whipple, K.L. & Foster, D. (2008) Ice thickness and topographic relief in glaciated landscapes of the western USA. *Geomorphology*, *97*, 35–51.

Burtner, R.L., Nirgini, A. & Donelick, R.A. (1994) Thermochronology of Lower Cretaceous Source Rocks in the Idaho-Wyoming Thrust Belt. *AAPG Bulletin*, *78*, 1613–1636.

Campani, M., Herman, F. & Mancktelow, N. (2010) Two- and three- dimensional thermal modeling of a low-angle detachment: Exhumation history of the Simplon Fault Zone, central Alps. *Journal of Geophysical Research*, *115*, B10420, doi:10.1029/2009JB007036.

Carlson, W.D., Donelick, R.A. & Ketcham, R.A. (1999) Variability of apatite fission-track annealing kinetics: I. Experimental results. *American Mineralogist*, *84*, 1213–1223.

Cederbom, C.E., Sinclair, H.D., Schlunegger, F. & Rahn, M.K. (2004) Climate-induced rebound and exhumation of the European Alps. *Geology*, *32*, 709–712.

Cederbom, C.E., van der Beek, P., Schlunegger, F., Sinclair, H.D. & Oncken, O. (2011) Rapid extensive erosion of the North Alpine foreland basin at 5-4 Ma. *Basin Research*, *23*, 528–550.

Champagnac, J.-D., Schlunegger, F., Norton, K., von Blanckenburg, F., Abbühl, L.M. & Schwab, M. (2009) Erosion-driven uplift of the modern Central Alps. *Tectonophysics*, *474*, 236–249.

Ciancaleoni, L. (2005) *Deformation processes during the last stages of the continental collision:*

the brittle–ductile fault systems in the Bergell and Insubric areas (Eastern Central Alps, Switzerland–Italy). Ph.D. thesis, University Neuchâtel, Switzerland.

Clauzon, G. (1990) *Genèse et évolution du piémont néogène subalpin du Bas-Dauphiné*. Livret-Guide du 3e Forum National de Géomorphologie, Université d'Aix-Marseille II, Aix-en-Provence, 71 pp.

Danišik, M., Pfaff, K., Evans, N.J., Manoloukos, C., Staude, S., McDonald, M.J. & Markl, G. (2010) Tectonothermal history of the Schwarzwald Ore District (Germany): An apatite triple dating approach. *Chemical Geology*, *278*, 58–69.

Dézes, P., Schmid, S.M. & Ziegler, P.A. (2004) Evolution of the European Cenozoic Rift System: interaction of the Alpine and Pyrenean orogens with their foreland lithosphere. *Tectonophysics*, *389*, 1–33.

Donelick, R.A., Ketcham, R.A. & Carlson, W.D. (1999) Variability of apatite fission-track annealing kinetics: II. Crystallographic orientation effects. *American Mineralogist*, *84*, 1224–1234.

Dunkl, I. (2002) Trackkey: A windows program for calculation and graphical presentation of fission track data. *Comput. Geosci.*, *28*, 3–12.

Ehlers, J. & Gibbard, P.L. (2007) The extent and chronology of Cenozoic Global Glaciation. *Quaternary International*, *164–165*, 6–20.

Ehlers, T.A. & Farley, K.A. (2003) Apatite (U-Th)/He thermochronometry: methods and applications to problems in tectonic and surface problems. *Earth and Planetary Science Letters*, *206*, 1–14.

Elfert, S., Reiter, W. & Spiegel, C. (2011) Doming and unroofing of the Lepontine Dome (Central European Alps). New insights from Low-Temperature thermochronology. *Geophysical Research Abstracts*, *13*, EGU2011-11983.

Ellwanger, D., Wielandt-Schuster, U., Franz, M. & Simon, T. (2011). The Quaternary of the southwest German Alpine Foreland (Bodensee, Oberschwaben, Baden-Württemberg, Southwest Germany). *Quaternary Science Journal*, *60*, 306–328.

Farley, K. (2000) Helium diffusion from apatite: General behaviour as illustrated by Durango flourapatite. *Journal of Geophysical Research*, *105*, 2903–2914.

Farley, K. (2002) (U-Th)/He Dating: Techniques, Calibrations, and Applications. *Reviews in Mineralogy and Geochemistry*, *47*, 819–844.

Farley, K., Wolf, R.A. & Silver, L.T. (1996) The effects of long alpha-stopping distances on (U-Th)/He ages. *Geochimica et Cosmochimica Acta*, *60*, 4223–4229.

Flisch, M. (1986) Die Hebungsgeschichte der oberostalpinen Silvretta-Decke seit der mittleren Kreide. *Bulletin der Vereinigung schweizerische Petroleum-Geologen und Ingenieure*, *53*, 23–49.

Frisch, W. (1979) Tectonic progradation and plate tectonic evolution of the Alps. *Tectonophysics*, *60*, 121–139.

Frisch, W., Dunkl, I. & Kuhlemann, J. (2000) Post-collisional orogen-parallel large-scale extension in the Eastern Alps. *Tectonophysics*, *327*, 239–265.

Füchtbauer, H. (1959) Zur Nomenklatur der Sedimentgesteine. *Erdöl Kohle*, *12*, 605–613.

Fügenschuh, B. & Schmid, S.M. (2003) Late stages of deformation and exhumation of an orogen constrained by fission-track data: A case study in the Western Alps. *Geological Society of America Bulletin*, *115*, 1425–1440.

Gabriel, G., Ellwanger, D., Hoselmann, C. & Weidenfeller, M. (2010) The Heidelberg Basin Drilling Project – Characteristics of an outstanding archive of Quaternary sediments. *Geophysical Research Abstracts EGU General Assembly*, *12*, EGU2010-7791.

Garibaldi, C., Guillou-Frottier, L., Lardeaux, J.-M., Bonté, D., Lopez, S., Bouchot, V. & Ledru, P.

(2010) Thermal anomalies and geological structures in the Provence basin: Implications for hydrothermal circulations at depth. *Bull. Soc. géol. Fr.*, *181*, 363–376.

Garver, J.I., Brandon, M.T., Roden-Tice, M. & Kamp, P.J.J. (1999) Exhumation history of orogenic highlands determined by detrital fission-track thermochronology. *Geological Society Special Publications*, *154*, 283–304.

Garzanti, E., Vezzoli, G. & Andò, S. (2011) Paleogeographic and paleodrainage changes during Pleistocene glaciations (Po Plain, Northern Italy). *Earth-Science Reviews*, *105*, 25–48.

Gautheron, C., Tassan-Got, L., Barbarand, J. & Pagel, M. (2009) Effect of alpha-damage annealing on apatite (U-Th)/He thermochronology. *Chemical Geology*, *266*, 157–170.

Giamboni, M., Ustaszewski, K., Schmid, S.M., Schumacher, M.E. & Wetzel, A. (2004) Plio-Pleistocene transpressional reactivation of Paleozoic and Paleogene structures in the Rhine-Bresse transform zone (northern Switzerland and eastern France). *Int J Earth Sci*, *93*, 207–223.

Giger, M. (1991) *Geochronologische und petrographische Studien an Geröllen und Sedimenten der Gonfolite Lombarda Gruppe (Südschweiz und Norditalien) und ihr Vergleich mit dem alpinen Hinterland*. Ph.D. thesis, University Bern, Switzerland.

Gleadow, A.J.W. (1981) Fission track dating methods: what are the real alternatives? *Nuclear Tracks and Radiation Measurements*, *5*, 3–14.

Gleadow, A.J.W. & Duddy, I.R. (1981) A natural long-term annealing experiment for apatite. *Nuclear Tracks and Radiation Measurements*, *5*, 169–174.

Glotzbach, C., Reinecker, J., Danišik, M., Rahn, M., Frisch, W. & Spiegel, C. (2008) Neogene exhumation history of the Mont Blanc massif, western Alps. *Tectonics*, *27*, TC4011, doi:10.1029/2008TC002257.

Glotzbach, C., Reinecker, J., Danišik, M., Rahn, M., Frisch, W. & Spiegel, C. (2010) Thermal history of the central Gotthard and Aar massifs, European Alps: Evidence for steady state, long-term exhumation. *J Geophys Res*, *115*, F03017, doi:10.1029/2009JF001304.

Glotzbach, C., van der Beek, P., Carcaillet, J. & Delunel, R. (in revision): Deciphering the driving forces of erosion rates on millennial to million year timescales in glacially impacted landscapes, an example from the Western Alps. *J Geophys Res,* in revision.

Glotzbach, C., van der Beek, P. & Spiegel, C. (2011) Episodic exhumation and relief growth in the Mont Blanc massif, Western Alps from numerical modelling of thermochronology data. *Earth and Planetary Science Letters*, *304*, 417–430.

Graf, H.R. (1993) *Die Deckenschotter der zentralen Nordschweiz*. Ph.D thesis, ETH Zürich, URL: http://e-collection.library.ethz.ch/view/eth:39047.

Graf, H.R. (2009) Stratigraphie und Morphogenese von frühpleistozänen Ablagerungen zwischen Bodensee und Klettgau. *Quaternary Science Journal*, *58*, 12–53.

Green, P.F., Duddy, I.R., Gleadow, A.J.W., Tingate, P.R. & Laslett, G.M. (1986) Thermal annealing of fission tracks in apatite 1. A Qualitative Description. *Chemical Geology, 59*, 237–253.

Habbe, K.A., Ellwanger, D. & Becker-Haumann, R. (2007) Stratigraphische Begriffe für das Quartär des süddeutschen Alpenvorlandes. *Quaternary Science Journal*, *56*, 66–83.

Haeuselmann, P., Granger, D.E., Jeannin, P.-Y. & Lauritzen, S.-E. (2007) Abrupt glacial valley incision at 0.8 Ma dated from cave deposits in Switzerland. *Geology*, *35*, 143–146.

Hagedorn, E.-M. & Boenigk, W. (2008) The Pliocene and Quaternary sedimentary and fluvial history in the Upper Rhine Graben based on heavy mineral analyses. *Netherlands Journal of Geosciences*, *87*, 21–32.

Hoselmann, C. (2008) The Pliocene and Pleistocene fluvial evolution in the northern Upper Rhine Graben based on results of the research borehole at Viernheim (Hessen, Germany). *Quaternary Science Journal*, *57*, 286–315.

Howat, I.M., Joughin, I., Tulaczyk, S. & Gogineni, S. (2005) Rapid retreat and acceleration of Helheim Glacier, east Greenland. *Geophysical Research Letters*, *32*, L22502, doi:10.1029/2005GL024737.

Hunze, S. & Wonik, T. (2008) Sediment Input into the Heidelberg Basin as determined from Downhole Logs. *Quaternary Science Journal*, *57*, 367–381.

Hurford, A.J. (1986) Cooling and uplift patterns in the Lepontine Alps South Central Switzerland and an age of vertical movement on the Insubric fault line. *Contrib Mineral Petrol*, *92*, 413–427.

Hurford, A.J., Flisch, M. & Jäger, E. (1989) Unravelling the thermo-tectonic evolution of the Alps: a contribution from fission track analysis and mica dating. In: *Alpine Tectonics*, (Ed. by M. P. Coward, D. Dietrich and R. G. Park), *Geological Society Special Publication*, *45*, 369–398.

Hurford, A.J. & Green, P.F. (1983) The zeta age calibration of fission-track dating. *Chem. Geol.*, *41*, 285–317.

Ivy-Ochs, S., Poschinger, A.V., Synal, H.-A. & Maisch, M. (2009) Surface exposure dating of the Flims landslide, Graubünden, Switzerland. *Geomorphology*, *103*, 104–112.

Keller, L.M., Hess, M., Fügenschuh, B. & Schmid, S. (2005) Structural and metamorphic evolution of the Camughera–Moncucco, Antrona and Monte Rosa units southwest of the Simplon line, Western Alps. *Eclogae geol. Helv.*, *98*, 19–49.

Keller, J., Kraml, M. & Henjes-Kunst, F. (2002) $^{40}Ar/^{39}Ar$ single crystal dating of early volcanism in the Upper Rhine Graben and tectonic implications. *Schweiz. Mineral. Petrogr. Mitt.*, *82*, 121– 130.

Ketcham, R.A. (2005) Forward and Inverse Modeling of Low-Temperature Thermochronometry Data. *Reviews in Mineralogy & Geochemistry*, *58*, 275–314.

Ketcham, R.A., Carter, A., Donelick, R.A., Barbarand, J. & Hurford, A.J. (2007) Improved modeling of fission-track annealing in apatite. *American Mineralogist*, *92*, 799–810.

Knipping, M. (2008) Early and Middle Pleistocene pollen assemblages of deep core drillings in the northern Upper Rhine Graben, Germany. *Netherlands Journal of Geosciences*, *87*, 51–65.

Koppes, M.N. & Montgomery, D.R. (2009) The relative efficacy of fluvial and glacial erosion over modern to orogenic timescales. *Nature Geosciences*, *2*, doi:10.1038/NGEO616.

Kraml, M., Pik, R., Rahn, M., Selbekk, R., Carignan, J. & Keller, J. (2007) A New Multi-mineral Age Reference Material for 40Ar/39Ar, (U-Th)/He and Fission Track Dating Methods: The Limberg t3 Tuff. *Geostandards and Geoanalytical Research*, *30*, 73–86.

Krogh, T.E. (1982) Improved accuracy of U-Pb zircon ages by the creation of more concordant systems using an air abrasion technique. *Geochimica et Cosmochimica Acta*, *46*, 637–649.

Kuhlemann, J., Frisch, W., Székely, B., Dunkl, I. & Kázmer, M. (2002) Post-collisional sediment budget history of the Alps: tectonic versus climatic control. *Int J Earth Sci*, *91*, 818–837.

Kuhlemann, J., Frisch, W., Dunkl, I., Székely, B. & Spiegel, C. (2001) Miocene shifts of the drainage divide in the Alps and their foreland basin. *Z. Geomorph. N. F.*, *45*, 239–265.

Kuhlemann, A. & Kempf, O. (2002) Post-Eocene evolution of the North Alpine Foreland Basin and its response to Alpine tectonics. *Sedimentary Geology*, *152*, 45–78.

Larsen, I.J. & Montgomery, D.R. (2012) Landslide erosion coupled to tectonics and river incision. *Nature Geoscience*, *5*, doi:10.1038/NGEO1479.

Laubscher, H.P. (1986) The eastern Jura: relations between thin-skinned and basement tectonics, local and regional. *Geol Rundsch*, *75*, 535–553.

Lauer, T., Frechen, M., Hoselmann, C. & Tsukatomo, S. (2010) Fluvial aggradation phases in the Upper Rhine Graben - new insights by quartz OSL dating. *Proceedings of the Geologists' Association*, *121*, 154–161.

Lelarge, M.L. (1993) *Thermochronologie par la methode des traces de fission d'une marge passiv (Dome de Ponta Grossa, Se Bresil) et au sein d'une chaine de collision (Zone externe de l'arc alpin, France)*. Ph.D. thesis, Université Joseph Fourier Grenoble, France, URL: http://tel.archives-ouvertes.fr/docs/00/60/32/09/PDF/These-Lelarge-1993.pdf

Liniger, H. (1966) Das plio-altpleistozäne Flussnetz der Nordschweiz. *Regio Bas*, *7*, 158–177.

Liniger, H. (1967) Pliozän und Tektonik des Juragebirges. *Eclogae geol Helv*, *60*, 407–490.

Link, K. (2010) *Die thermo-tektonische Entwicklung des Oberrheingraben-Gebietes seit der Kreide*. Ph.D. thesis, Albert-Ludwigs Universität Freiburg, Germany, URL: http://www.freidok.uni-freiburg.de/volltexte/7847/.

Lippolt, H.J., Gentner, W. & Wimmenauer, W. (1963) Altersbestimmungen nach der Kalium-Argon-Methode an tertiären Eruptivgesteinen Südwestdeutschlands. *Jh. geol. Landesamt Baden-Württemberg*, *6*, 507–538.

Litt, T. (2007) Das Quartär als chronostratigraphische Einheit. *Quaternary Science Journal*, *57*, 3–6.

Litt, T., Ellwanger, D., Villinger, E. & Wansa, S. (2005) Das Quartär in der Stratigraphischen Tabelle von Deutschland 2002. *Newsletters on Stratigraphy*, *41*, 385–399.

Litt, T., Schmincke, H.-U., Frechen, M. & Schlüchter, C. (2008) *Quaternary*. In: The Geology of Central Europe – Vol. 2: Mesozoic and Cenozoic (Ed. by T. McCann), pp. 1287–1340, The Geological Society, London.

Madritsch, H., Schmid, S.M. & Fabbri, O. (2008) Interactions between thin- and thick-skinned tectonics at the northwestern front of the Jura fold-and-thrust belt (eastern France). *Tectonics*, *27*, TC5005, doi:10.1029/2008TC002282.

Merle, O., Cobbold, P.R. & Schmid, S. (1989) *Tertiary kinematics in the Lepontine Dome*. In: Alpine Tectonics (Ed. by M.P. Coward, Dietrich, D. & Park, R.G.), pp. 113–134, Geological Society Special Publication No. 45, London.

Michalski, I. & Soom, M. (1990) The Alpine thermo-tectonic evolution of the Aar and Gotthard massifs, Central Switzerland: Fission Track ages on zircon and apatite and K-Ar mica ages. *Schweiz. Mineral. Petrogr. Mitt.*, *70*, 373–387.

Miller, G.H., Briner, J.P., Lifton, N.A. & Finkel, R.C. (2006) Limited ice-sheet erosion and complex exposure histories derived from in situ cosmogenic ^{10}Be, ^{26}Al, and ^{14}C on Baffin Island, Arctic Canada. *Quaternary Geochronology*, *1*, 74–85.

Molnar, P. & England, P. (1990) Late Cenozoic uplift of mountain ranges and global climate change: chicken or egg? *Nature*, *346*, 29–34.

Mortaz-Djalili, D. & Perriaux, J. (1979) Le Néogène du Plateau de Chambaran (Bas-Dauphiné, France). *Géologie Alpine*, *55*, 133–152.

Moss, S. (1992) Organic maturation in the French Subalpine Chains: regional differences in the burial history and the size of tectonic loads. *Journal of the Geological Society*, *149*, 503–515.

Muttoni, G., Carcano, C., Garzanti, E., Ghielmi, E.M., Piccin, A., Pini, R., Rogledi, S. & Sciunnach, D. (2003) Onset of major Pleistocene glaciations in the Alps. *Geology*, *31*, 989–992.

Nehlig, P., Boivin, P., de Goër, A., Mergoil, J., Prouteau, G., Sustrac, G. & Thiéblemont, D. (2003) *Les volcans du Massif central*. Revue Géologues Numéro spécial Massif central, BRGM, Orleans, 41 pp.

Nesbitt, H.W. & Young, G.M. (1996) Petrogenesis of sediments in the absence of chemical weathering: effects of abrasion and sorting on bulk composition and mineralogy. *Sedimentology*, *43*, 341–358.

Nie, J., Horton, B.K., Saylor, J.E., Mora, A., Mange, M., Garzione, C.N., Basu, A., Moreno, C.J.,

Caballero, V. & Parra, M. (2012) Integrated provenance analysis of a convergent retroarc foreland system: U–Pb ages, heavy minerals, Nd isotopes, and sandstone compositions of the Middle Magdalena Valley basin, northern Andes, Colombia. *Earth-Science Reviews*, *110*, 111–126.

Petit, C., Campy, M., Chaline, J. & Bonvalot, J. (1996) Major palaeohydrographic changes in Alpine foreland during the Pliocene-Pleistocene. *Boreas*, *25*, 131–143.

Pignalosa, A., Zattin, M., Massironi, M. & Cavazza, W. (2011) Thermochronological evidence of a late Pliocene climate-induced erosion rate increase in the Alps. *Int J Earth Sci*, *100*, 847–859.

Preusser, F., Graf, H.R., Keller, O., Krayss, E. & Schlüchter, C. (2011) Quaternary glaciation history of northern Switzerland. *Quaternary Science Journal*, *60*, 282–305.

Preusser, F., Reitner, J.M. & Schlüchter, C. (2010) Distribution, geometry, age and origin of overdeepened valleys and basins in the Alps and their foreland. *Swiss J Geosci, 103*, 407–426.

Rahn, M.K., Hurford, A.J. & Frey, M. (1997) Rotation and exhumation of a thrust plane: Apatite fission-track data from the Glarus thrust, Switzerland. *Geology, 25*, 599–602.

Rahn, M.K. & Selbekk, R. (2007) Absolute dating of the youngest sediments of the Swiss Molasse basin by apatite fission track analysis. *Swiss J Geosci*, *100*, 371–381.

Raymo, M.E. & Ruddiman, W.F. (1992) Tectonic forcing of late Cenozoic climate. *Nature, 359*, 117–122.

Reinecker, J., Danišik, M., Schmid, C., Glotzbach, C., Rahn, M., Frisch, W. & Spiegel, C. (2008) Tectonic control on the late stage exhumation of the Aar Massif (Switzerland): Constraints from apatite fission track and (U-Th)/He data. *Tectonics*, *27*, TC6009, doi:10.1029/2007TC002247.

Reinecker, J. & Kuhlemann, J. (2008) Timing of orogen-parallel Rhône valley incision, Switzerland. *Geophysical Research Abstracts*, *10*, EGU2008-A-00000.

Reiter, W., Elfert, S., Bernet, M., Glotzbach, C. & Spiegel, M. (in press) Relations between denudation, glaciation, and sediment deposition: implications from the Plio-Pleistocene Central Alps. *Basin Research*, doi: 10.1111/bre.12023.

Reiter, W., Elfert, S., Glotzbach, C. & Spiegel, C. (in preparation) Plio-Pleistocene evolution of the north-Alpine drainage system – implications from Neogene foreland deposits.

Rignot, E., Rivera, A. & Casassa, G. (2003) Contribution of the Patagonia Icefields of South America to Sea Level Rise. *Science*, *302*, 434–437.

Rolf, C., Hambach, U. & Weidenfeller, M. (2008) Rock and palaeomagnetic evidence for the Plio-Pleistocene palaeoclimatic change recorded in Upper Rhine Graben sediments (Core Ludwigshafen-Parkinsel). *Netherlands Journal of Geosciences*, *87*, 41–50.

Rotstein, Y. & Schaming, M. (2011) The Upper Rhine Graben (URG) revisited: Miocene transtension and transpression account for the observed first-order structures. *Tectonics*, *30*, TC3007, doi:10.1029/2010TC002767.

Schaer, J.P., Reimer, G.M. & Wagner, G.A. (1975) Actual and ancient uplift rate in the Gotthard region, Swiss Alps: A comparison between precise levelling and fission-track apatite age. *Tectonophysics*, *29*, 293–300.

Schlunegger, F. & Mosar, J. (2011) The last erosional stage of the Molasse Basin and the Alps. *Int J Earth Sci*, *100*, 1147–1162.

Schlunegger, F., Rieke-Zapp, D. & Ramseyer, K. (2007) Possible environmental effects on the evolution of the Alps-Molasse Basin system. *Swiss J. Geosci.*, *100*, 383–405.

Schlunegger, F. & Willett, S. (1999) *Spatial and temporal variations in exhumation of the central Swiss Alps and implications for exhumation mechanisms*. In: "Exhumation Processes:

Normal Faulting, Ductile Flow and Erosion" (Ed. by Ring, U., Brandon, M.T., Lister, G.S. & Willett, S.). p. 157–179, Geological Society, London, Special Publication 154.

Schmid, S.M., Fügenschuh, B., Kissling, E. & Schuster, R. (2004) Tectonic map and overall architecture of the Alpine orogen. *Eclogae geol Helv*, *97*, 93–117.

Schreiner, A. (1992) *Erläuterungen zu Blatt Hegau und westlicher Bodensee*. Geologisches Landesamt Baden-Württemberg, Freiburg, Stuttgart.

Shuster, D.L., Ehlers, T.A., Rusmore, M.E. & Farley, K.A. (2005) Rapid Glacial Erosion at 1.8 Ma Revealed by $^{4}He/^{3}He$ thermochronometry. *Science*, *310*, 1668–1670.

Sissing, W. (1998) Comparative Tertiary stratigraphy of the Rhine Graben, Bresse Graben and Molasse Basin: correlation of Alpine foreland events. *Tectonophysics*, *300*, 249–284.

Sissingh, W. (2001) Tectonostratigraphy of the West Alpine Foreland: correlation of Tertiary sedimentary sequences, changes in eustatic sea-level and stress regimes. *Tectonophysics*, *333*, 361-400.

Sissingh, W. (2006) Syn-kinematic palaeogeographic evolution of the West European Platform: correlation with Alpine plate collision and foreland deformation. *Netherlands J Geosc*, *85*, 131–180.

Soom, M. (1990) *Abkühlungs- und Hebungsgeschichte der Externmassive und der penninischen Decken beidseits der Simplon-Rhône-Linie seit dem Oligozän: Spaltspurendatierung an Apatit/Zirkon und K-Ar-Datierungen an Biotit/Muskovit (Westliche Zentralalpen)*. Ph.D. thesis, University of Bern, Switzerland.

Spiegel, C., Kohn, B., Belton, D., Berner, Z. & Gleadow, A. (2009) Apatite (U–Th–Sm)/He thermochronology of rapidly cooled samples: The effect of He implantation. *Earth and Planetary Science Letters*, *285*, 105–114.

Spiegel, C., Kohn, B., Raza, A., Rainer, T. & Gleadow, A. (2007) The effect of long-term low-temperature exposure on apatite fission track stability: A natural annealing experiment in the deep ocean. *Geochimica et Cosmochimica Acta*, *71*, 4512–4537.

Spiegel, C., Kuhlemann, J., Dunkl, I. & Frisch, W. (2001) Paleogeography and catchment evolution in a mobile orogenic belt: the Central Alps in Oligo–Miocene times. *Tectonophysics*, *341*, 33–47.

Spiegel, C., Kuhlemann, J., Dunkl, I., Frisch, W., von Eynatten, H. & Balogh, K. (2000) The erosion history of the Central Alps: evidence from zircon fission track data of the foreland basins. *Terra Nova*, *12*, 163–170.

Spiegel, C., Siebel, W. & Berner, Z. (2002) Sr and Nd isotope ratios and trace element geochemistry of detrital epidote as provenance indicators: implications for the reconstruction of the exhumation history of the Central Alps. *Chemical Geology*, *189*, 231–250.

Spiegel, C., Siebel, W., Kuhlemann, J. & Frisch, W. (2004) *Toward a comprehensive provenance analysis: A multi-method approach and its implications for the evolution of the Central Alp*s. In: "Detrital thermochronology – Provenance Analysis, Exhumation, and Landscape Evolution in Mountain Belts" (Ed. by M. Bernet and C. Spiegel). pp. 37–50, GSA Special Paper 378.

Steck, A. & Hunziker, J. (1994) The Tertiary structural and thermal evolution of the Central Alps - compressional and extensional structures in an orogenic belt. *Tectonophysics*, *238*, 229–254.

Steiner, H. (1984) Mineralogisch-petrographische, geochemische und isotopengeologische Untersuchungen an einem Meta-Lamprophyr und seinem granodioritischen Nebengestein (Matorello-Gneis) aus der Maggia-Decke. *Schweiz. Mineral. Petrogr. Mitt.*, *64*, 227–259.

Stewart, R.J. & Brandon, M.T. (2004) Detrital-zircon fission-track ages for the "Hoh Formation": Implications for late Cenozoic evolution of the Cascadia subduction wedge. *Geological Society of America Bulletin*, *116*, 60–75.

Stock, G.M., Ehlers, T.A. & Farley, K.A. (2006) Where does sediment come from? Quantifying catchment erosion with detrital apatite (U-Th)/He thermochronometry. *Geology*, *34*, 725–728.

Sue, C., Delacou, B., Champagnac, J.-D., Allanic, C., Tricart, P. & Burkhard, M. (2007) Extensional neotectonics around the bend of the Western/Central Alps: an overview. *Int J Earth Sci*, *96*, 1101–1129.

Suess, E. (1875) *Die Entstehung der Alpen*. Verlag W. Braumüller, Wien.

Teichmüller, R. & Teichmüller, M. (1986) Relations between coalification and palaeogeothermics in Variscan and Alpidic foredeeps of western Europe. *Paleogeothermics, Lecture Notes in Earth Sciences*, *5*, 53–78.

Thomson, S.N., Brandon, M.T., Tomkin, J.H., Reiners, P.W., Vásquez, C. & Wilson, N.J. (2010) Glaciation as a destructive and constructive control on mountain building. *Nature*, *467*, doi:10.1038/nature09365.

Timar-Geng, Z., Fügenschuh, B., Wetzel, A. & Dresmann, H. (2006) Low-temperature thermochronology of the flanks of the southern Upper Rhine Graben. *Int J Earth Sci*, *95*, 685–702.

Timar-Geng, Z., Grujic, D. & Rahn, M. (2004) Deformation at the Leventina–Simano nappe boundary, Central Alps, Switzerland. *Eclogae geol. Helv.*, *97*, 265–278.

Trautwein, B., Dunkl, I. & Frisch, W. (2001) Accretionary history of the Rhenodanubian Flysch zone in the Eastern Alps – evidence from apatite fission-track geochronology. *Int J Earth Sci*, *90*, 703–713.

Trümpy, R. (1960) Paleotectonic evolution of the Central and Western Alps. *Bulletin of the Geological Society of America*, *71*, 843–908.

Ustaszewski, K. & Schmid, S.M. (2007) Latest Pliocene to recent thick-skinned tectonics at the Upper Rhine Graben – Jura Mountains junction. *Swiss J. Geosc.*, *100*, 293–312.

Valla, P.G., Shuster, D.L. & van der Beek, P. (2011) Significant increase in relief of the European Alps during mid-Pleistocene glaciations. *Nature Geoscience*, *4*, 688–692.

Valla, P.G., van der Beek, P., Shuster, D., Braun, J., Herman, F., Tassan-Got, L. & Gautheron, C. (2012) Late-Neogene exhumation and relief development of the Aar and Aiguilles Rouges massifs (Swiss Alps) from low-temperature thermochronology modeling and $^{4}He/^{3}He$ thermochronometry. *J. Geophys. Res.*, *117*, F01004.

Van der Beek, P., Valla, P.G., Herman, F., Braun, J, Persano, C., Dobson, K.J. & Labrin, E. (2010) Inversion of thermochronological age-elevation profiles to extract independent estimates of denudation and relief history – II: Application to the French Western Alps. *Earth and Planetary Science Letters*, *296*, 9–22.

Vermeesch, P. (2004) How many grains are needed for a provenance study? *Earth and Planetary Science Letters*, *224*, 441–451.

Vermeesch, P. (2008) Three new ways to calculate average (U-Th)/He ages. *Chemical Geology*, *249*, 339–347.

Vernon, A., van der Beek, P.A., Sinclair, H.D., Persano, C., Foeken, J. & Stuart, F.M. (2009) Variable late Neogene exhumation of the central European Alps: Low-temperature thermochronology from the Aar Massif, Switzerland, and the Lepontine Dome, Italy. *Tectonics*, *28*, TC5004, doi:10.1029/2008TC002387.

Vernon, A.J., van der Beek, P.A., Sinclair, H.D. & Rahn, M.K. (2008) Increase in late Neogene denudation of the European Alps confirmed by analysis of a fission-track thermochronology database. *Earth and Planetary Science Letters*, *270*, 316–329.

Villinger, E. (1998) Zur Flussgeschichte von Rhein und Donau in Südwestdeutschland. *Jahresberichte und Mitteilungen des Oberrheinischen Geologischen Vereins, 80*, 361–398.

Villinger, E. (2003) Zur Paläogeographie von Alpenrhein und oberer Donau. *Zeitschrift der deutschen geologischen Gesellschaft*, *154*, 193–253.

Von Hagke, C., Cederbom, C.E., Oncken, O., Stöckli, D.F., Rahn, M.K. & Schlunegger, F. (2012) Linking the northern Alps with their foreland: The latest exhumation history resolved by low-temperature thermochronology. *Tectonics*, *31*, TC5010, doi:10.1029/2011TC003078.

Wagner, G.A. & Reimer, G.M. (1972) Fission track tectonics: The tectonic interpretation of fission track apatite ages. *Earth and Planetary Science Letters*, *14*, 263–268.

Wagner, G.A., Reimer, G.M. & Jager, E. (1977) Cooling ages derived by apatite fission-track, mica Rb-Sr and K-Ar dating: The uplift and cooling history of the Central Alps. *Mem Ist Geo Min Univ Padova*, Vol. XXX.

Wedel, J. (2008) Pleistocene molluscs from research boreholes in the Heidelberg Basin. *Quaternary Science Journal*, *57*, 382–402.

Weh, M. (1998) *Tektonische Entwicklung der penninischen Sediment-Decken in Graubünden (Prättigau bis Oberhalbstein)*. Ph.D. thesis, University Basel, Switzerland.

Weidenfeller, M. & Kärcher, T. (2008) Tectonic influence on fluvial preservation: aspects of the architecture of Middle and Late Pleistocene sediments in the northern Upper Rhine Graben, Germany. *Netherlands Journal of Geosciences*, *87*, 33–40.

Weidenfeller, M. & Knipping, M. (2008) Correlation of Pleistocene sediments from boreholes in the Ludwigshafen area, western Heidelberg Basin. *Quaternary Science Journal*, *57*, 270–285.

Willenbring Staiger, J., Gosse, J., Little, E.C., Utting, D.J., Finkel, R., Johnson, J.V. & Fastook, J. (2006) Glacial erosion and sediment dispersion from detrital cosmogenic nuclide analyses of till. *Quaternary Geochronology*, *1*, 29–42.

Willenbring, J.K. & von Blanckenburg, F. (2010) Long-term stability of global erosion rates and weathering during late-Cenozoic cooling. *Nature*, *465*, 211–214.

Willett, S.D., Schlunegger, F. & Picotti, V. (2006) Messinian climate change and erosional destruction of the central European Alps. *Geology*, *34*, 613–616.

Wolf, R.A., Farley, K.A. & Kass, D.M. (1998) Modeling of the temperature sensitivity of apatite (U-Th)/He thermochronometer. *Chemical Geology*, *148*, 105–114.

Zhang, P., Molnar, P. & Downs, W.R. (2001) Increased sedimentation rates and grain sizes 2-4 Myr ago due to the influence of climate change on erosion rates. *Nature*, *410*, 891–897.

Ziegler, P.A. & Dèzes, P. (2007) Cenozoic uplift of Variscan Massifs in the Alpine foreland: Timing and controlling mechanisms. *Global and Planetary Change*, *58*, 237–269.

Ziegler, P.A. & Fraefel, M. (2009) Response of drainage systems to Neogene evolution of the Jura fold-thrust belt and Upper Rhine Graben. *Swiss J. Geosci.*, *102*, 57–75.

10 Acknowledgements

For people who know that I grew up at the foot of the Alps, it might looks strange to go to Bremen to study the Alps, but that is how life works. Things very often come a lot different than we are expecting. Now looking back at the start of my PhD, I don´t regret my decision to come to northern Germany. I appreciate very much all the support I received from all working group members during my PhD time, therefore I want to thank the whole working group! Please be soft on me, if I don´t mention every person of my PhD time, they are not forgotten.

Special thanks goes to my supervisor Prof. Dr. Cornelia Spiegel for giving me this great opportunity to study "my" beloved mountain belt, and also for the constructive scientific discussions, and financial support after the original funding (DFG project SP673/5-1) was finished. Also special thanks to Dr. Joachim Kuhlemann, without Connys and his motivation to raise funding I could have not worked in this project. Many thanks to Frank Lisker and Barbara Ventura for their support and especially for the awesome Italian cheese. Many thanks to Andreas Klügel for being the second assessor of this thesis.

Thanks to the YTE organisation committee who supported me with literature, reading drafts (especially David "may the force be with you" Fernández-Blanco), and for the cheerfulness prior, during and after the two workshops.

And last but not least, the support of my parents, Christophe, Anne, Shantala, Simon, Tim, and all the nice people at Linie7, which helped me through this challenging period of my life!

11 Curriculum vitae

Education and career

2009 – 2013	Ph.D. student at Department of Geosciences, University of Bremen, Germany within the ESF-project Thermo-Europe – IP2: 'Sources and Sinks of Pliocene erosion: Investigating the latest-stage exhumation history of the Alps'
2003 – 2008	Diploma in Geosciences (equivalent to M.Sc.) with a major in Sedimentary Geology, Institute of Geosciences, University of Tübingen, Germany. Thesis: 'Climate changes in the Middle and Late Jurassic: Isotope analyses of radiolarites from the Northern Calcareous Alps' (Supervisor: Prof. em. Dr. Wolfgang Frisch) & mapping part: 'Kartierung der miozänen Karbonatrampe und der umgebenden alpinen Einheiten im NE von Saint Forent, Korsika / Frankreich' (Supervisor: Prof. Dr. Joachim Kuhlemann)
2005 – 2008	Undergraduate assistant at the geodynamics and micropalaeontology research groups, Department of Geosciences, University of Tübingen, Germany
2000 – 2003	Study of Bioinformatics, University of Tübingen, Germany

Special activities

September 2012	Member of the organisation committee of the Second Topo-Europe Young Researchers Workshop YTE2 in Utrecht, The Netherlands
April 2012	Member of the organisation committee of the First Topo-Europe Young Researchers Workshop YTE1 in Bratislava, Slowakian Republic
October 2011	Oral presentation at the 4th Workshop Forschungsbohrungen Heidelberger Becken in Grubenhagen, Germany
June 2010	Summer School on Modelling Surface Processes on Geological Timescales in Davos, Switzerland
January 2010	Thermo-Europe meeting in Grenoble, France
September 2009	Summer School on Modelling Thermochronology Data in Aussois, France
January 2009	Topo Alps/Thermo Europe meeting in Zürich, Switzerland

Peer reviewed publications

Reiter, **W**., Elfert, S., Glotzbach, C., Bernet, M. & Spiegel, C. (in press) Relations between denudation, glaciation, and sediment deposition: implications from the Central Alps. *Basin Research*, doi:10.1111/bre.12023.

Reiter, **W**., Elfert, S., Glotzbach, C. & Spiegel, C. (in prep) Plio-Pleistocene evolution of the north-Alpine drainage system – implications from Neogene foreland deposits.

Reiter, **W**., Elfert, S., Glotzbach, C. & Spiegel, C. (in prep) Reconstructing hinterland cooling history from foreland deposits – a detrital apatite (U-Th-Sm)/He case study from the Western Alps.

Talks

Reiter, **W**., Elfert, S., Bernet, M. & Spiegel, C. (2011) Denudation and drainage evolution of the Central European Alps since the Pliocene - Implications from detrital thermochronology. Oral presentation. 7th Topo-Europe Workshop. Davos/Switzerland.

Reiter, **W**., Elfert, S. & Spiegel, C. (2011) Plio-Pleistocene changes in drainage evolution and implications for the denudation history of the Central European Alps. Oral presentation. 10th Alpine Workshop - CorseAlp 2011.

Abstracts

Spiegel, C., Dörr, N., Lindow, J. & **Reiter**, **W**. (2012) Efficiency of glacial erosion - examples from the Arctic, Antarctica and the Alps. 13th International Conference on Thermochronology. Guilin/China.

Elfert, S., **Reiter**, **W**. & Spiegel, C. (2011) Late Miocene exhumation history of the Lepontine Dome. Poster presentation. 7th Topo-Europe Workshop. Davos/Switzerland.

Elfert S., **Reiter**, **W**. & Spiegel C. (2011) Timing and evolution of Neogene updoming of the Lepontine Dome. Constraints through new fission track and (U-Th-Sm)/He data on apatites. Oral presentation. 10th Alpine Workshop - CorseAlp 2011.

Reiter, **W**., Elfert, S. & Spiegel, C. (2011) Plio-Pleistocene denudation history of the Central European Alps revealed through detrital thermochronology. Poster presentation. European Geosciences Union General Assembly 2011. Vienna/Austria.

Elfert, S., **Reiter**, **W**. & Spiegel, C. (2011) Doming and unroofing of the Lepontine Dome (Central European Alps). New insights from low-temperature thermochronology. Poster presentation. European Geosciences Union General Assembly 2011. Vienna/Austria.

Reiter, **W**., Elfert, S. & Spiegel, C. (2010) Reconstructing circum-Alpine drainage evolution since the Pliocene using detrital thermochronology. Poster presentation at Thermo2010. 12th International Conference on Thermochronology. Glasgow/UK.

Elfert, S., **Reiter**, **W**. & Spiegel, C. (2010) Interrelations between the exhumation history and the drainage evolution of the European Alps during the Neogene. Poster presentation at Thermo2010. 12th International Conference on Thermochronology. Glasgow/UK.

Reiter, **W**., Elfert, S. & Spiegel, C. (2009) Pliocene erosion and drainage evolution of the Alps: Constraints from Neogene sedimentary deposits. Poster presentation at the 9th Workshop Alpine Geological Studies. Cogne/Italy.

Elfert, S., **Reiter**, **W**., Dörr, N. & Spiegel, C. (2009) Sources of Pliocene erosion of the Alps - The

Lepontine Dome as a potential source area. Poster presentation at 9th Workshop on Alpine Geological Studies. Cogne/Italy.